LAPPEENRANTA UNIVERSITY OF TECHNOLOGY
LUT School of Energy Systems
LUT Mechanical Engineering

Eero Ukkonen

CONVENIENCE OF SCALLOPS IN PLATE STRUCTURES

Examiners: Professor Timo Björk
M.Sc. (Tech.) Tuomas Skriko

ABSTRACT

Lappeenranta University of Technology
LUT School of Energy Systems
LUT Mechanical Engineering

Eero Ukkonen

Convenience of scallops in plate structures

Master's Thesis

2016

93 pages, 85 figures and 20 tables

Supervisors: Professor Timo Björk and M.Sc. (Tech.) Tuomas Skriko

Keywords: scallop; cope hole; weld; fatigue; stiffener

In this thesis was performed comprehensive study about the convenience of scallops in plate structures. A literature review was performed and lack of knowledge was fulfilled with fatigue tests performed in the laboratory of Steel Structures at the Lappeenranta University of Technology and with finite element method.

The aim of this thesis was to produce design guidance for the use of scallops for different structural details and different loading conditions. An additional aim was to include more precise instructions for scallop design to produce good fatigue resistance and appropriate manufacturing quality.

The literature review was performed searching bridge engineering and maritime standards and design guides and studies from scientific databases and reference lists from the literature of this field. Fatigue tests were used to research the effect of using scallops or not using scallops to fatigue strength of bracket specimen. Tests were performed on three specimens with different scallop radii and to five specimens without scallops with different weld penetration depths. Finite element method using solid elements, symmetry and submodels was used to determine stress concentration factors for I-beams with scallops. Stresses were defined with hot spot stress method.

Choosing to use a scallop or not in the structure is affected by many factors, such as structural and loading conditions and manufacturability. As a rule of thumb, scallops should be avoided because those cause stress concentration points to the structure and take a lot of time to manufacture. When scallops are not used, good quality welding should be provided and full weld penetration is recommended to be used in load carrying corner weld areas. In some cases, it is advisable to use scallops. In that case, circular scallops are recommended to be used and radius should be chosen from fatigue strength or manufacturing point of view.

TIIVISTELMÄ

Lappeenrannan teknillinen yliopisto
LUT School of Energy Systems
LUT Kone

Eero Ukkonen

Levyrakenteiden nurkkakolojen tarkoituksenmukaisuus

Diplomityö

2016

93 sivua, 85 kuvaa ja 20 taulukkoa

Tarkastajat: Professori Timo Björk ja DI Tuomas Skriko

Hakusanat: notsikolo; nurkkakolo; hitsi; väsyminen; jäykiste

Tässä työssä tehtiin kattava tutkimus nurkkakolojen tarpeellisuudesta levyrakenteissa. Aiheesta suoritettiin kirjallisuustutkimus, jota täydennettiin Lappeenrannan teknillisen yliopiston Teräsrakenteiden Laboratoriossa tehdyillä väsytyskokeilla sekä FE-menetelmällä mallintamalla.

Työn tavoitteena oli tehdä ohjeistus nurkkakolojen suunnittelulle tai pois jättämiselle eri rakenne- ja kuormitustilanteissa. Lisätavoitteena oli sisällyttää ohjeistukseen tarkempia muotoiluohjeita tarkoituksenmukaisen laadun saavuttamiseksi.

Kirjallisuustutkimus suoritettiin etsimällä sillan- ja laivanrakennuksen standardeja sekä tutkimuksia tieteellisistä tietokannoista ja alan teosten lähdeluetteloista. Väsytyskokeilla tutkittiin kulmatuen loveamisen ja loveamattomuuden vaikutusta liitoksen kestoikään. Koe suoritettiin kolmella erikokoisella kololla varustetuilla kappaleilla ja viidellä koloamattomalla kappaleella eri syvyisillä tunkeumilla. FE-menetelmällä verrattiin I-palkin kolotun liitoksen jännityskonsentraatiokertoimia kirjallisuudessa oleviin ristiriitaisiin arvoihin. I-palkki mallinnettiin käyttäen solidi-elementtejä, symmetriareunaehtoja ja alimalleja. Jännitykset määritettiin hot spot -menetelmällä.

Nurkkakolojen tekemiseen tai tekemättä jättämiseen vaikuttaa moni asia, kuten rakenne- ja kuormitustilanne sekä valmistettavuus. Pääsääntönä voidaan todeta, että nurkkakoloja tulisi välttää, koska ne aiheuttavat rakenteisiin väsymiskestävyyden kannalta haitallisia jännityskeskittymiä sekä lisäävät valmistuksen työvaiheita ja kustannuksia. Kun nurkkakoloja ei käytetä, tulisi hitsauksen laadun olla hyvä ja suositeltavaa olisi käyttää täyden tunkeuman hitsejä voimaliitoksien nurkka-alueilla. On myös tilanteita, joissa nurkkakolon käyttäminen on suotavampaa kuin koloamatta jättäminen. Tällöin ympyrän kaaren muotoista koloa tulisi käyttää, jonka säde tulisi valita väsymiskestävyyden ja valmistuksen vaatimusten mukaisesti.

ACKNOWLEDGEMENTS

First, I would like to thank my student mates and especially other research assistants in steel structures department who helped me through this Thesis work. Thanks to Design Forum of optimized welded structures (HRO) for giving me this interesting topic and financing my thesis. Thanks to LUT Laboratory of Steel Structures for manufacturing laboratory test specimens and performing fatigue tests. Special thanks to my supervisors Professor Timo Björk and M.Sc. (Tech.) Tuomas Skriko for interesting conversations and knowledge that led me to the right direction.

Honorable mentions to my family and to my girlfriend for support along the way.

Eero Ukkonen
Lappeenranta 11.5.16

TABLE OF CONTENTS

LIST OF SYMBOLS AND ABBREVIATIONS

$\Delta\sigma$	Design value of the constant amplitude stress range [MPa]
ΔP	Given load range [N]
σ	Normal stress [MPa]
$\sigma_{0.4*t}$	Nodal stress at a reference point at a distance of 0.4 * *t* [MPa]
$\sigma_{1.0*t}$	Nodal stress at a reference point at a distance of 1.0 * *t* from weld toe [MPa]
σ_b	Shell bending stress [MPa]
σ_{hs}	Structural hot spot stress [MPa]
σ_k	Effective notch stress [MPa]
σ_m	Membrane stress [MPa]
σ_n	Nominal stress [MPa]
$\sigma_{n,\ effective}$	Effective nominal stress [MPa]
σ_{nl}	Non-linear peak stress [MPa]
$\sigma(x)$	Measured stress at point *x*
τ	Shear stress [GPa]
a	Weld throat thickness [mm]
A	Minimum elongation [%]
C_f	Constant for fatigue category
E	Young's modulus [MPa]
F_{TH}	Threshold allowable stress range, maximum stress range for infinite design life [MPa]
g	Lack of weld penetration depth [mm]
h	Height of scallop [mm]
k_s	Stress concentration factor
m	Slope of the S-N curve
M	bending moment [Nm]
N	Number of life cycles
N_c	Number of cycles to crack detection
N_f	Number of cycles to failure
r	Radius [mm]
R	Radius of scallop [mm]

R_m	Tensile strength [MPa]
$R_{p0.2}$	Offset yield strength defined at the amount of stress that will results in a plastic strain of 0.2% [MPa]
S_r	Nominal bending tensile stress range [MPa]
t	Plate thickness [mm]
t_f	Flange thickness [mm]
t_w	Web thickness [mm]
Vb	Shear force by flange width [Nm]
Q	Heat input [kJ/mm^2]

AASHTO	American Association of State Highway and Transportation Officials
BNS	Bracket without scallop
BWS	Bracket with scallop
DFMA	Design for manufacturing and assembly
DNV	Det Norske Veritas
ENS	Effective notch stress
FAT	Fatigue class
FEA	Finite element analysis
FEM	Finite element method
HN	H-shaped specimen without scallop
HS	H-shaped specimen with scallop
IIW	International Institute of Welding
JSSC	Japanese Society of Steel Construction
LSE	Linear surface extrapolation
LUT	Lappeenranta University of Technology
MAG	Metal active gas
SCF	Stress concentration factor
S-N	Wöhler curve
TIG	Tungsten inert gas
TN	T-shaped specimen without scallop
TS	T-shaped specimen with scallop
TTWT	Through thickness at the weld toe

1 INTRODUCTION

Fatigue is a phenomenon due to cyclic loading leading to microscopic physical damage to the material of the affected structure. Continuous cyclic loading may raise microscopic damage into a macroscopic crack which can cause failure of the structure. The stress leading to fatigue failure may be significantly below material's ultimate strength. (Dowling, 2007, pp. 391–392.) Welded joints are typical places to start fatigue failure thus fatigue strength of connections should be taken into account in structural designing. Fatigue is a major problem in bridges and it does not show until the bridge has been used for many years. Many railroad bridges have shown fatigue cracks after 30 to 50 years of service. (Munse & Grover, 1964, pp. 2–3.) Analysed data from 164 cases of metallic bridge failures shows that 13 % of bridge collapses were caused by fatigue failure and 67 % of non-collapsed bridge failures were caused by fatigue. Results are shown in figure 1. The high percentage of fatigue caused failure modes for non-collapsed bridges shows that much attention has been paid to fatigue failures by inspectors. (Imam & Chryssanthopoulos, 2010, pp. 4–5.)

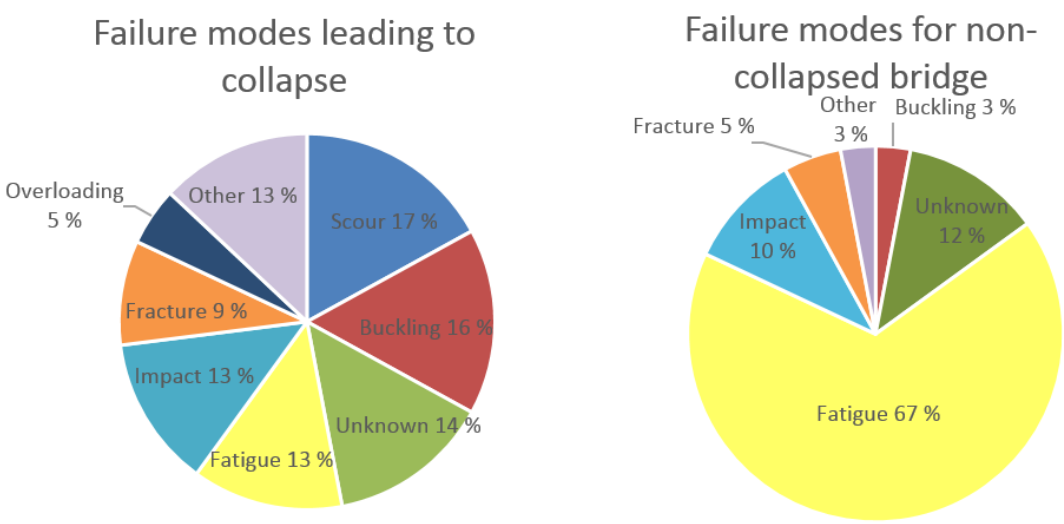

Figure 1. Failure modes of metallic bridges (modified from Imam & Chryssanthopoulos, 2010, pp. 4–5).

Scallops are cut outs in weld corners which are used in many structures as in bridges, decks and offshore structures for several reasons. Usually, scallops are used in connections

between girders' web and flanges with or without stiffener to avoid intersecting welds. Scallops are also known as cope holes, cut outs, weld access holes and mouse holes. Figure 2 shows different types of scallops. Scallops are used for several reasons. Three usual reasons are:

- To ensure good welding quality between web and flange (figure 2a).
- To reduce the welding length and plate distortion (figure 2b).
- To provide drain or air holes (figures 2a and 2b).

(Fricke & Paetzold, 1995, pp. 423–424.)

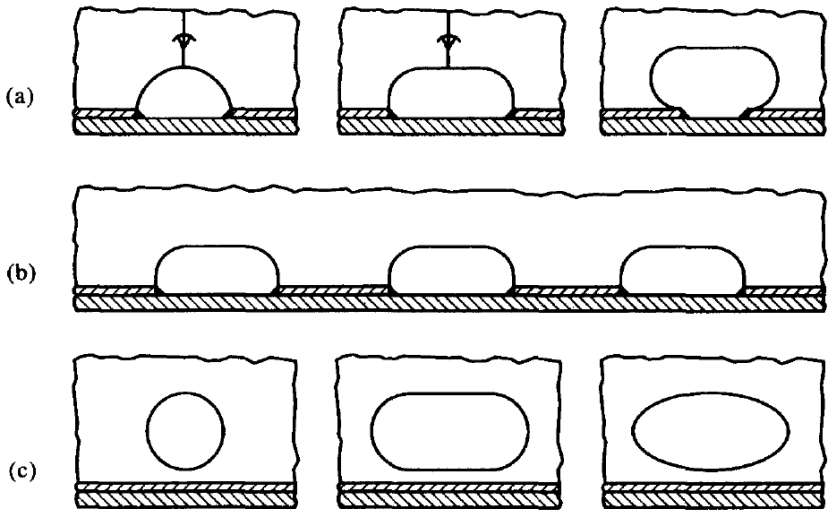

Figure 2. Different scallop types and different reasons for those (Fricke & Paetzold, 1995, p. 424).

Steel girders in bridges are usually fabricated in pieces and welded together at field. To ease the welding and avoiding crossing welds, scallops have been used as shown in figure 3. Scallops can be used at splices due to section change. (Heshmati & Al-Emrani, 2012, pp. 2–3.) Actually Intersecting welds are not a bad thing but residual stress distributions are.

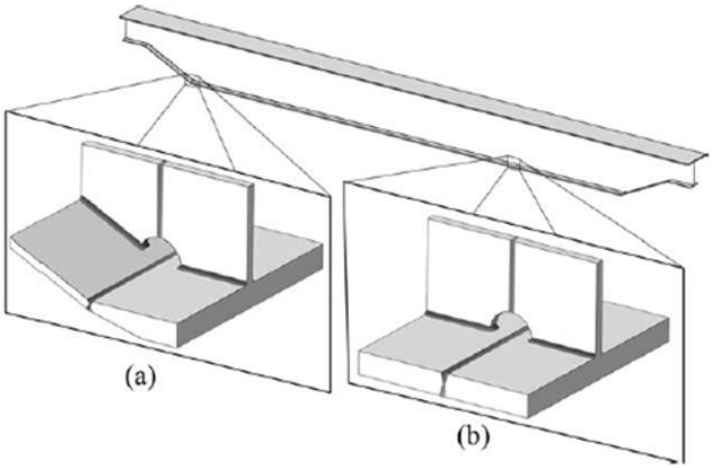

Figure 3. Scallops in a steel bridge girder (Heshmati & Al-Emrani, 2012, p. 3).

Cutting the inner corners of I-beams' stiffeners comes from era when unkilled steel, insufficiently deoxidized steel, was used in rolled sectional girders. The corner of web and flange had to remain uninfluenced by welding. Welding the corner used to cause cracking. Later the scallops were used to help welding, avoid bad fitting and residual stresses at the weld crossing. (Radaj, 1990, p. 111.) Nowadays, when welding quality is better and material properties have been improved, every intersecting weld should not be avoided (Niemi, 2003, p. 128).

1.1 Background of the research

This research is based on the field of steel structures and fatigue design. Some bridge design companies and experts in Finland prefer to use scallops, some don't and some are using scallops based on the situation. A comprehensive study was needed to clarify whether to use scallops or not.

A lot of research from the 1960's to these days have been made about scallops. Most of the studies are considering only one type of structure with one loading condition. This research summarizes previous studies and adds new knowledge from studies performed at Lappeenranta University of Technology.

1.2 Framework and research problem

The fatigue design and finite element method are the framework of this research. The research problem is that there is a lot of inherence when to use scallops and when not. It is unclear whether there are any benefits or disadvantages of using scallops.

1.3 The aims of the research, hypotheses and scope

The aim of this research is to produce a guidance for the use of scallops. The research question is when scallops should be used? The gained results are compared and guidance for using the scallops is made as a result of this research. Different structural details and loading conditions are included in the guidance, which is generally exploitable to ease engineers to create more fatigue resistant and cost-effective structures.

It is assumed that in some cases details with scallops have better fatigue strength than details without scallops, but in most cases the situation is opposite. It is also assumed that smaller scallop radius provides better fatigue strength for detail than bigger scallop radius.

The scope of this thesis narrows down to fatigue strength and fabrication aspects neglecting fluid dynamic cases and other obvious situations where scallops should be used. Closed stiffener to crossbeam connections are also neglected from this thesis.

1.4 Research methods

The research is performed mostly as a literature review. Laboratory measurements and Finite element analysis (FEA) are used to fulfill the lack of information from previous studies. Results are compared to each other and analysed.

2 FATIGUE ANALYSIS METHODS

Stresses in weld joints are not linear over the thickness. Total stress can be divided into three different parts as shown in figure 4. It consists of membrane stress σ_m, shell bending stress σ_b and non-linear peak stress σ_{nl}. (Hobbacher, 2014, pp. 14.) Residual stresses are also included to the total stress (Glenn et al., 1999, p. C-30).

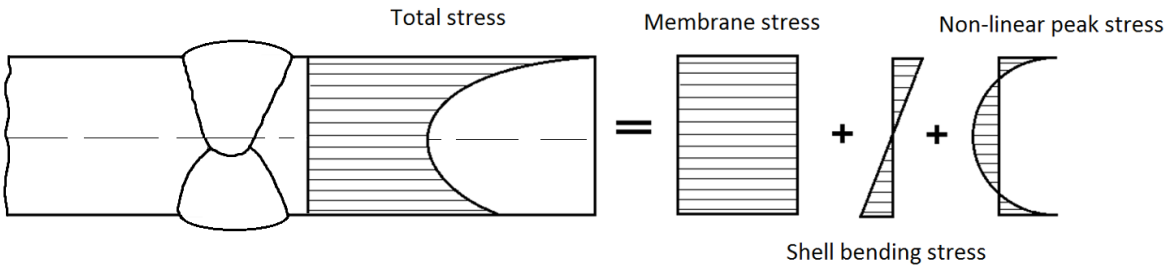

Figure 4. Stress components.

According to Hobbacher (2014, p. 12) five basic methods are used to determine fatigue life of a structure:

- "Nominal stress
- Structural hot spot stress
- Effective Notch stress (ENS)
- Linear elastic fracture mechanics
- Component testing."

Only nominal stress, structural hot spot stress and ENS are used in this research. Figure 5 shows what stresses these three techniques include. σ_n is nominal stress, σ_{hs} is structural stress and σ_k is ENS.

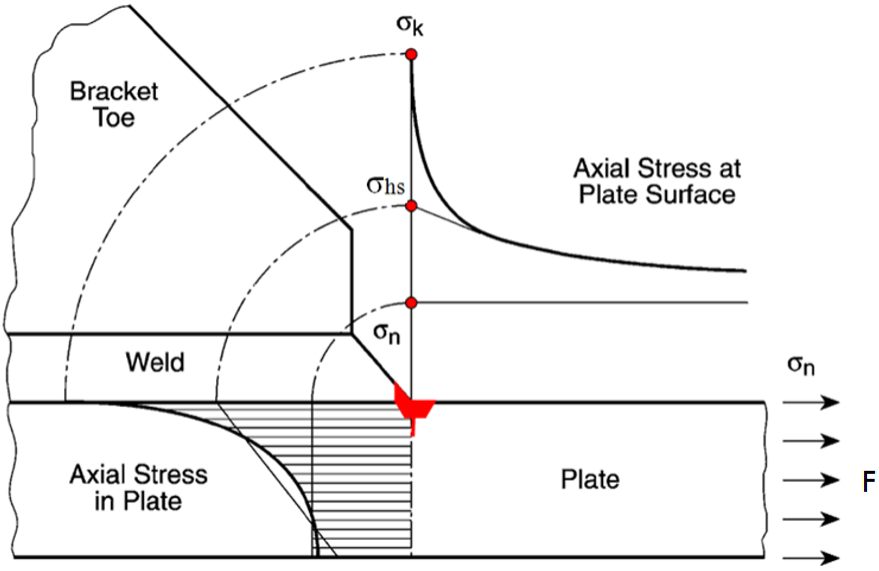

Figure 5. Stresses at plate surface (modified from Fricke, 2014, p. 2).

2.1 Nominal stress

Determining the fatigue life with nominal stress σ_n is based on experimental S-N curves (Wöhler curve) for different joint types (Hobbacher, 2012, pp. 45–74). Nominal stress includes stress raising effects of the macrogeometric features close to the joints but neglects stress raising effects of welded joints. Nominal stress is based on linear elastic theory. Depending on loading conditions the nominal stress may vary over the cross section of the structure as seen in figure 6. Simple beam theory can be used to calculate nominal stress for this kind of beam-like structure. The effect of the weld is not included to nominal stress. (Hobbacher, 2014, p. 15.)

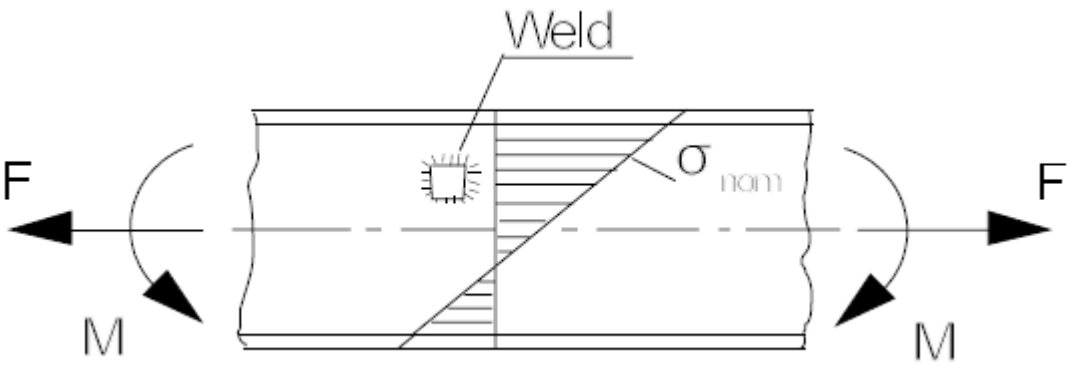

Figure 6. Nominal stress in a beam-like structure, where *F* is force and *M* is Bending moment (Hobbacher, 2014, p. 15).

Finite element method (FEM) should be used to include macrogeometric stress raisers to nominal stress because those are not included into standard S-N curves. Some examples of macrogeometric nominal stress raisers are shown in figure 7. (Niemi et al., 2004, p. 5.)

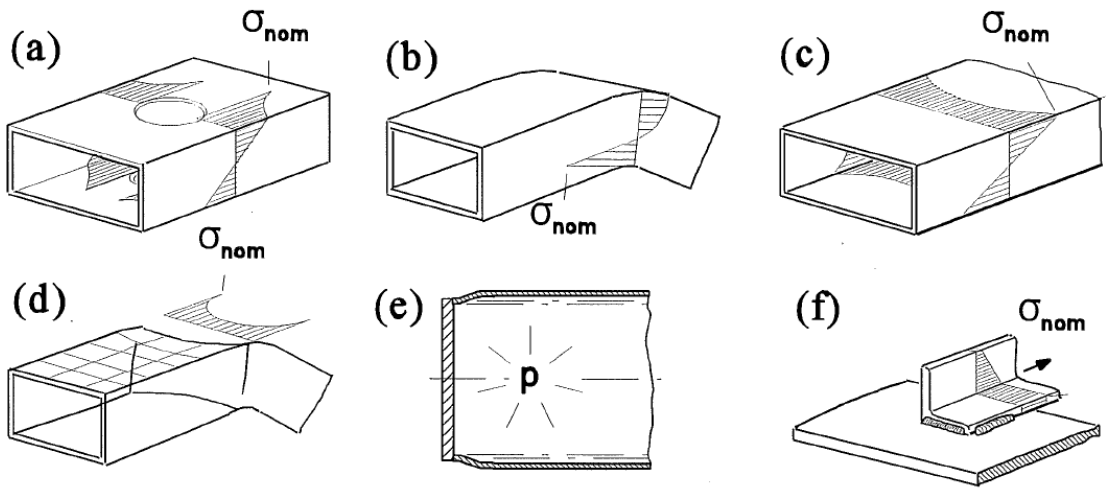

Figure 7. Macrogeometrical nominal stress raisers: a) large holes, b) curved beam, c) shear lag in wide flange, d) Distortion of curved beam's cross section, e) disorder of discontinuity in pressure vessel, f) bending in beam caused by eccentric lap joint (Hobbacher, 2014, p. 16).

Fatigue life with nominal stress is calculated using the following equation

$$\Delta\sigma^m N = FAT^m * 2 * 10^6, \qquad (1)$$

, where $\Delta\sigma$ is design value of the constant amplitude stress range, m is slope of the fatigue strength S-N curve, N is number of life cycles and FAT is design value of the fatigue resistance at $2 \cdot 10^6$ cycles for specified detail. (Hobbacher, 2014, p. 111.) IIW (International Institute of Welding) recommendations use FAT values but also different methods are used. In this paper also design rules from AASHTO (American Association of State Highway and Transportation Officials) are used. Design stresses for AASHTO detail categories are shown in table 1.

Table 1. AASHTO design stresses (Bowman el al., 2012, p. 31).

Detail category	Design stress at 2 million cycles
A	160 MPa
B	125 MPa
B’	100 MPa
C	90 MPa
D	71 MPa
E	56 MPa
E’	40 MPa

2.2 Structural stress (Hot spot)

In complex geometries where nominal stress is not clearly defined or there is no classified detail for the structure, other methods like structural hot spot stress should be used (Hobbacher, 2014, p. 19). The structural stress which is also known as geometric stress σ_{hs} at the hot spot includes membrane and bending stresses but excludes non-linear stress peak. All stress raising effects of a structural detail except effects due to weld are included to structural stress. Structural stress is traditionally derived by using reference points by extrapolation from specified distances from weld toe. The notch effect of the weld which is not included in structural stress disappears approximately at the distance of 0.4 * t from the weld toe, where t is the plate thickness. This is seen from figure 8. Two types of hot spots according to their location on the plate and orientation with respect to the weld are shown in figure 9. Hot spot type "a" is for weld toe on plate surface and type "b" is for weld toe at plate edge. (Hobbacher, 2014, pp. 19–28.)

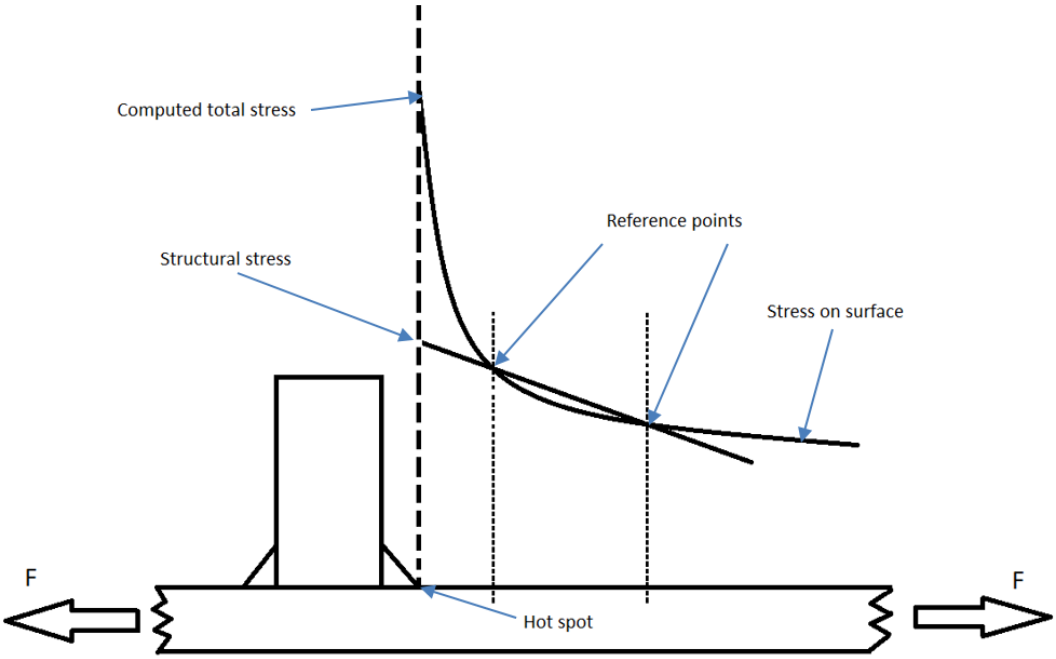

Figure 8. Definition of structural hot spot stress (Modified from Hobbacher, 2014, p. 20).

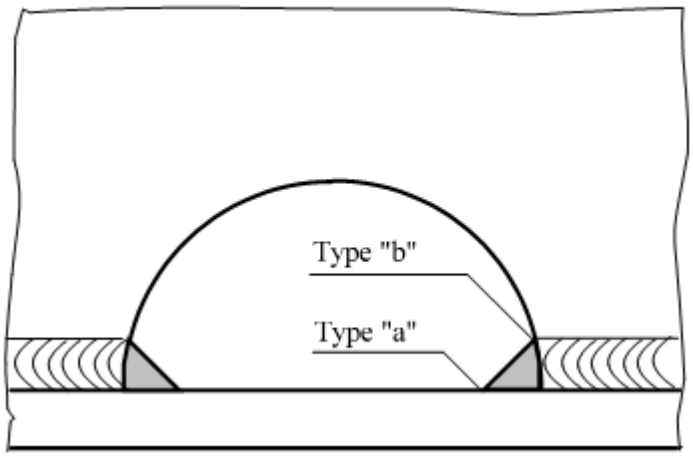

Figure 9. Type "a" and "b" hot spots at the edge in a scallop (Niemi, 1999, p. 17).

Three basic methods to determine structural stress are shown in figure 10. Method (a) is surface extrapolation technique which is the most commonly used. Alternative method (b) is to perform stress linearization through plate thickness at weld toe (TTWT). Method (c) by Dong (2001, p. 868) proposes to measure the element stresses in a distance δ from the weld toe.

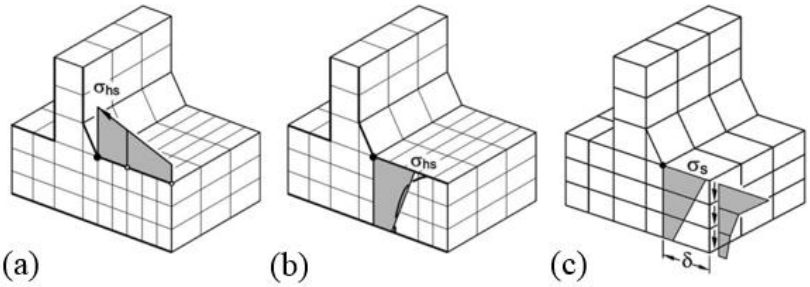

Figure 10. Three different methods to determine structural stress (Fricke & Kahl, 2005, p. 476).

International Institute of Welding (IIW) recommend using two or three quadratic extrapolation points in front of the weld toe when surface stress extrapolation is used. For type "a″ hot spots with fine mesh, structural hot spot stresses can be calculated as follows:

$$\sigma_{hs} = 1.67 * \sigma_{0.4*t} - 0.67 * \sigma_{1.0*t} \quad (2)$$

$$\sigma_{hs} = 2.52 * \sigma_{0.4*t} - 2.224 * \sigma_{0.9*t} + 2.224 * \sigma_{1.4*t} \quad (3)$$

In equation 2 σ_{hs} is structural hot spot stress, $\sigma_{0.4*t}$ is nodal stress at a reference point at a distance of 0.4 * *t* from weld toe where *t* is plate thickness. $\sigma_{1.0*t}$ is nodal stress at a reference point at a distance of 1.0 * *t* from weld toe. Distances of reference points in equation 3 are 0.4 * *t*, 0.9 * *t* and 1.4 * *t*. For coarse mesh, it is recommended to calculate hot spot stresses as follows:

$$\sigma_{hs} = 1.50 * \sigma_{0.5*t} - 0.50 * \sigma_{1.5*t}, \quad (4)$$

, where reference points are at distances of 0.5 * *t* and 1.5 * *t* from weld toe. Two equations are given for type "b" hot spot. Hot Spot Stress type "b" with fine mesh is calculated as follows:

$$\sigma_{hs} = 3 * \sigma_{4\ \mathrm{mm}} - 3 * \sigma_{8\ \mathrm{mm}} + \sigma_{12\ \mathrm{mm}}, \quad (5)$$

, where reference points are at distances of 4 mm, 8mm and 12 mm from weld toe. Hot Spot Stress type "b" with coarse mesh is calculated as follows:

$$\sigma_{hs} = 1.5 * \sigma_{5\ \mathrm{mm}} - 0.5 * \sigma_{15\ \mathrm{mm}}, \tag{6}$$

, where reference points are at distances of 4 mm, 8mm and 12 mm from weld toe. Reference points at different types of meshing for types "a" and "b" hot spots are shown in figure 11. (Hobbacher, 2014, pp. 24–25.)

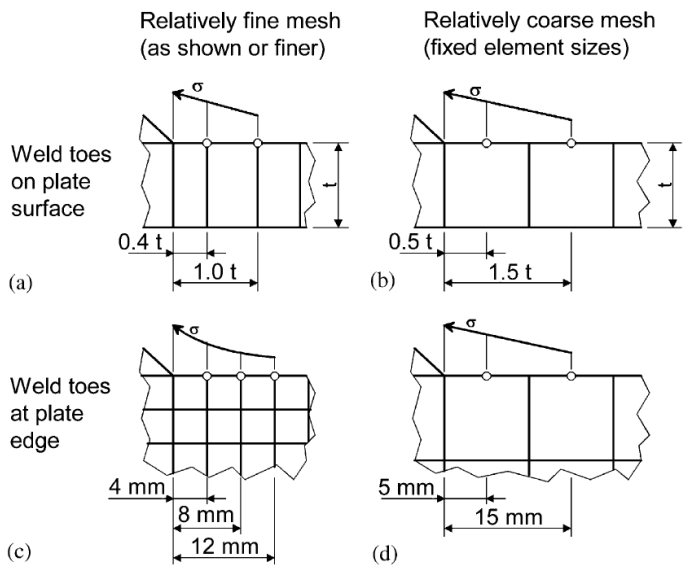

Figure 11. Reference points at different types of meshing (Fricke & Kahl, 2005, p. 476).

Specified S-N curves are made for structural hot spot stresses. Fatigue class FAT 100 applies for normal welded joint cases in steel structures. FAT 90 is used in longer attachments (length > 100 mm) at plate edges and in load carrying fillet welds. (Hobbacher, 2014, pp. 76–77.) Equation 1 is used to calculate fatigue lives for details (Hobbacher, 2014, p. 111).

Structural hot spot stress can be determined with stress concentration factor k_s and nominal stress σ_n. (DNV, 2011, p. 13).

$$\sigma_{hs} = k_s * \sigma_n \tag{7}$$

To calculate structural hot spot stress with TTWT method, membrane and shell bending stresses are separated from the total stress as follows:

$$\sigma_m = \frac{1}{t} * \int_{x=0}^{x=t} \sigma(x) * dx \tag{8}$$

$$\sigma_b = \frac{6}{t^2} * \int_{x=0}^{x=t} (\sigma(x) - \sigma_m) * \left(\frac{t}{2} - x\right) * dx, \tag{9}$$

, where σ_m is membrane stress, σ_b is shell bending stress, t is plate thickness, $\sigma(x)$ is measured stress at point x and x is a distance from plate surface to measure point. (Hobbacher, 2014, pp. 15.) Structural hot spot stress is gained by summing the membrane and shell bending stresses. (Hobbacher, 2014, p. 19).

$$\sigma_{hs} = \sigma_m + \sigma_b \tag{10}$$

2.3 Effective notch stress (ENS)

Effective notch stress is the total stress which includes membrane, bending and peak stresses as shown in figure 12. ENS can be used to define stresses at weld toe and also at weld root. (Hobbacher, 2014, pp. 29–30.)

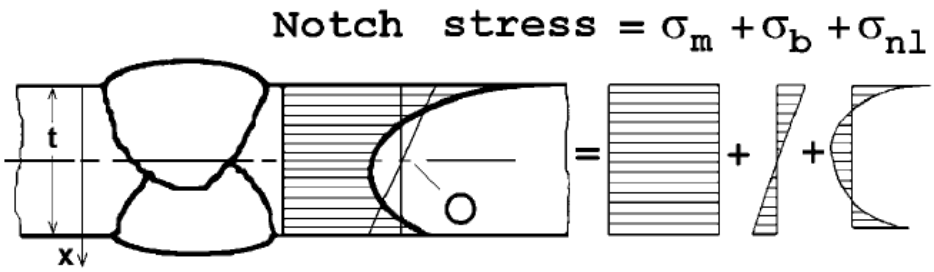

Figure 12. Stresses in notch stress (Hobbacher, 2014, p. 14).

For steel and aluminum structures with plate thickness not less than 5 mm, radius r = 1 mm for toe and root gives reliable results. Figure 13 represents rounding of weld toes and roots. Single S-N curve is determined to ENS specimens. When principal stresses are determined, FAT 225 is used for steel structures and FAT 71 is used for aluminum alloys when plate thickness is not less than 5 mm. (Hobbacher, 2014, pp. 29–30.) When plate thickness less than 5 mm is used, radius r = 0.05 mm should be used for toe and root. FAT 630 is used for steel structures and FAT 180 for aluminum alloys when plate thickness is less than 5 mm. (Fricke, 2010, p. 21.) It is recommended to model fillet welds to 30° angle and butt welds to

45° angle. Figure 14 shows modelling guidance for weld toes and roots. (Hobbacher, 2014, pp. 29–30.)

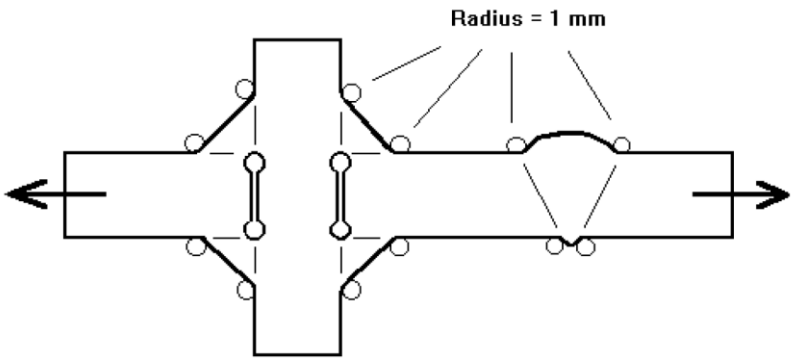

Figure 13. Radius to be used in ENS method (Hobbacher, 2014, p. 30).

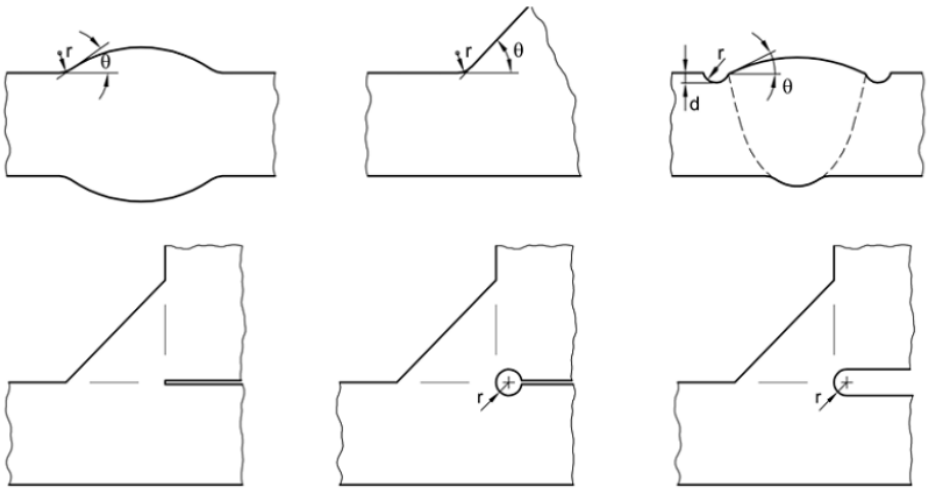

Figure 14. Examples for modelling weld toes and roots (Hobbacher, 2014, p. 30).

ENS at weld toe should be more than 1.6 times the structural hot spot stress. A relative fine mesh is needed to determine effective notch stress at weld toes and roots. It is recommended to use at least three elements at 45° arc of weld toe and at least twenty-four element around 360° arc at weld root. When quadratic elements with mid-side nodes are used the mesh size should not be more than 0.25 mm at the arc and close to the measured point. When using linear elements the mesh size should be not more than 0.15 mm. (Hobbacher, 2014, pp. 29–30.) This is an official rule for engineering design. For scientific analysing, Kranz and Sonsino (2010) recommend a mesh size of 0.05 mm to be used.

3 CASES

This chapter gathers together results from many experimental fatigue tests and finite element model studies. Cases are gathered using scientific databases like Scopus and ScienceDirect. Bridge engineering and maritime standards and design guides from different countries are important part of this chapter. Critical analysing is performed due to incongruities between some of the test results.

3.1 T- and H-shaped specimens

Xiao and Yamada (2005) studied the effect of scallops to fatigue strength with T- and H-shaped specimens which were fillet welded to both surfaces of a tensile plate. Test specimens with loading conditions are shown in figure 15. Tests for T-shaped specimens with scallops (TS) and without scallops (TN) were done with 100 mm and 200 mm long brackets to define the influence of bracket length to fatigue strength. For H-shaped specimens with scallops (HS) and without scallops (HN) tests were done only with 200 mm long brackets. Also a 50 mm bracket was used in TN specimen. Fatigue tests were applied with constant amplitude tensile cyclic loading. All specimens were fillet welded using the design weld leg length of 6 mm. (Xiao &Yamada, 2005, pp. 924–925.)

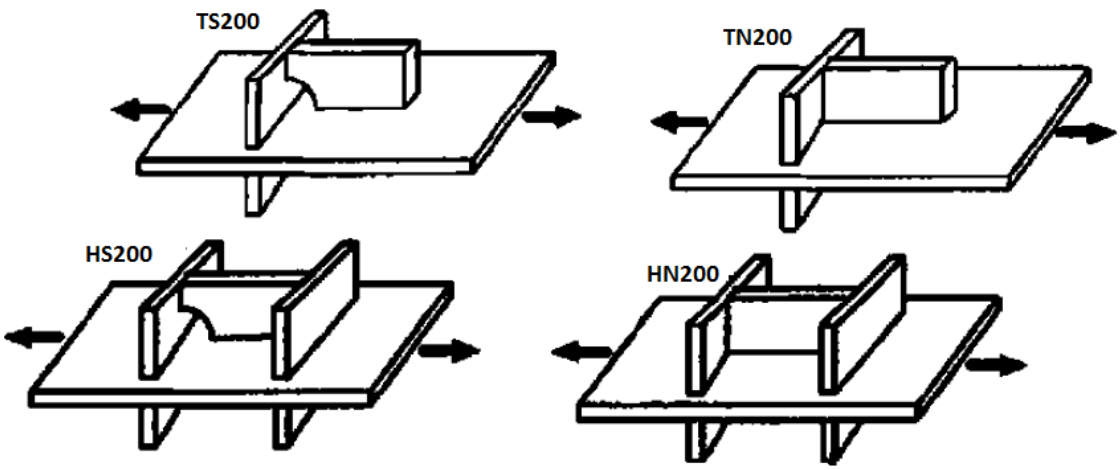

Figure 15. T- and H-shaped specimens (modified from Xiao & Yamada, 2005, p. 927).

Fatigue test results are shown in table 2. Nominal stresses are used to determine the fatigue strengths of specimens. It is seen that increasing the bracket length degreases fatigue strength of the specimen. With 100 mm longitudinal attachment length, T-shaped specimen with a scallop has slightly better fatigue strength than specimen without a scallop. With 200 mm longitudinal attachment length, specimen without a scallop has better fatigue strength than specimen with a scallop. Fatigue cracks developed at weld toes of bracket ends. (Xiao & Yamada, 2005, pp. 927–928.) Scallops degrease the effective length of brackets which is seen in slightly better fatigue strength than in specimens without scallops. When bracket length is increased the effect of the scallop degreases.

Table 2. Fatigue test results of T and H-shaped specimens (modified from Xiao & Yamada, 2005, p. 927).

Specimen	Mean strength at 2 million cycles [MPa]
TN50	90.5
TN100	81.5
TN200	78.7
TS100	83.3
TS200	73.6
HN200	89.6
HS200	89.5

H-shaped specimens with and without scallop with 200 mm bracket have almost the same fatigue strength. Fatigue cracks in HS200 specimens developed at toes of the longitudinal brackets at scallop edges. Fatigue cracks in HN200 specimens developed at fillet weld toes at outside welds in transverse attachments. Stress distributions at the edges of transverse attachments for T and H-shaped specimens are shown in figure 16. (Xiao & Yamada, 2005, pp. 927–929.)

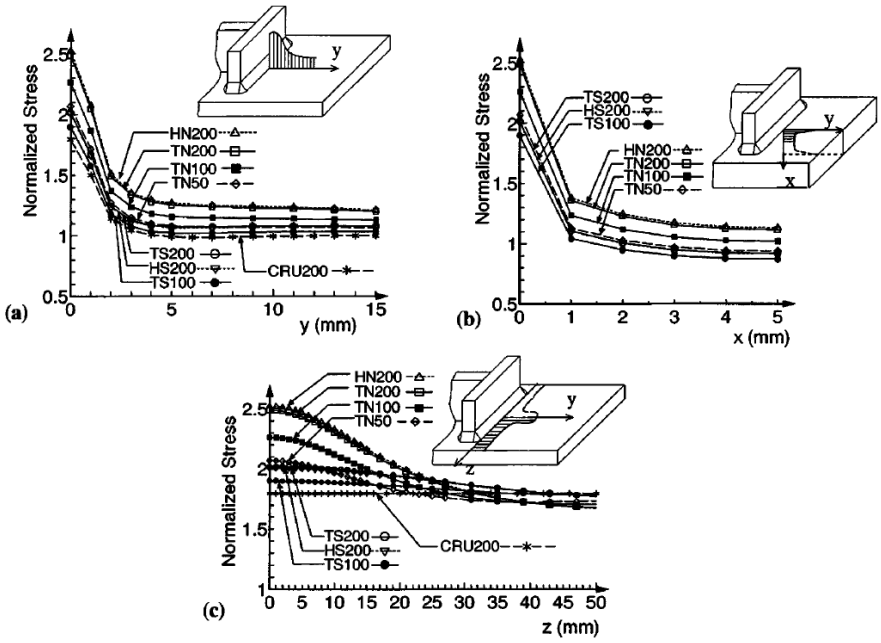

Figure 16. Stress distributions at the edges of transverse attachments: (a) in longitudinal direction; (b) through thickness; (c) in transverse direction (Xiao & Yamada, 2005, p. 929).

Solomon, Björk and Nykänen (2010) investigated the effect of scallops for loaded and non-loaded brackets using effective notch stress method (ENS). Figure 17 shows one quarter model of the examined specimen. Green arrows represent the primarily loaded case and blue arrows represents the non-primarily loaded case. The effect of different weld throat thicknesses, plate thicknesses and scallop sizes were studied. Results from shell element models showed that increasing the length of the bracket reduces stress concentration due to the presence of the scallop. These results are opposite than results from Xiao and Yamada (2005). Different loading conditions are one reason for opposite results. Other reason is that Solomon, Björk and Nykänen used ENS method to determine stresses but Xiao and Yamada used nominal stress method which is not as accurate as ENS method.

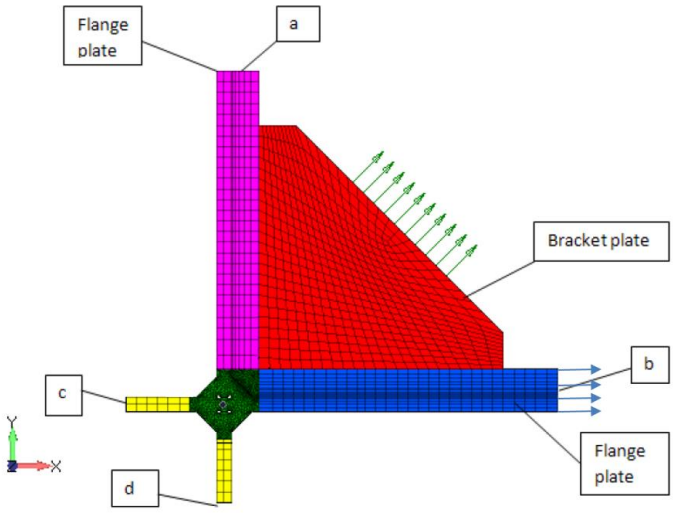

Figure 17. Bracket without a scallop with two different loading conditions (Modified from Solomon, Björk & Nykänen, 2010, p. 6).

Solomon, Björk and Nykänen (2010) concluded that when a bracket is primarily loaded the best fatigue strength is achieved using full penetration weld at corner area for bracket with no scallop (BNS). If filled weld is used, bracket with scallop (BWS) has better fatigue life than BNS. Increasing the radius of scallop degreases the fatigue strength. This means that small scallops with radii as 20 mm are recommended. Depending on the lack of weld penetration depth, BNS have better fatigue strength than BWS with large scallop. BNS is vulnerable for bad welding quality. If full penetration weld cannot be achieved, using a scallop should be considered. Good quality is required at corner area, which can be reached and repeated reliably only by using robotic welding. (Solomon, Björk & Nykänen, 2010, p. 19.)

When the bracket is non-primarily loaded the bracket end weld toe is the critical location for fatigue failure for BNS and BWS. BNS with full penetration weld has the lowest von Mises stress at the bracket plate end when compared to the other cases but the difference in fatigue strength is minor. When fillet weld is used specimen with 20 mm radius scallop has slightly better fatigue strength at the bracket plate end when compared to BNS. Based on stresses at the scallop corner and crossing weld, BNS with fillet or full penetration welds has better fatigue strength than BWS. Because it is almost the same to use BWS or BNS at the bracket and BNS is better at weld crossing, BNS is recommended to be used with full penetration weld at critical zone. (Solomon, Björk and Nykänen, 2010, p. 19.)

3.2 Flange and web with tensile stress

EN 1993-1-9 Eurocode 3 (2005) gives fatigue detail categories for I-shaped rolled section beams with various requirements. These recommendations which are presented in table 3 shows that using a scallop reduces the fatigue strength, increasing the thickness of the beam degreases the fatigue strength and quality of welding has an influence to fatigue strength. *t* is the thickness of the flange and k_s is a reduction factor for fatigue stress to account for size effects. (EN 1993-1-9, 2005, pp. 21–22.)

Table 3. Rolled sections with and without scallops (EN 1993-1-9, 2005, pp. 21–22).

	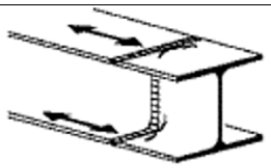			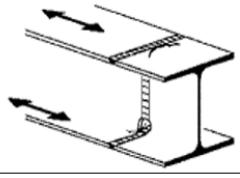	
Detailed requirements	Rolled sections without scallops			Rolled sections with scallops	
All welds ground flush to plate surface parallel to direction of arrows	x			x	
The high of the weld convexity to be not greater than 10 % of the weld width, with smooth transition to the plate surface		x			x
Size effect when $t > 25$ mm: $k_s = (25/t)^{0.2}$	x	x		x	x
Weld run-on and run-out pieces to be used and subsequently removed, plate edges to be ground flush in direction of stress	x	x	x	x	x
Welded from both sides	x	x	x	x	x
Checked by NDT (nondestructive testing)	x	x		x	x
Fatigue strength (FAT)	112	90	63	90	80

Continuous fillet or butt welds in flange and web have a fatigue strength of 100 MPa. If intermittent welds are used the detail have a fatigue strength of 80 MPa and if scallops are used the detail have a fatigue strength of 71 MPa. If the height of the scallop *h* is larger than 60 mm, then the fatigue strength degreases. FAT is 63 when *h* is over 60 mm but not more than 100 mm and FAT is 56 when *h* is more than 100 mm. (EN 1993-1-9, 2005, pp. 21–22.) IIW document by Hobbacher (2014, p. 56) gives the same FAT classes for details B and C (without flange crossing weld) as EN 1993-1-9 Eurocode 3 (2005), but with a correlation

factor. The ratio of shear stress τ in web at weld ends to normal stress σ in flange affects to the fatigue strength (Hobbacher, 2014, p. 56). Results are shown in table 4.

Table 4. Specimens with manual continuous weld (A), intermittent welds (B) and weld with a scallop (C) (EN 1993-1-9, 2005, pp. 21–22; Hobbacher, 2014, p. 56).

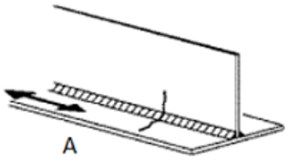 A	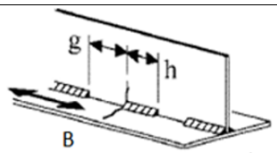 B $g/h \leq 2.5$	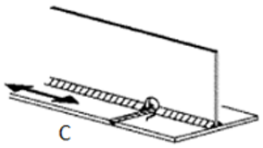 C	τ/σ
FAT = 100	FAT = 80 x (1 − $\Delta\tau$ / $\Delta\sigma$)	FAT = 71 x (1 − $\Delta\tau$ / $\Delta\sigma$)	
	80	71	0
	71	63	0.0 – 0.2
	63	56	0.2 – 0.3
	56	50	0.3 – 0.4
	50	45	0.4 – 0.5
	45	40	0.5 – 0.6
	-	36	> 0.6
	40	-	0.6 – 0.7
	36	-	> 0.7

Fricke and Paetzold (1995) made fatigue tests with specimens with different sized and shaped scallops. The results of three different studies were plotted in figure 18 together with the scatter line calculated by Gurney and Maddox (1972). This figure shows that the scallop with radius of 25 mm has better fatigue strength than scallop with radius of 40 mm. Small radius should be used and large radius is not recommended to be used even it would ease the welding and thus improve quality. Hot spot and notch stress methods were used to define the fatigue behavior of different scallop shapes. Investigated shapes were rectangular, elliptical and half-round scallops. Theoretical and experimental investigations shows that half-round scallops have the best fatigue strength under axial loading. (Fricke & Paetzold, 1995, p. 427.)

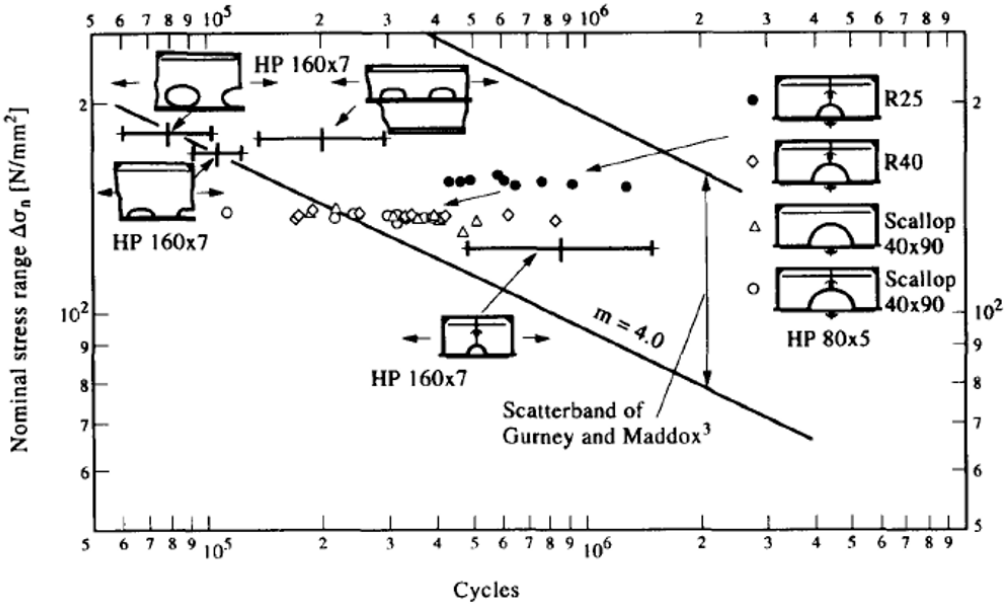

Figure 18. Fatigue test results for axial loaded scallops (Fricke & Paetzold, 1995, p. 427).

The difference in fatigue strength between rolled cross sections with cope holes and welded cross sections with cope holes is specified by American Institute of Steel Construction (2010). This is shown in table 5. Rolled cross sections have better fatigue strength than welded cross sections. C_f is a constant for fatigue category and F_{TH} is threshold allowable stress range, maximum stress range for infinite design life. (American Institute of Steel Construction, 2010, pp. 198–199.)

Table 5. Rolled vs. welded cross sections (modified from American Institute of Steel Construction, 2010, pp. 198–199).

Description		Stress category	Constant C_f	Threshold F_{TH} MPa
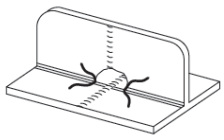	Rolled cross sections	*C*	44 x 10^8	69
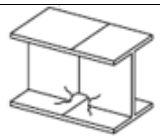	Welded cross sections	*D*	22 X 10^8	48
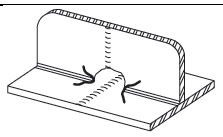				

3.3 Tensile stress at I-profile with brackets

Bramat, Gerbeaus and Vix (1973) made fatigue tests for specimens where brackets were welded to flanges and web. Tensile stress is acting on the directions of the arrows as shown in figure 19. Before types 2, 3, 4 and 6 were preferred but nowadays fatigue tests are verified those to have lower fatigue strength than types 1 and 5. Type 5 has the best fatigue strength with a value of over 163.7 MPa. Brackets with a 30 mm radius scallops (type 1) have fatigue strength of 131.4 MPa. (Bramat, Gerbeaus and Vix, 1972, pp. 129–130.)

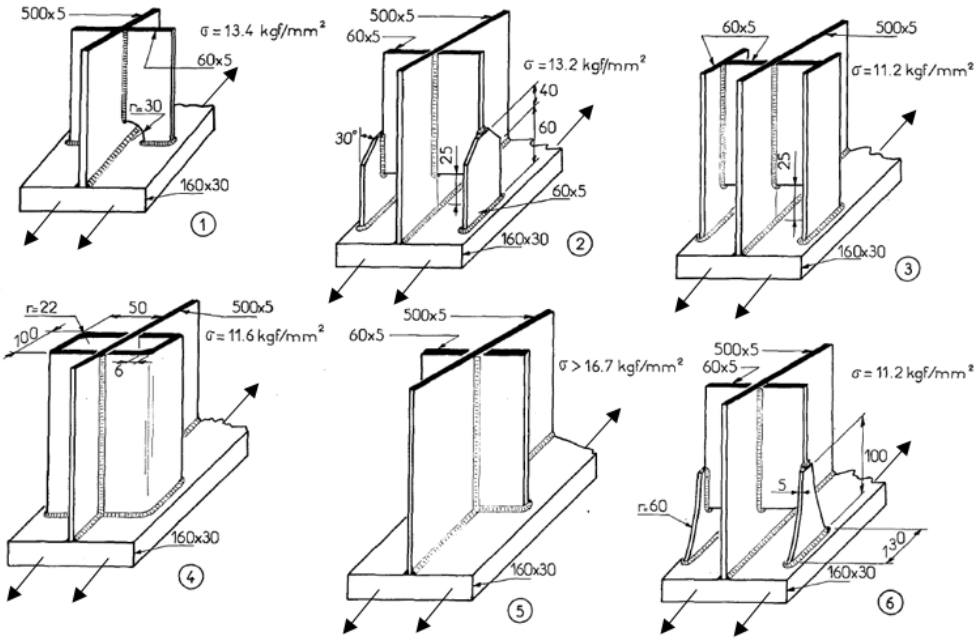

Figure 19. Tensile stress at I-profile with stiffeners (modified from Bramat, Gerbeaus & Vix, 1972, p.130).

3.4 Brittle fracture in highly constrained details with tensile stress

Mahmoud, Conner and Fisher (2005) have studied the effect of triaxial stresses in the girder's web. When the structure is highly constrained the yielding of the material is not possible and brittle facture can occur. Model of a bridge detail which is shown in figure 20 was studied without a web gap and with a web gap. Web gap was located at the corner of the toe of the vertical fillet weld and the toe of the gusset termination. Results showed that without a web gap high triaxial stresses will occur. There triaxial stresses can be avoided by using a small web gap. For example, 6.5 mm web gap would result smaller stresses. (Mahmoud, Connor & Fisher, 2005, pp. 385–392.)

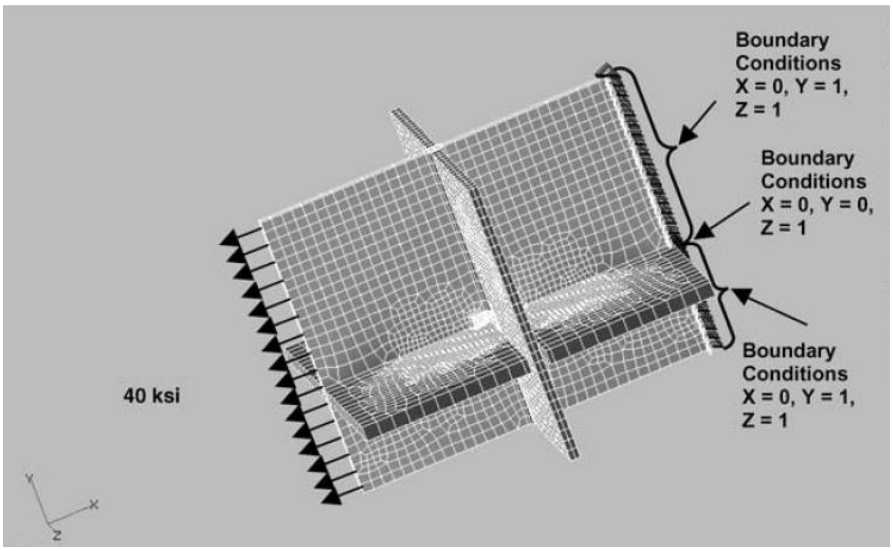

Figure 20. Model to study highly constrained detail (Mahmoud, Connor & Fisher, 2005, p. 386).

3.5 Bending of I-beams with vertical stiffeners

Many studies have been performed to investigate the fatigue strength of I-beams with vertical stiffeners. Six different studies are discussed in this chapter. Glinka and Krzyżecki (1981) studied details shown in figure 21. The fatigue tests were performed as four point bending tests using both constant and variable amplitude loadings. Results showed that using a scallop in the stiffener has no effect on the fatigue strength of this type of structures. (Glinka & Krzyżecki, 1981, pp. 36–48.)

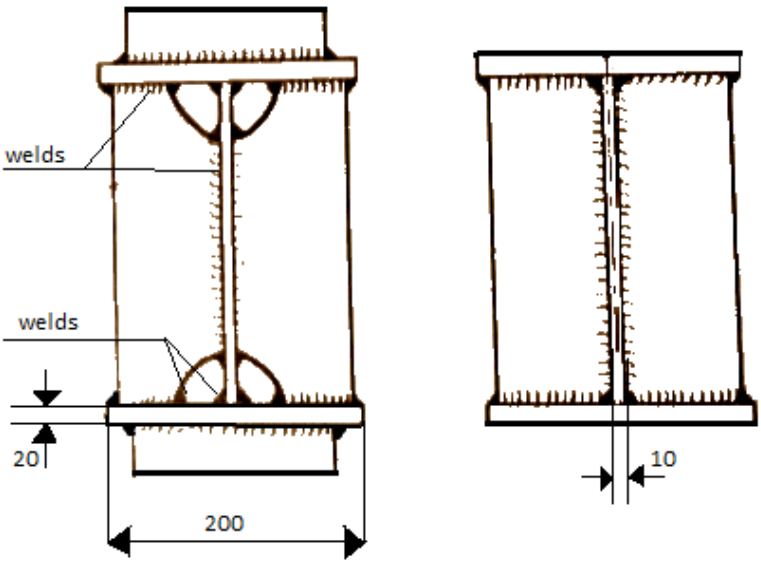

Figure 21. I-beam specimens (modified from Glinka & Krzyżecki, 1981, p. 36).

DeLong and Bowman (2010) made fatigue tests for I-beams with vertical stiffeners with gaps larger than 6.35 mm and without gaps, which are shown in figure 22. Fatigue tests were performed with a three point bending machine shown in figure 23. The results showed that there is no significant difference in fatigue strength between specimens with gaps and specimens without gaps. It is stated that to avoid the risk of brittle fracture, web gaps smaller than 6.35 mm should not be used. DeLong and Bowman also made tests with specimens where vertical stiffeners are intersecting with horizontal stiffeners. Those tests showed that fatigue cracks formed earlier when small gaps (less than 6.35 mm) were used than when large gaps (25.4 mm) were used. (DeLong & Bowman, 2010, pp. 46–47, 52–59, 151–153.)

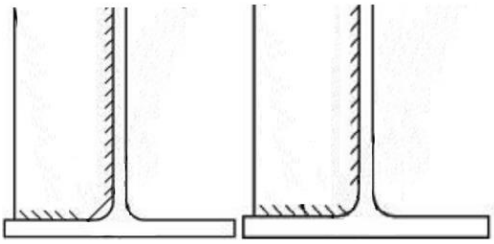

Figure 22. Stiffeners with and without a gap (modified from DeLong & Bowman, 2010, p. 54).

Figure 23. Three point bending procedure (DeLong & Bowman, 2010, p. 59).

Miki and Tateishi (1997) studied the effect of scallops and scallop size to the fatigue strength with a three point bending machine. Specimen 2A has boxing welds at end points of scallops and specimen 2B does not. Specimen 2A has six varieties of scallops of radii of 25, 30, 35, 40, 45 and 50 mm. First three are set to the tension side of the structure. Specimen 2B has the same scallop sizes, but it is turned up-side-down because it was found that increasing the scallop radius degreases the fatigue strength. Test specimens and cracking points are shown in figures 24 and 25. (Miki & Tateishi, 1997, p. 445.)

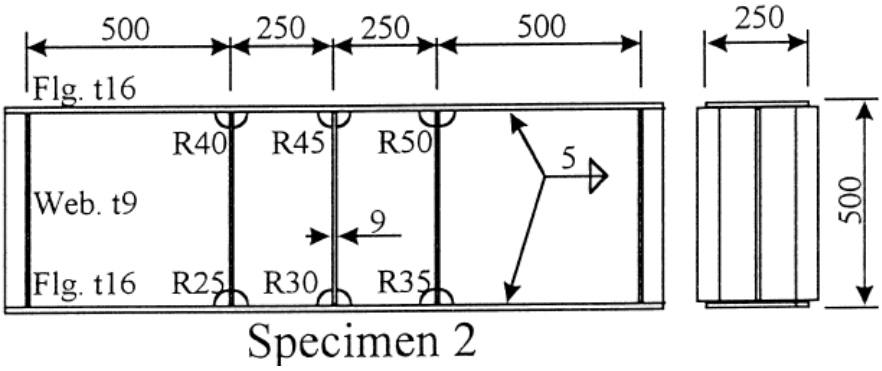

Figure 24. Specimen 2 at A position (Miki & Tateishi, 1997, p. 446).

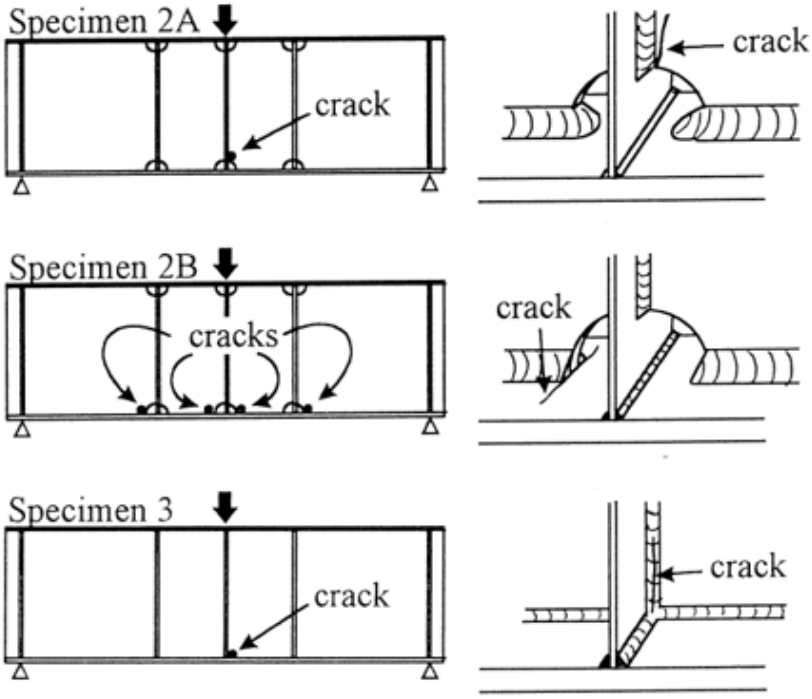

Figure 25. Test specimens with crack locations (Miki & Tateishi, 1997, p. 447).

Fatigue tests showed that when nominal bending stress is used, a scallop detail has lower fatigue life than a detail without a scallop, this is seen from figure 26 (Miki & Tateishi, 1997, p. 447). When hot spot bending stress is analysed, the fatigue lives of details with scallops increases and overtakes the fatigue lives of details without scallops, this is seen from figure 27 (Miki &Tateishi, 1997, p. 455). In this case nominal stress gives more reliable results than hot stop stress method. The problem with hot spot method is that scallops cause major, even oversized, hot spots. ENS method should be used to get more precise results.

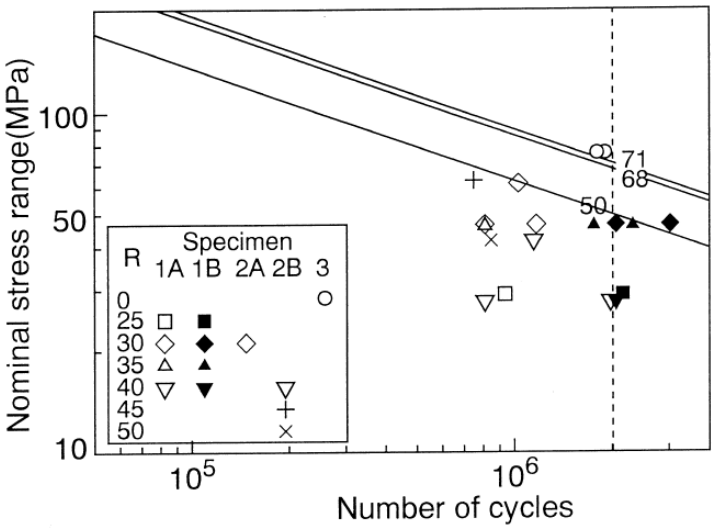

Figure 26. Nominal fatigue life when crack length is 20 mm (Miki & Tateishi, 1997, p. 447).

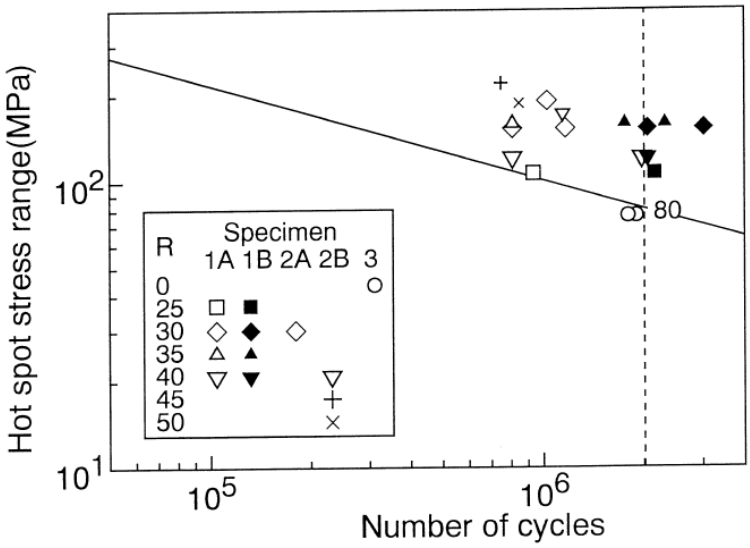

Figure 27. Hot spot fatigue life when crack length is 20 mm (Miki & Tateishi, 1997, p. 455).

The stress concentration inside a scallop becomes smaller as the size of the scallop is degreased, hence it is recommended to use a small scallop radius. The shear force is a reason for high local stresses at scallops thus the influence of shear force should be considered. (Miki & Tateishi, 1997, p. 454.)

Sakano et al. (1992) performed fatigue tests for vertical stiffeners with and without scallops at the University of Kansai. The fatigue testing was performed with thee point bending machine. (Sakano et al., 1992, p. 152.) The specimens used in fatigue tests are shown in figure 28 (Sakano et al., 1992, p. 150). The fatigue limits of details 1 and 2 are 85 MPa, detail 4 have a fatigue limit of 65 MPa and tests for detail 3 gave a fatigue limit of over 100 MPa. Tests showed that detail 3 is superior and the detail with a scallop is better than the detail without a scallop. (Sakano et al., 1992, pp. 159–160.) Later FEM analyse by Sakano et al. (1993) showed that intersecting welds cause higher stress concentrations than details 1, 2 and 3. Only a few tests were made and fatigue lives of every specimen were still above Japanese Society of Steel Construction's (JSSC) design life category *E* (Sakano et al., 1992, pp. 160). Only four tests were made and one test had to be retested because the used force was not enough to produce fatigue failure. Test results are shown in table 6 where ΔP is given load range, S_r is nominal bending tensile stress range, N_c is a number of cycles to crack detection and N_f is a number of cycles to failure. BH1 and BH2 represents initiation of cracks from blow holes occurring in the weld between web and flange. (Sakano et al., 1992, p. 155.)

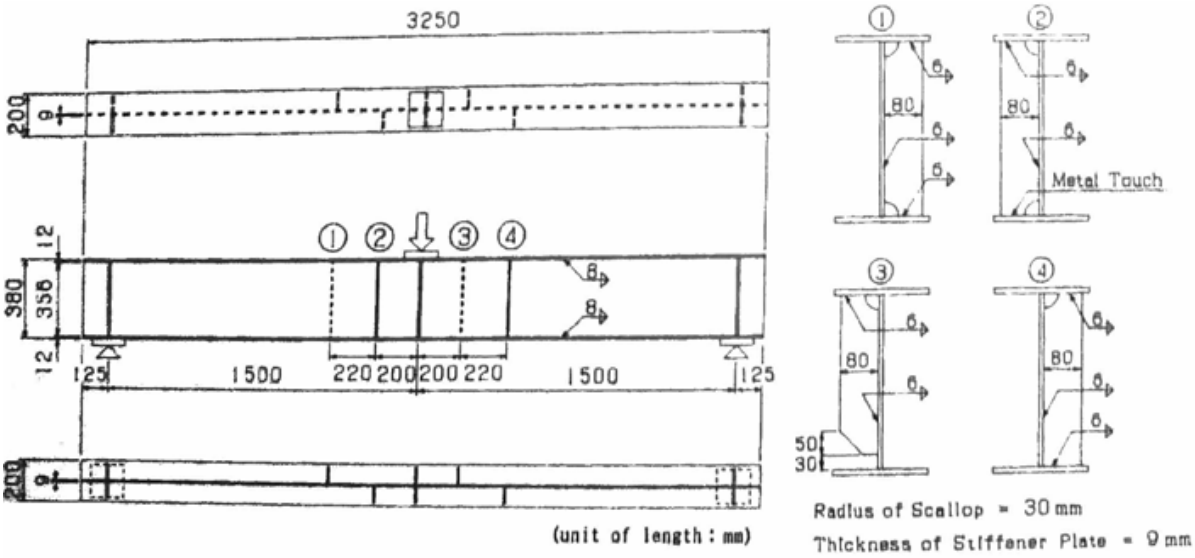

Figure 28. Plate girder specimen with vertical stiffeners (Sakano et al., 1992, p. 150).

Table 6. Fatigue test results (modified from Sakano et al., 1992, p. 155).

Specimen	ΔP [kN]	Detail	S_r [MPa]	N_c x 10^4 [cycles]	N_f x 10^4 [cycles]
No. 1	216	1	84	240	335
		2	103	80	294
		3	102	> 581	> 581
		4	98	120	256
No. 2	176	1	82	> 678	> 678
		2	85	> 678	> 678
		3	85	> 678	> 678
		4	85	493	678
		BH1	118	493	493
		BH2	94	593	678
No. 3	137	1	65	> 1047	> 1047
		2	65	> 1047	> 1047
		3	65	> 1047	> 1047
		4	65	> 1047	> 1047
No 3. (retest)	196	1	93	> 661	> 661
		2	95	661	661
		3	96	> 661	> 661
		4	95	329	329

Bridge standards and procedure manual by British Columbia Ministry of Transportation (2007) shows the design instruction for cutting out the corner of the vertical stiffener of an I-beam in figure 29 which is based on a research by Fisher (1977). The cut out should be 4 to 6 times the thickness of girder web but not less than 50 mm. These cut outs prevent the possibility of intersecting welds, allow drainage, ease the welding procedure and reduce the high weld shrinkage strains caused by small cut outs. (British Columbia Ministry of Transportation, 2007, section 10, pp. 8–9.)

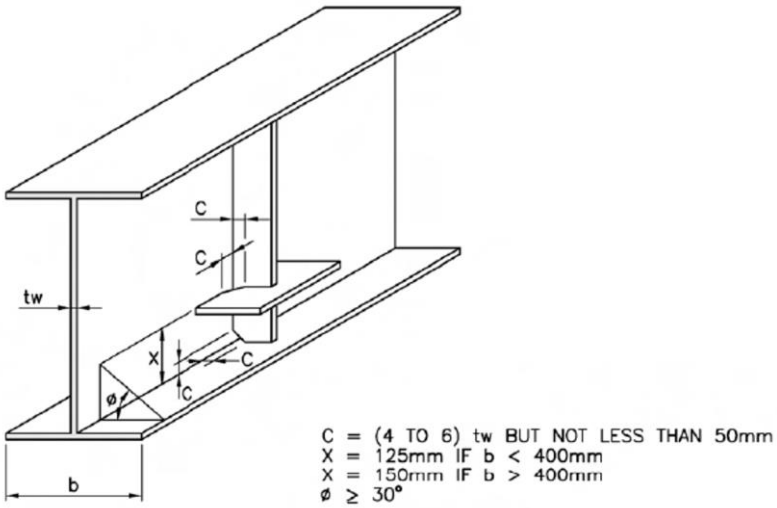

Figure 29. Cut out in stiffeners and location of gusset plates (British Columbia Ministry of Transportation, 2007, section 10, p. 8).

Jordan and Krumpen (1990) give doubtful proposition for better construction for detail shown in figure 30. This thesis work does not suggest to use this kind of modification because welding additional plate, like in the figure 30, to the structure is a stress riser which degreases fatigue strength of the detail.

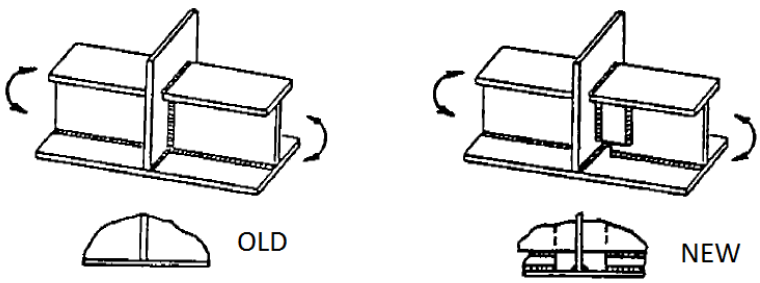

Figure 30. Local fatigue detail in ship structures (Jordan & Krumpen, 1990, section 2 p. 10).

DeLong and Bowman (2010) have gathered together results from four different studies into one graph shown in figure 31. VS-1, VS-2 and VS-3 specimens are shown in figure 22. Specimens by Sakano et al. (1992) are shown in figure 28. It is seen that most of the measured results are close to design life category C which equals 90 MPa as shown in table 1. There is no significant difference in fatigue strength between specimens with a gap and specimens without a gap. (DeLong & Bowman, 2010, p. 160.)

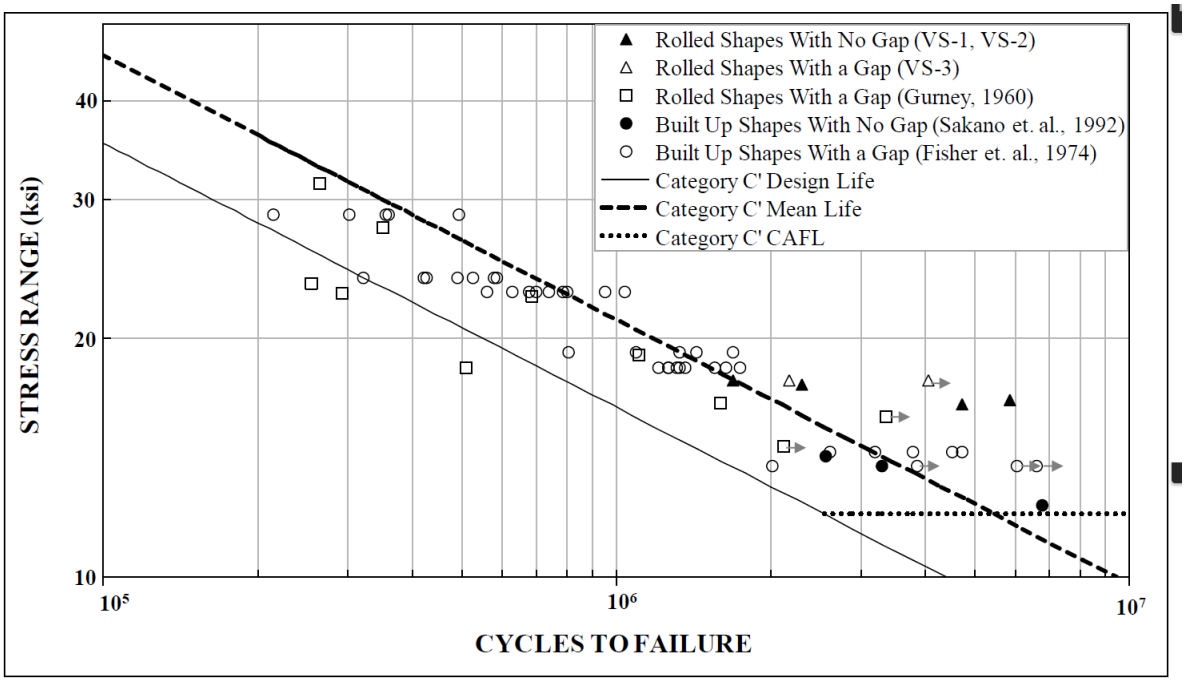

Figure 31. Combined test results (DeLong & Bowman, 2010, p. 160).

3.6 Bending of I-beams without stiffeners

Miki and Tateishi (1997) also made experiments with I-beams without stiffeners to study the effect of scallop size to fatigue strength. Specimen 1A has boxing welds at end points of scallops and specimen 1B does not. Specimens 1A and 1B have four varieties of scallops of radii of 25, 30, 35 and 40 mm. One of each are set on tension side and one of each is set to the compression side of the structure. Test specimens and cracking points are shown in figures 32 and 33. (Miki & Tateishi, 1997, p. 445.)

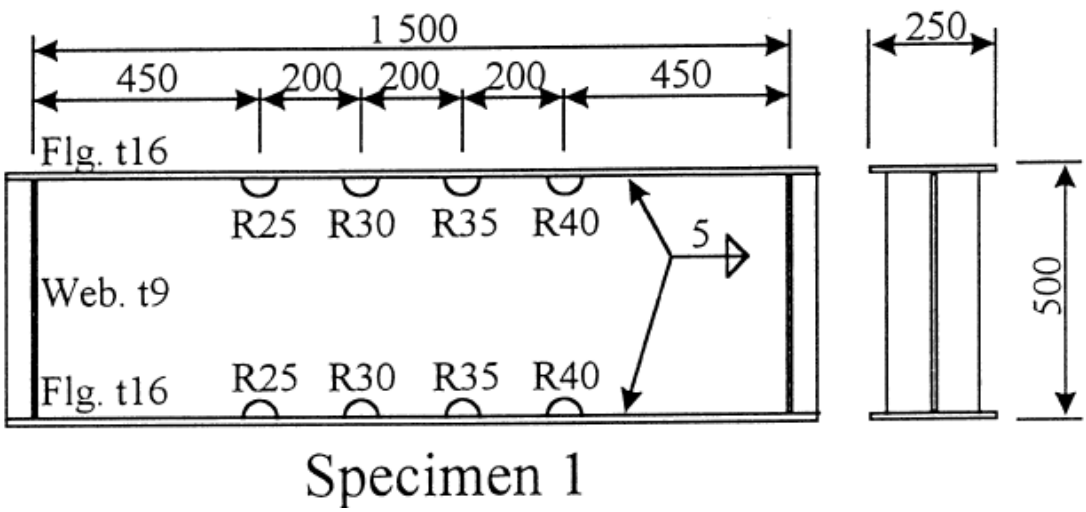

Figure 32. Specimen 1 (Miki & Tateishi, 1997, p. 446).

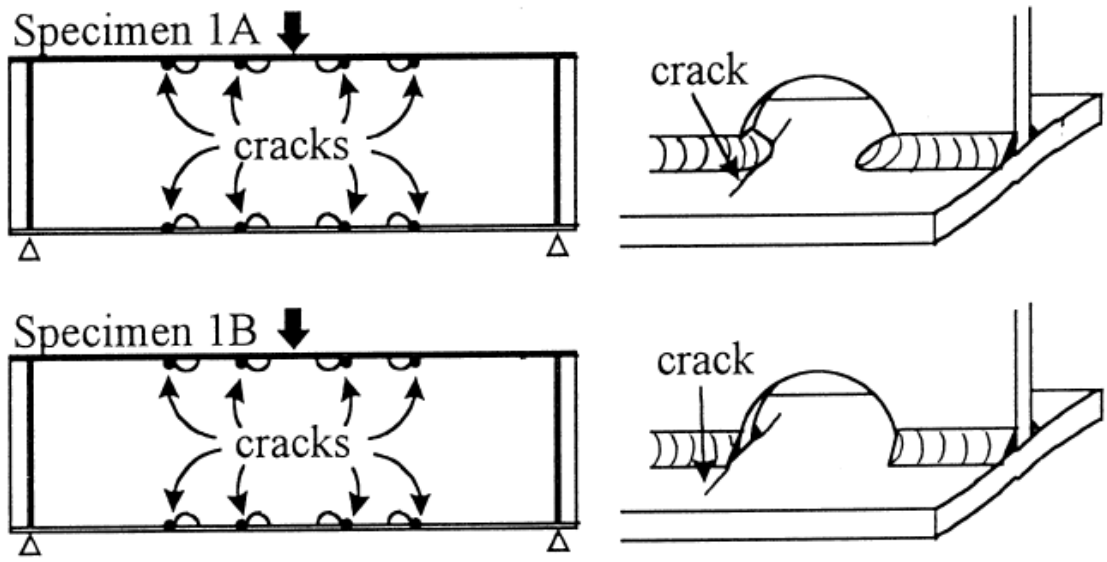

Figure 33. Test specimens 1A and 1B with crack locations (Miki & Tateishi, 1997, p. 447).

Test results showed that the stress concentration inside a scallop degreases as the ratio of scallop radius to flange thickness degreases. This means that scallops with small radii should be used. The shear force is a reason for high local stresses at scallops thus the influence of shear force should be considered. Measured results show that using a boxing weld at the end of a scallop as in figure 33, has higher local stress than a scallop without a boxing weld. Figure 34 shows arrangements of strain gauges. Miki and Tateishi defined (1997) an equation for stress concentration factors of scallops

$$SCF = 1 + 1.2\left(\frac{t_f}{t_w}\right)^{-0.54}\left(\frac{R}{t_f}\right)^{0.21} + 2.6\left(\frac{t_f}{t_w}\right)^{0.23}\left(\frac{R}{t_f}\right)^{0.54}\left(\frac{Vb}{M}\right), \qquad (11)$$

, where t_f is flange thickness, t_w is web thickness, R is the radius of scallop, Vb is shear force by flange width and M is bending moment. It is seen that increasing the ratios of VB/M, R/t_f and t_f/t_w increases SCFs degreasing fatigue lives of specimens. (Miki & Tateishi, 1997, pp. 453–454.)

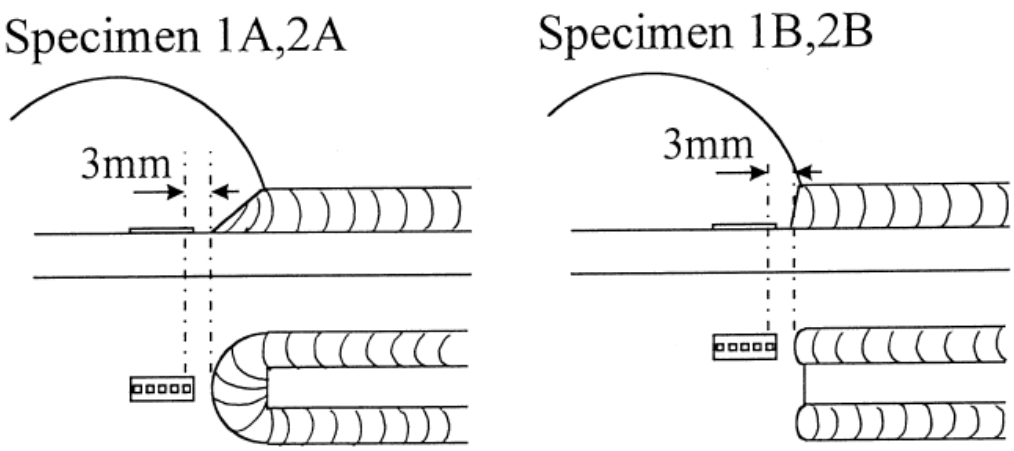

Figure 34. Arrangement of strain gauges (Miki & Tateishi, 1997, pp. 447).

Heshmati and Al-Emrani (2012) studied the influence of scallop shapes to fatigue strength. FEM-models were used to analyse the four point bending tests with circular, triangular, semi-elliptical and elliptical scallops. Investigated models are shown in figure 35, where the used dimensions are in mm. (Heshmati & Al-Emrani, 2012, p. 11.)

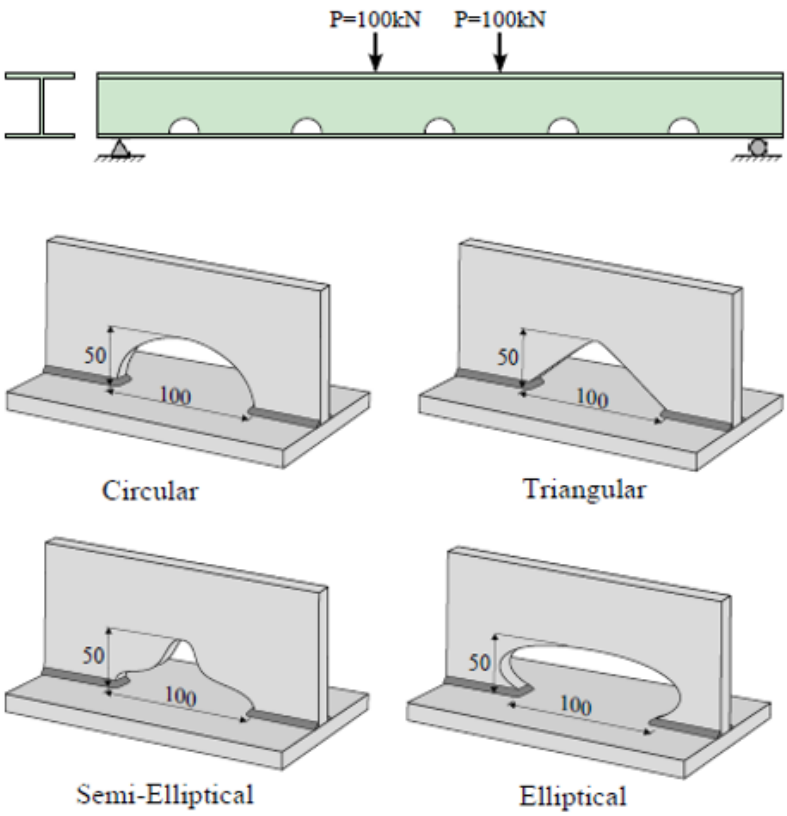

Figure 35. Four point bending test with four different scallop shapes (Heshmati & Al-Emrani, 2012, p. 11).

Five scallops were used in one model. The scallop at the middle of the structure experienced only bending stresses. When the scallop is closer the support, the ratio of shear stress to bending stress is higher than in the middle where shear stress is close to the zero. Table 7 presents the SCF for each scallop shape and compares the fatigue strengths of different shapes using the fatigue strength of circular scallop as a baseline. The elliptical shape is the most unfavorable and the triangular shape has the highest fatigue strength. It should be noted that only few analyses were made, it's not sure if using triangular shaped scallops would improve the fatigue life of the specimen. (Heshmati & Al-Emrani, 2012, pp. 11–13.)

Table 7. Fatigue tests for different scallop shapes (modified from Heshmati and Al-Emrani, 2012, p. 13).

Scallop shape	Hot Spot SCF			Variation in fatigue strength		
	First hole	Second hole	Center hole	First hole	Second hole	Center hole
Circular	3.24	2.42	1.79	-	-	-
Triangular	3.15	2.36	1.63	9 %	8.1 %	31.2 %
Semi-elliptical	3.43	2.56	1.73	-15.4 %	-15.2 %	11.2 %
Elliptical	3.42	2.58	1.89	-14.5 %	-17.3 %	-14.6 %

Fisher and Stallmeyer (1958) made fatigue tests with I-beams in the 1950's. Three point bending fatigue tests were made to determine the difference in fatigue life between four different cases where two I-beams were weld to one longer beam. In type A flanges and web were welded at the same plane and scallops were used. In type B scallops and welds in the web and flanges were staggered. Type D is the same as type A without scallops and type E is the same as type B without scallops. Scallops with 1 inch radius were used. Test specimens are shown in figure 36. (Fisher & Stallmeyer, 1958, pp. 7–8.)

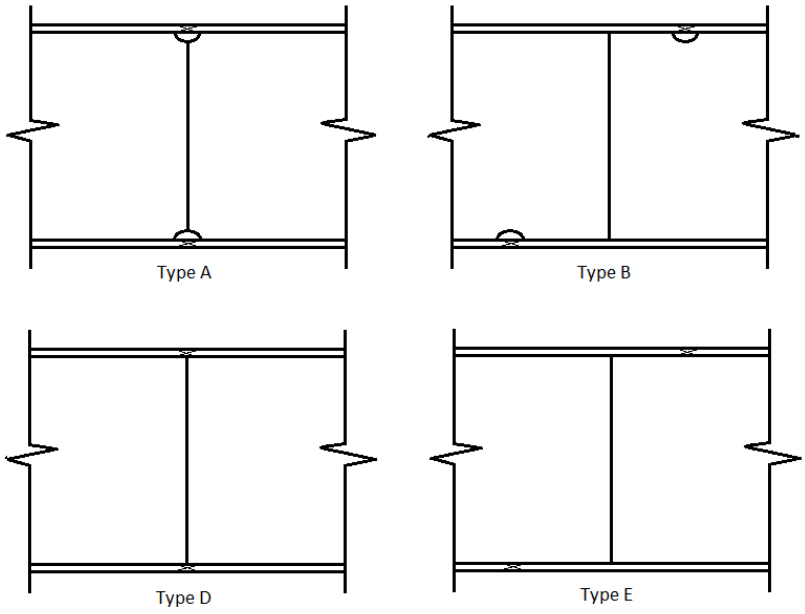

Figure 36. Spliced I-beams.

Altogether ten specimens of each type A and E were tested and eight specimens of type B and D, respectively (Fisher & Stallmeyer, 1958, pp. 60–61). Cycles to failure were plotted to one graph which is shown in figure 37. At long endurances Type E has the best fatigue strength followed by type B. Type D has the second lowest fatigue strength and type A has the poorest fatigue strength. This means that Specimens having the welds in the flanges and beam staggered have better fatigue strength than specimens having the welds in the same plane. Fatigue curves were extrapolated to get fatigue strength when fatigue failure occurs at 10^5 cycles. Interesting is that in that case the results are opposite. In general, the use of scallops reduces the fatigue strength of the spliced I-beam. Fatigue strength at 10^5 cycles and 2×10^6 cycles are presented in table 8. (Fisher & Stallmeyer, 1958, p. 44.)

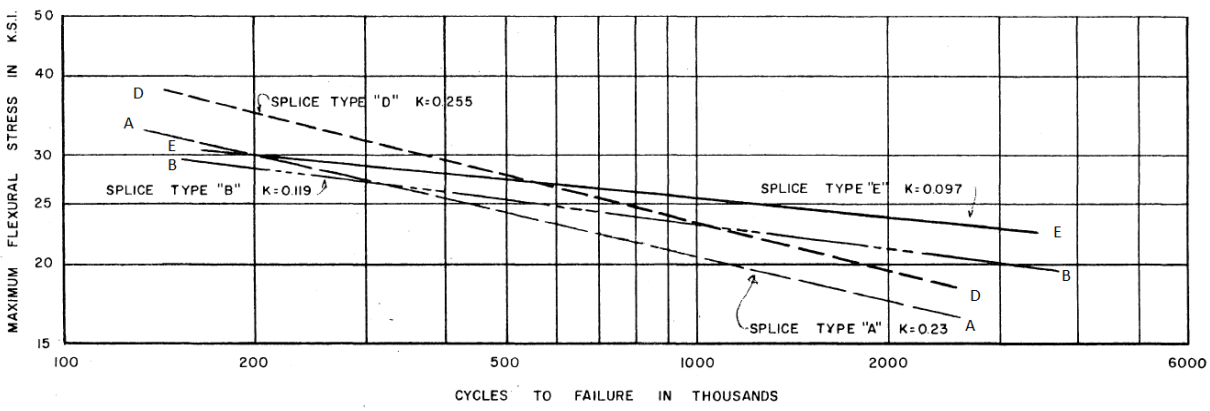

Figure 37. Fatigue lives of spliced I-beams (Fisher & Stallmeyer, 1958, p. 44).

Table 8. Fatigue strengths of spliced beams (modified from Gurney, 1972, p. 163).

type	Detail of splice	Fatigue strength [N/mm^2]	
		10^5 cycles	2 x 10^6 cycles
A	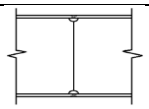	234	120
B	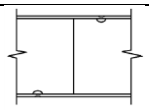	212	145
C	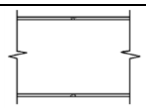	-	178
D	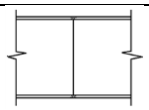	276	134
E	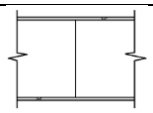	221	159
F	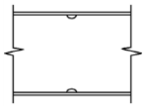	-	159

Details C and F were also tested. Details F are not splices at all but were tested to clarify the effect of scallops. (Gurney, 1979, p. 163).

Detail categories by National Board of Housing, Building and Planning (2003) show different results for spliced details. Figure 38 shows that same fatigue strength is given to splices where welds are staggered and to splices where welds are at the same plane. Also same fatigue strength, when welding classes are WC and WB, is given to splices where welds are on the same plane and scallops are used. (National Board of Housing, Building and Planning, 2003, p. 167.) Welding classes are corresponding on SS-ISO 5817 (National Board of Housing, Building and Planning, 2003, p. 109). These values are guidelines for designers which usually are quite conservative because those are set based on the worst-case scenario.

No	Type of connection	Welding Class	$C_{\parallel}$	$C_{\perp}$	Remarks
18	Butt weld at girder splice 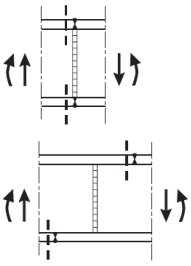	WC WB WA	– – –	63 80 100	Butt weld with sealing run on root [1]. Rolled or welded girder. However, the *C* value for WA applies only for welded girders. In a welded girder, other sections should also be checked, see e.g. No. 30.
19	Butt weld at girder splice (rolled girder) 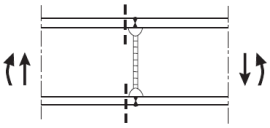	WC WB WA	– – –	63 80 90	Root with sealing run [1]. Drilled or ground hole. For WA, edge of hole must also be dressed (see No. 08) (See Nos. 25 and 33 for welded girder.)

Figure 38. Detail categories for Girder splices (National Board of Housing, Building and Planning, 2003, p. 167).

Radaj (1990) represents structural stress concentration factors for I-beams with different shaped scallops. Loading conditions, SCF values and crack points are shown in figure 39, where can be seen that the I-beam is subjected to bending (Radaj, 1990, p. 134). These results are correct but the loading conditions are incorrectly referred because the original loading conditions for these SCF values also include tensile stress component. This is not a major mistake because shear force is not affecting to either of cases. Results are based on the paper from Matoba et al. (1983). The I-beam is subjected to combined loading, which is seen in figure 40 (Matoba et al., 1983, p. 134).

134 **Design and analysis of fatigue resistant welded structures**

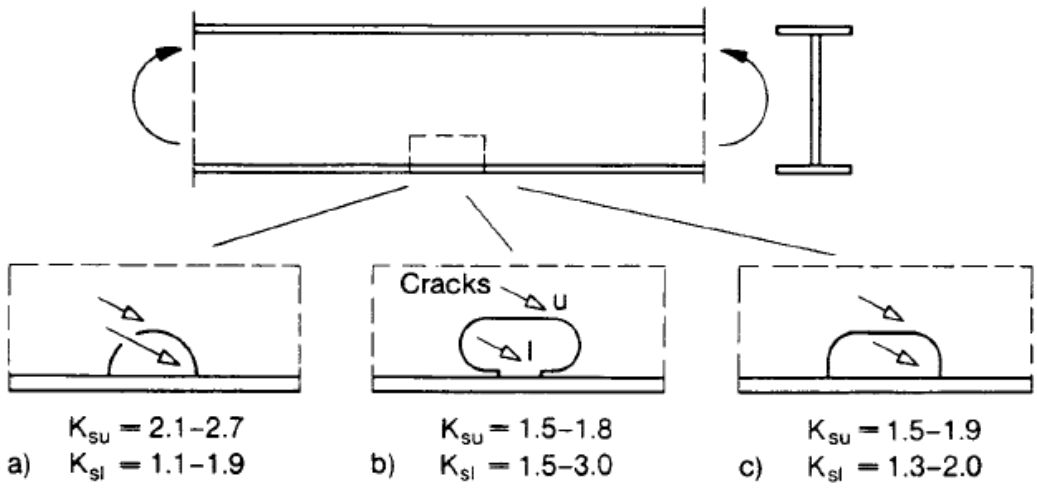

118 Weld end cope holes, design variants (a) to (c), structural stress concentration factors, K_{sl}, for upper (index u) and lower (index l) notch, after Matoba *et al.*[91]

Figure 39. Stress concentration factors for different scallop shapes with incorrect loading condition (Radaj, 1990, p. 134).

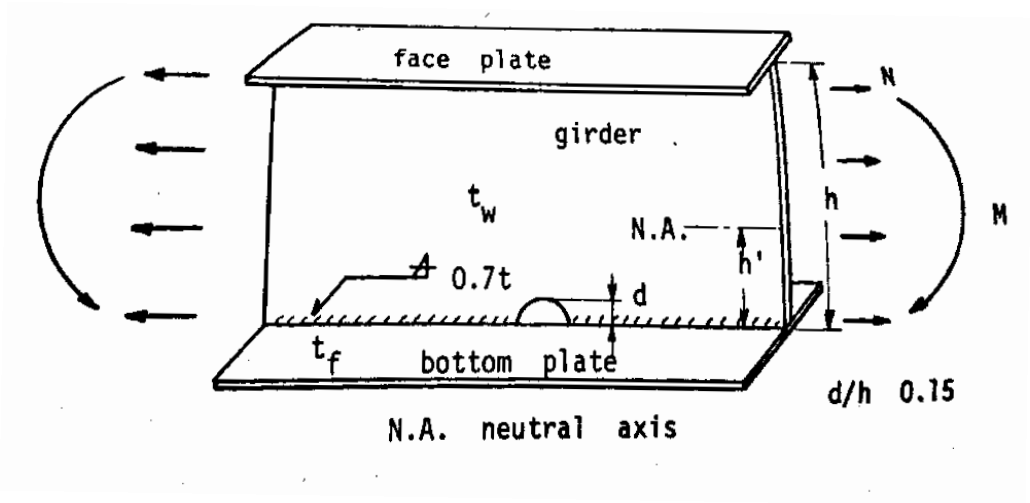

Figure 40. Original loading conditions for SCF tests by Matoba et al. (1983, p. 29).

SCF values are dependent on the ratio of flange thickness to web thickness and also on the shapes of the scallops. SCF curves for three different shaped scallops are shown in figure 41. For all of the three different scallop shapes, the SCF degreases when the ratio of flange and web thickness increases. SCF for half-round scallops, which are recommended to use, also degreases when the ratio of scallop radius *d* and the length of the scallop *2c* degreases.

This means that a segment of full half-round scallop has better fatigue strength than a full half-round scallop. (Matoba et al., 1983, p. 29.) It should be noted that the results are without shear stress which would affect a lot to the results.

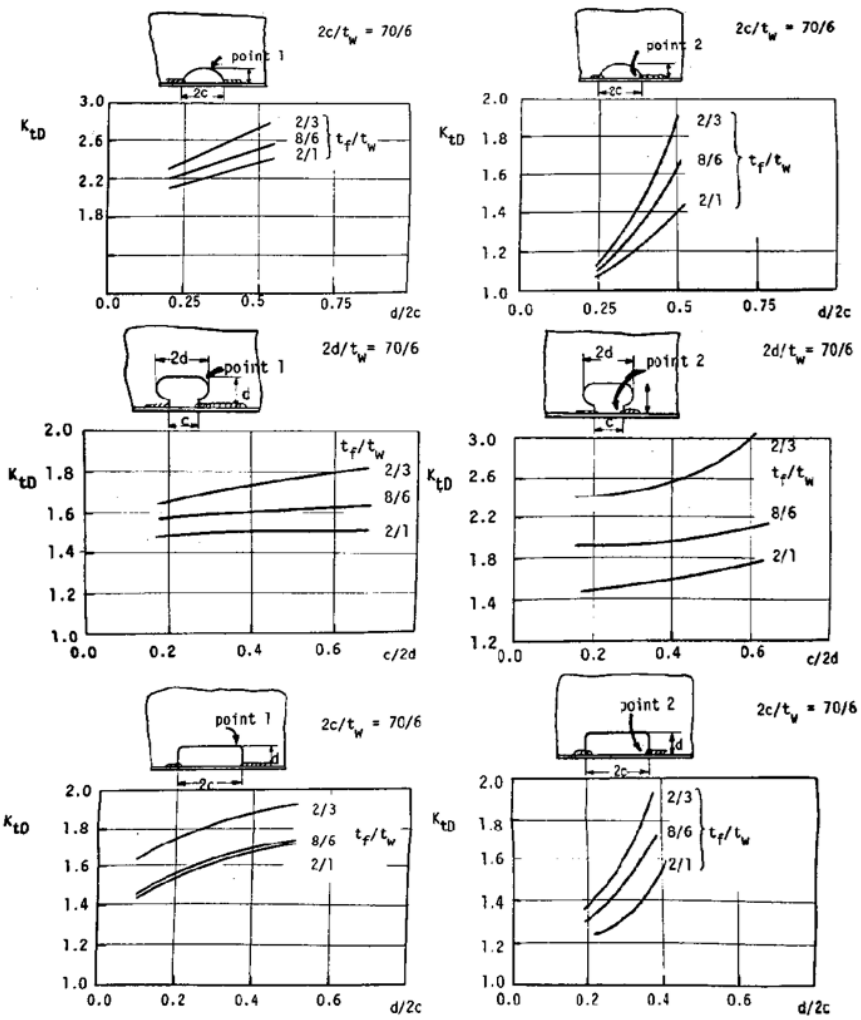

Figure 41. SCF values for different scallop shapes without shear stress (Matoba et al., 1983, p. 29).

Fricke and Paetzold (1995) computed hot spot and notch stresses for rectangular and elliptical scallops exposed to different loading conditions. Dimensions of elliptical and rectangular scallops are shown in figure 42. Dimension *b'* from the figure 42 is calculated by using dimensions *b* and *d* from figure 42. (Fricke & Paetzold, 1995, p. 433).

$$b' = (8 + b/d)/18 \qquad (12)$$

The results showed that elliptical scallops are the best shape under combined stress especially when shear stress is acting to the web. Local stresses at different locations in the longitudinal in the bottom structure of tanker are shown in figure 43 where *x* is the distance in longitudinal. (Fricke & Paetzold, 1995, pp. 441–443.) Results from Matoba et al. (1983) shows that rectangular scallops have better fatigue strength than elliptical. When shear stress is affecting to the rectangular scallop, structure bends between points a and b and the slope is zero at points a and b. In elliptical scallop case the bending moment is not zero at points a and b because bending starts before point a and stops after point b, but the vertical displacement is equal as in rectangular case making the bending to be smoother in elliptical case than in rectangular case. This is shown in figure 44 where red line represent the displacement of the flange. When structural stress method is used elliptical scallops have better fatigue strength than rectangular scallops. Notch stress method may give different results. When tensile stress is affecting to the rectangular scallop specimen, bending is zero at vertical edges. When tensile stress is affecting to the elliptical scallop, vertical edges bend outside.

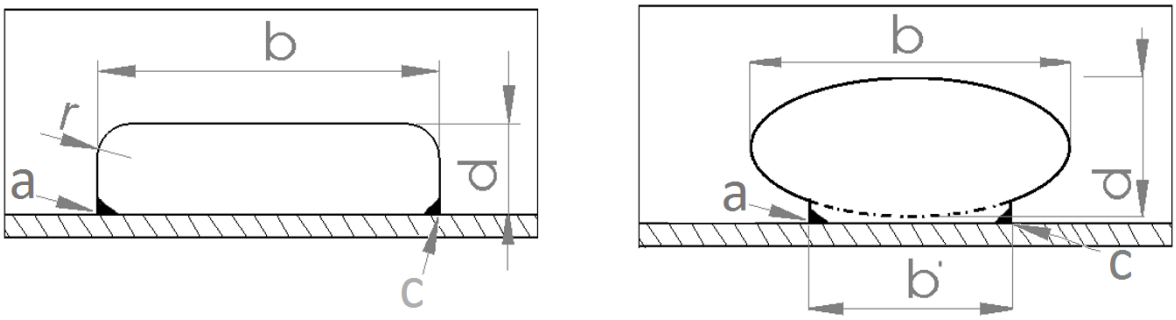

Figure 42. Rectangular and elliptical scallops (modified from Fricke and Paetzold, 1995, p. 433).

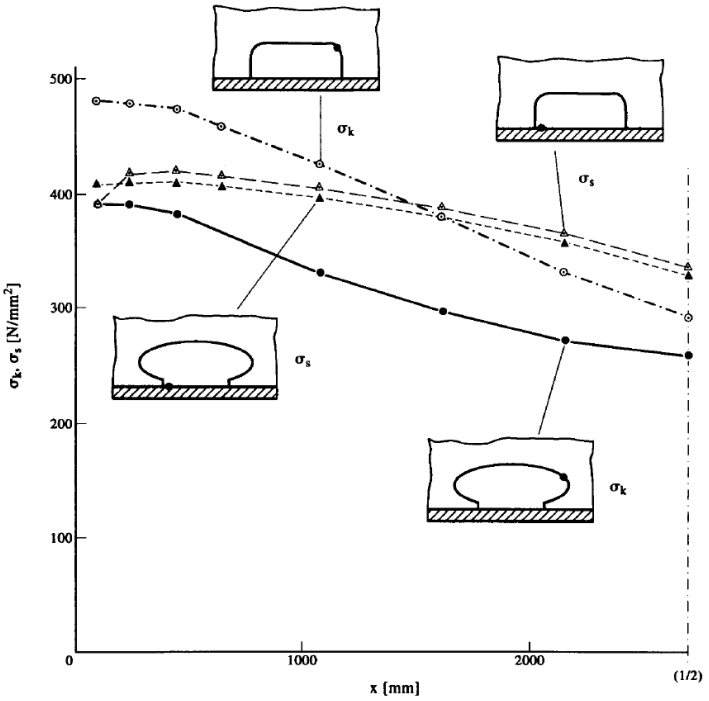

Figure 43. Local stresses for scallops at different locations in longitudinal in the bottom structure of tanker (Fricke and Paetzold, 1995, p. 441).

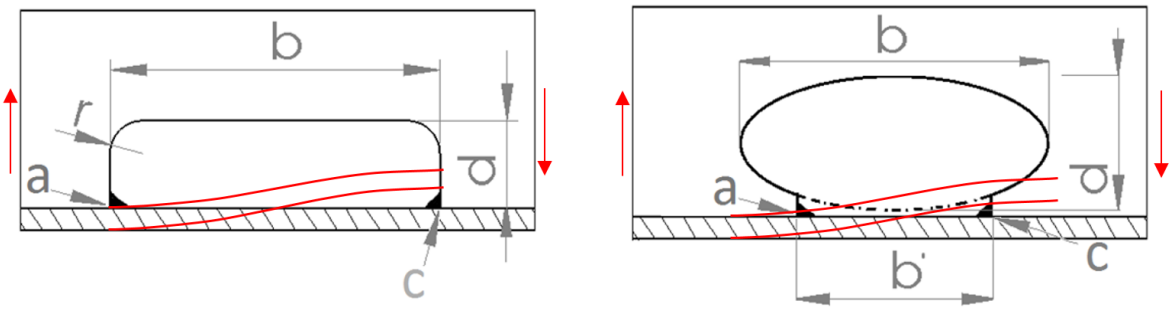

Figure 44. Deformations of rectangular and elliptical scallops affected to shear stress.

3.7 Design for manufacturing and assembly (DFMA)

Finnish guidance from InfraRYL 2006 (2008) suggests cutting the inside corners of web stiffeners to ease the welding and surface treatment processes. Figure 45 shows the preferred scallop shape and dimensions. (InfraRYL 2006, 2008, p. 147.)

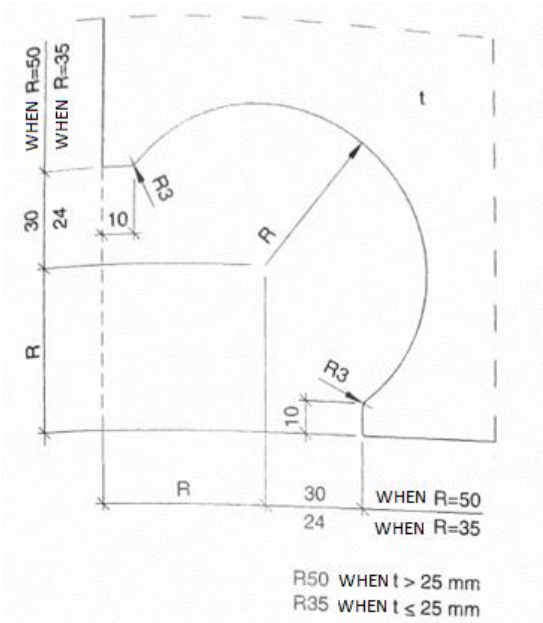

Figure 45. Scallop shape to help manufacturing (modified from InfraRYL 2006, 2008, p. 147).

3.8 Other design rules

Many books and research papers give general design rules for scallops. This chapter gathers some of those together.

American Bureau of Shipping (2007) gives design rules for the distance between welds when scallops are over weld seams. The illustrative specimen is shown in figure 46. For significant member, the distance from the toe of the fillet weld to the toe of the butt weld should not be less than 5 mm. (American Bureau of Shipping, 2007, p.23.)

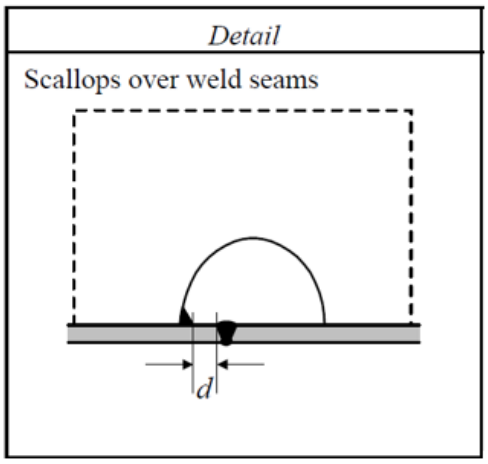

Figure 46. Distance between welds (American Bureau of Shipping, 2007, p.23).

Paper from DNV (2016) (Det Norske Veritas) states that when intermittent welds are allowed to be used, scallops should be used in tanks where are liquids like fresh water and cargo oil. Chain and staggered welds can be used in dry places or tanks where are only fuel oil. Figure 47 shows some design rules for using scallops. Scallop radius should not be less than 25 mm and the maximum length is 150 mm. The depth of the notch should be 0.25 times the height of the web but not greater than 75 mm. (DNV, 2016, p. 137.)

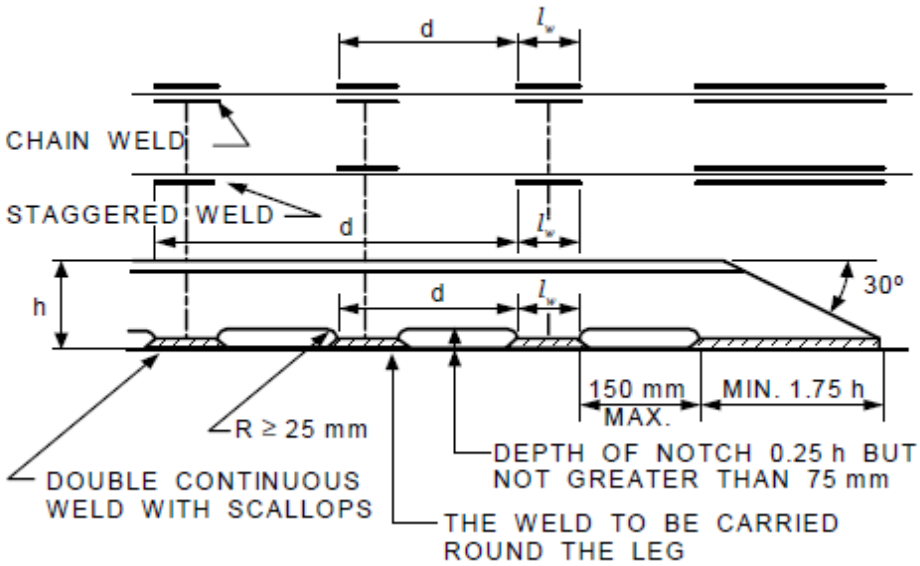

Figure 47. Other design rules by DNV (DNV, 2016, p. 138).

Okumoto et al. (2009) guide engineers to avoid using scallops as much as possible. Studies show that intersecting welding lines do not cause loss of fatigue strength or decay the structure. Scallops are stress raisers for the structure and take a lot of time to manufacture. When scallops are not used designers should pay attention to welding quality to make a smooth surface. If deleted scallops were worked as air or drain holes, additional holes should be made to replace the scallops. Scallop should be used in the corner of a web plate of right angled triangle where the corner touches the fillet weld of a stiffener as shown in figure 48. (Okumoto et al., 2009, pp. 309–310.)

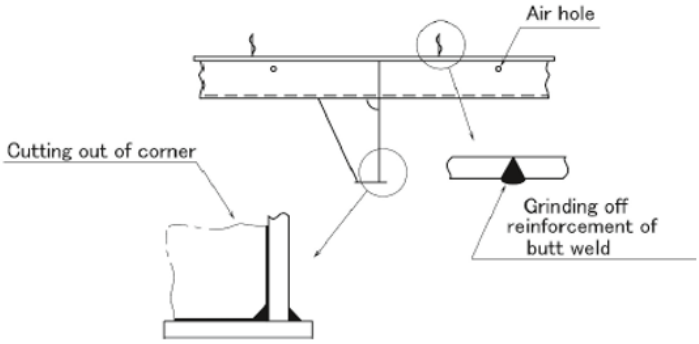

Figure 48. Deletion of scallop (Okumoto et al., 2009, p. 310).

Scallops are recommended to be cut ground back as shown in figure 49 (American Bureau of Shipping, 1995, p. 22). Other cases included in this thesis doesn't show similar recommendations. The welds at a distance of at least 75 mm from the scallop should be full penetrated (American Bureau of Shipping, 1995, p. 22).

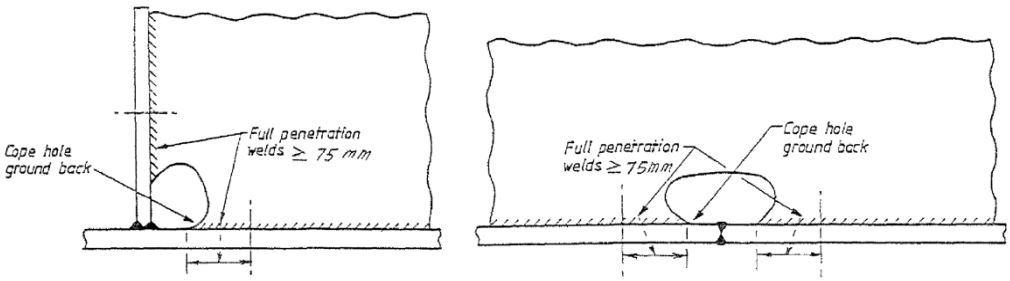

Figure 49. Design rules for details with scallops (American Bureau of Shipping, 1995, p. 22).

Scallop details can be strengthened by adding filler plate or fiber reinforced plastic strips, using full penetration welding and surface treatments like Tungsten inert gas (TIG) dressing, hammer peening or grinding. Improving the shape of scallop like increasing curvature ratios of scallop increase the fatigue strength of the detail. (Kühn et al., 2008, p. 69.)

Design instructions for ship structure details by Glenn et al. (1999) shows that increasing the fatigue strength of the detail increases manufacturing and maintenance costs. Figure 50 shows how fatigue strength of intersection of side shell longitudinal and transverse web frame stiffener can be increased. Adding soft toe and soft backing bracket increases fatigue

strength of the detail but also increases manufacturing and maintenance costs and makes inspection harder. Table 9 shows how this affects on design attributes of figure 50 details. (Glenn et al., 1999, p. B-11.)

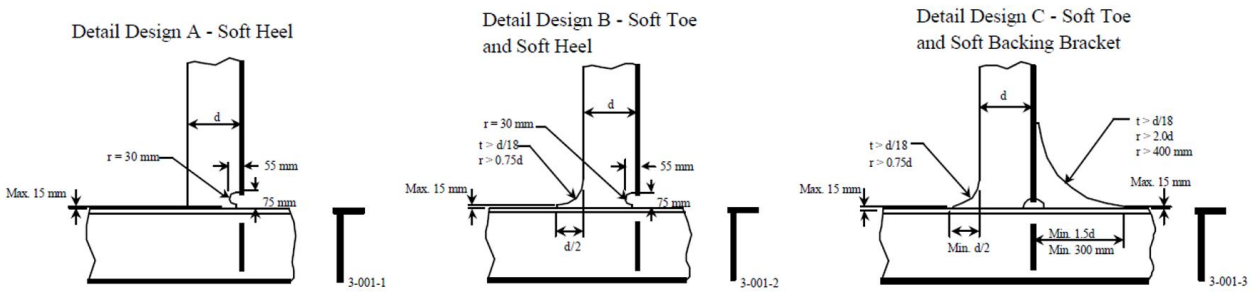

Figure 50. Increasing the fatigue strength of intersection of side shell longitudinal and transverse web frame (Glenn et al., 1999, p. B-11).

Table 9. Effect of increasing fatigue strength to other detail attributes (modified from Glenn et al., 1999, p. B-11).

Detail attributes	Detail rankings		
	A	B	C
Fatigue performance	3	2	1
Ease of inspection	1	1	2
Maintenance cost	1	2	3
Fabrication cost	1	2	3

3.9 Repairing cracks

When fatigue crack has been initiated at the fillet weld toe in the flange or web, repairing is possible to avoid failure. Adding filler plate or fiber reinforced plastic strips can be used to repair failure. Also stop holes can be used to retrofit holes. (Kühn et al., 2008, p. 69.) The diameter of the hole should be large enough to avoid the crack re-initiate. If required hole diameter is too large, then other alternatives should be considered like bolded splice repair. Retrofit holes may increase stress concentrations of nearby details by reducing the fatigue strength of details close to the hole, leading to fatigue failure. (DeLong & Bowman, 2010, pp. 174–175.) Caution should be used with these methods because cracks may reinitiate and another repair is needed.

3.10 Discussions of reliability of results from cases

When different cases and loading conditions are categorised, most of the results are consistent with each other. A couple of studies show results which are not reliable due to the results from other studies or false loading conditions. These unreliable results are neglected from guidance for using scallops which is the main result of this thesis. The oldest cases are investigated in the 1950's and in the 1960's when the quality of welding and materials were not as good as in nowadays. At that time, a lot of experimental laboratory measurements were done because it was not possible to use computers to calculate stresses using FEM. The high amount of used test specimens make these test results more reliable but it is still hard to tell how the use of old materials and welding techniques affect the results. Reliability of some results is hard to analyses because only results are shown and no explanation about determination methods or measures of specimens have been given. Other research cases and FEA is used to clarify the reliability of these kind of unclear cases. Different fatigue analysing methods may lead to incorrect conclusions. For example, hot spot method is may give results where scallops cause major, even oversized, hot spots. In this kind of cases ENS method should be used to get more precise results. In nominal stress method the effect of effective cross section should be considered when comparing different sized scallops. In large specimens the effect of effective cross section is different than in small specimens and can affect to conclusions.

4 LABORATORY MEASUREMENTS AND TESTS AT LUT

Fatigue tests for brackets with scallops (BWS) and without scallops (BNS) were performed at Lappeenranta University of Technology (LUT). Constant amplitude tensile fatigue tests were performed with a 400 kN fatigue-testing machine. Cyclic loading was applied at the frequency of 3.5 Hz to the specimens. One of the specimens is shown in figure 51. Three different scallop radii were used with filled welds. BNS specimens were welded in load carrying corner weld areas with different weld penetration ratios. Red arrow in figure 52 shows the load carrying corner area. Optim 960 QC steel was used in the specimens which chemical composition and mechanical properties are shown in table 10. Geometries of the brackets are shown in table 11.

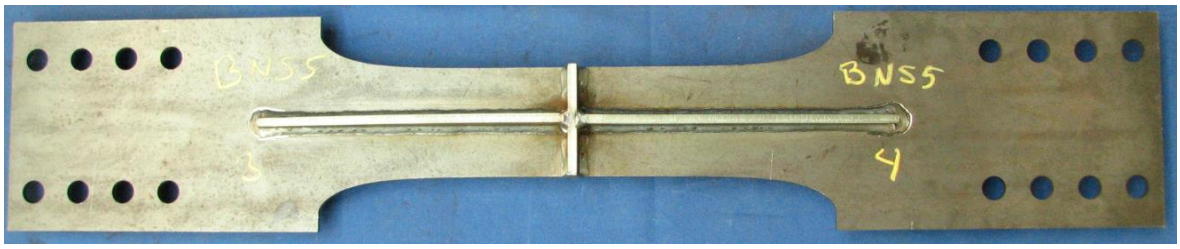

Figure 51. Test specimen.

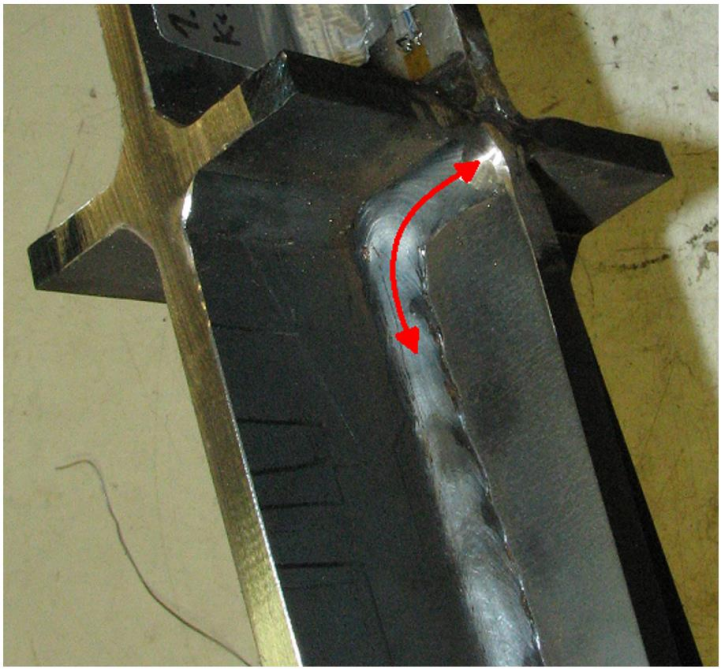

Figure 52. The load carrying corner area.

Table 10. Chemical composition and mechanical properties of Optim 960 QC steel (Rautaruukki Corporation, 2014, pp. 2–3).

	C	Si	Mn	P	S	Ti
Optim 960 QC	0.12	0.25	1.20	0.020	0.010	0.070
	0.2 % offset yield strength $R_{p0,2}$ [MPa] Minimum	Tensile strength R_m [MPa]	Elongation Minimum A %	Impact strength [J]		
				Temperature -40 °C	Temperature -20 °C	
	960	980–1250	7	27	40	

Table 11. Geometries of bracket specimens.

Number of specimen	t [mm]	a [mm]	Scallop radius r [mm]	$\frac{g}{t} = [\frac{mm}{mm}]$ Lack of weld penetration depths to thickness ratio	
1	8	4	20	-	Fillet weld with small penetration
2	8	4	35	-	Fillet weld with small penetration
3	8	4	50	-	Fillet weld with small penetration
4	8	4	-	1	Fillet weld, no penetration
5	8	4	-	0.75	Fillet weld, 25 % penetration
6	8	4	-	0.5	Fillet weld, 50 % penetration
7	8	4	-	0.25	Fillet weld, 75 % penetration
8	8	4	-	0	Fillet weld, full penetration

The main plate of the specimen was cut from 8 mm thick plate to designed measures shown in figure 53. Horizontal and vertical stiffeners which dimensions are shown in figures 54 to 57 are welded to the base plate with 4 mm design throat thickness. Welding specifications are shown in table 12. TIG welding was used to tack weld the parts for actual welding which was proceeded with metal active gas (MAG) welding.

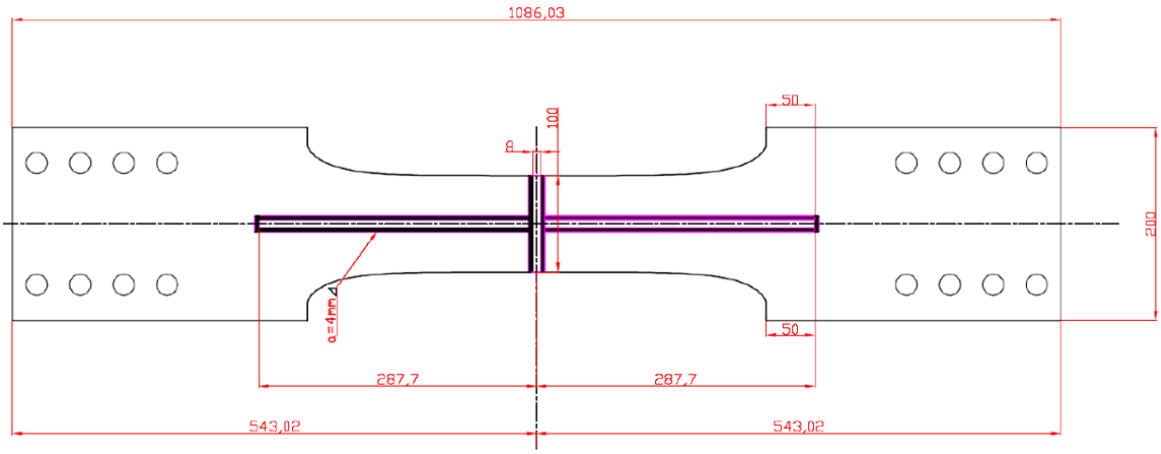

Figure 53. Design measures for specimen.

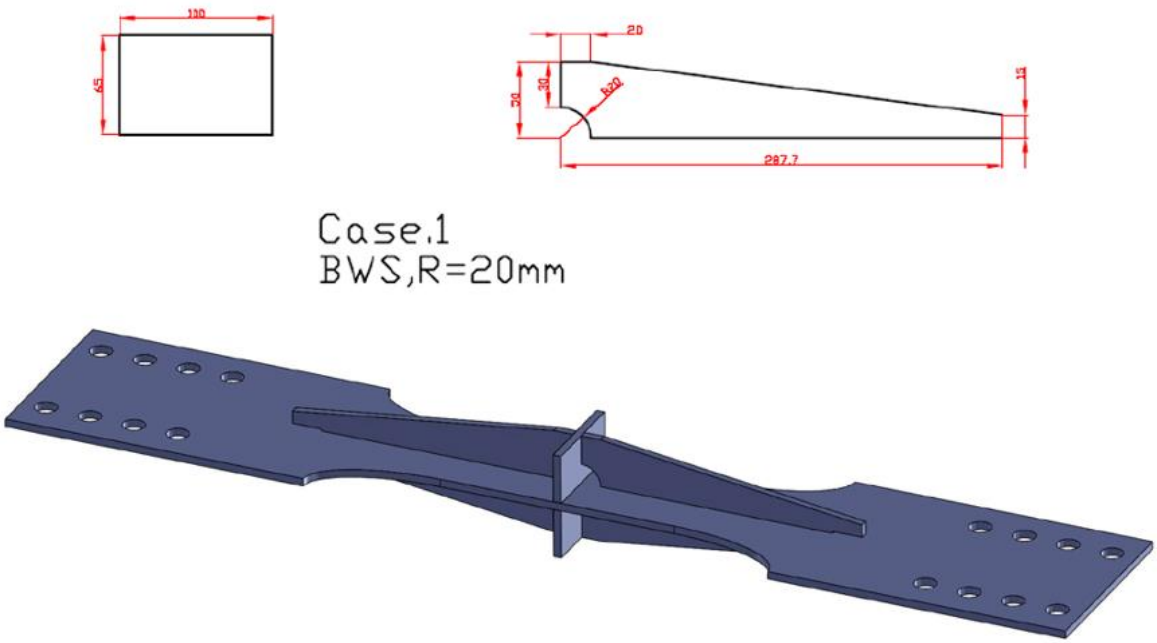

Figure 54. Dimensions of BWS specimen 1.

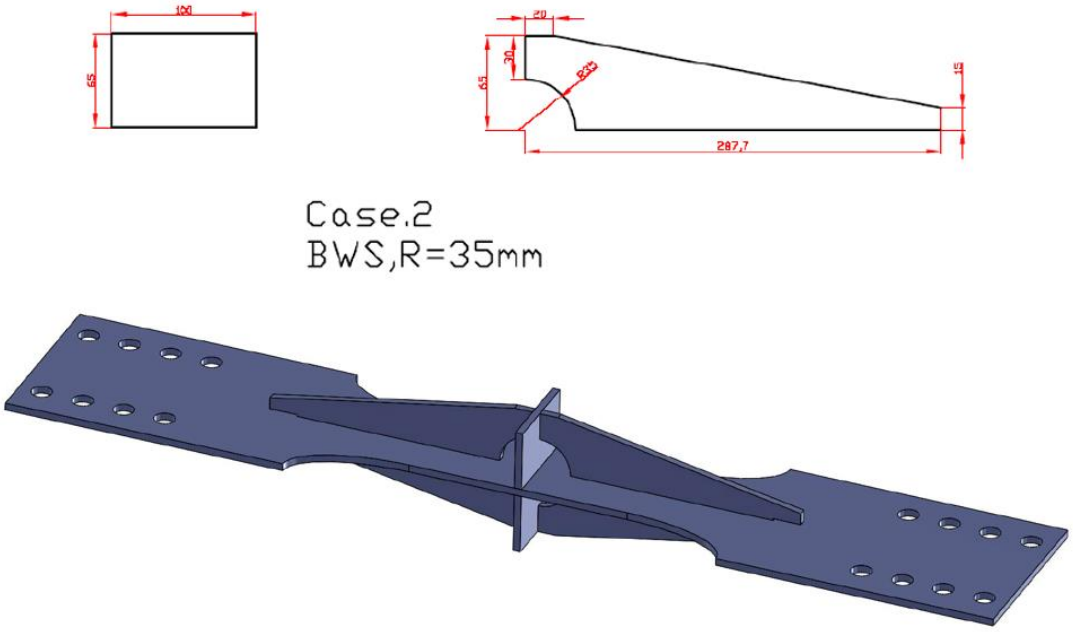

Figure 55. Dimensions of BWS specimen 2.

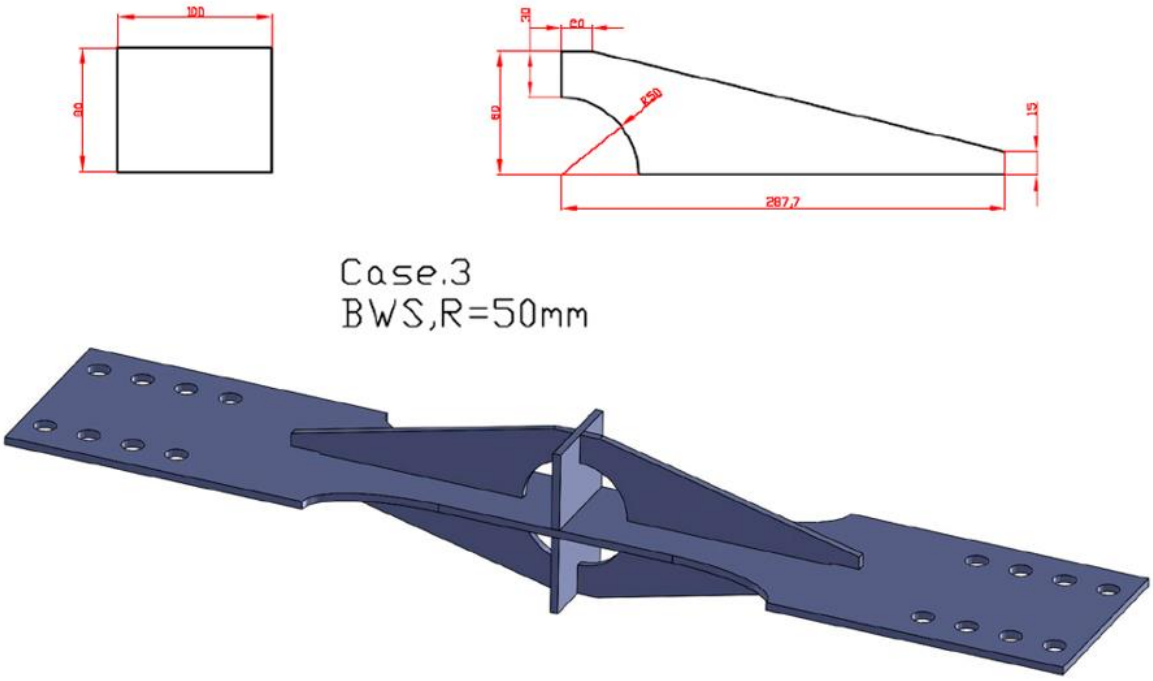

Figure 56. Dimensions of BWS specimen 3.

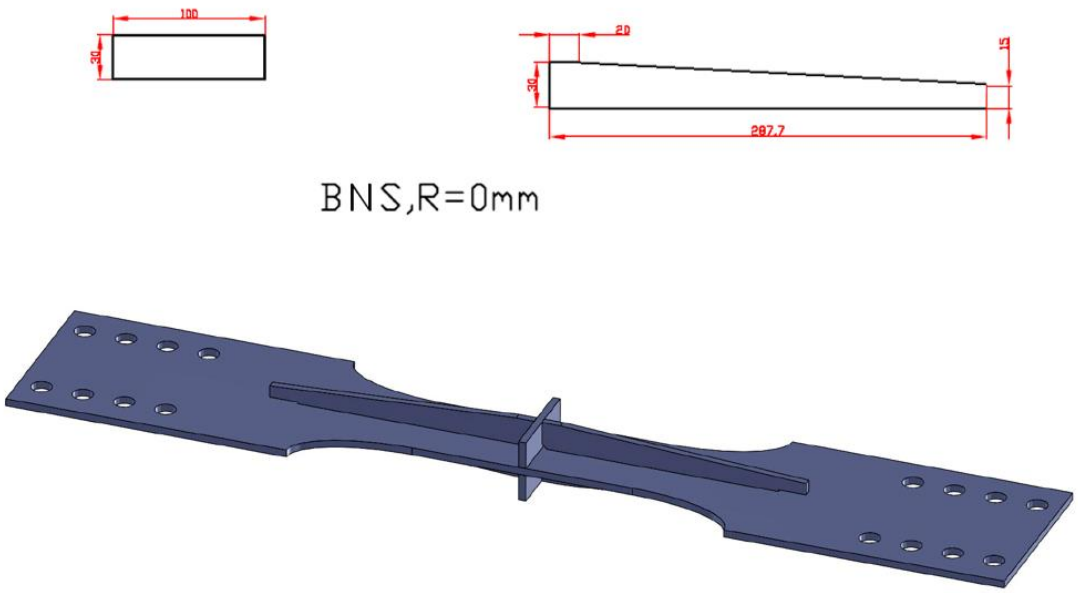

Figure 57. Dimensions of BNS specimen.

Table 12. Welding specifications for brackets.

Welding process	Filler metal	Shielding gas	Design throat thickness	Heat input *Q*
TIG (tack weld) and MAG (actual welding)	Union X96, Ø 1.0 mm	Ar + 8% CO2	4 mm	0.9 kJ/mm

Figure 58 shows welding penetrations of five different BNS specimens. All other dimensions are the same except measure *g* which is lack of weld penetration depth. Nominal stresses are calculated from measured force and area. Also, strain gauges were used to measure the structural stresses (notch stress) of the specimens. For BNS specimens' one strain gauge was attached to the corner of intersecting welds. Due to the small size of scallops, there were no space for two or more strain gauges to measure the hot spot stress. Figures 59 to 61 show clued strain gauges.

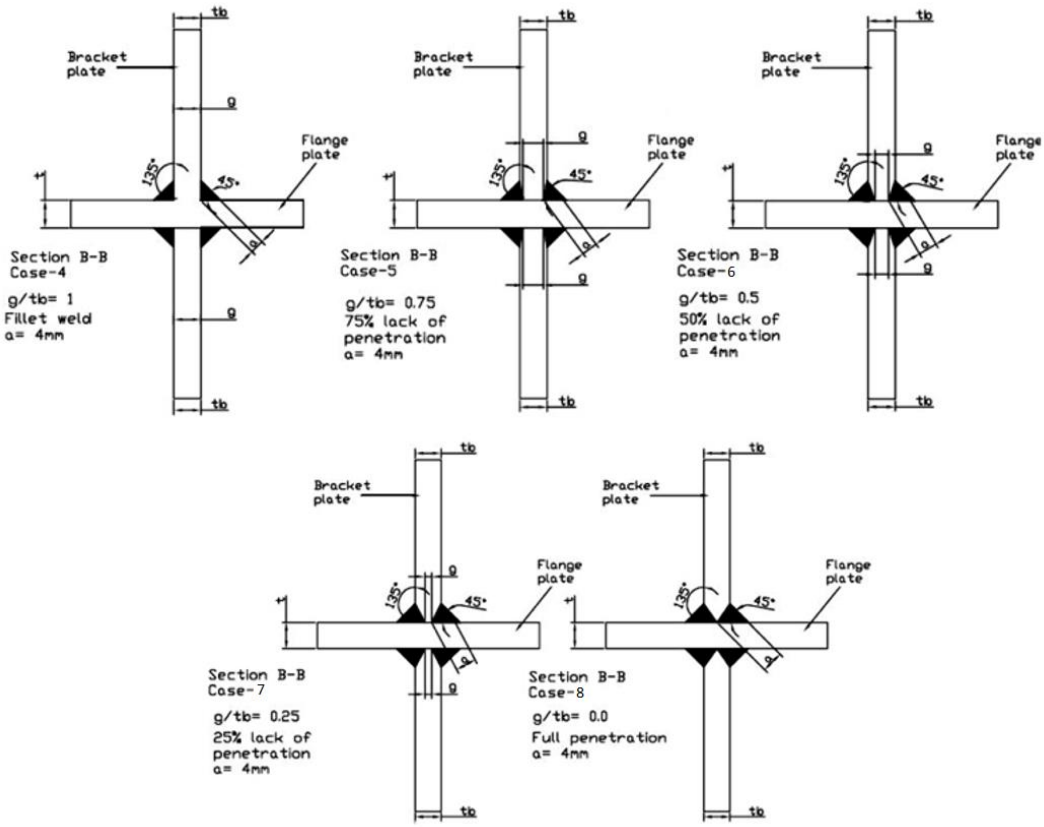

Figure 58. Welding penetrations of BNS specimens.

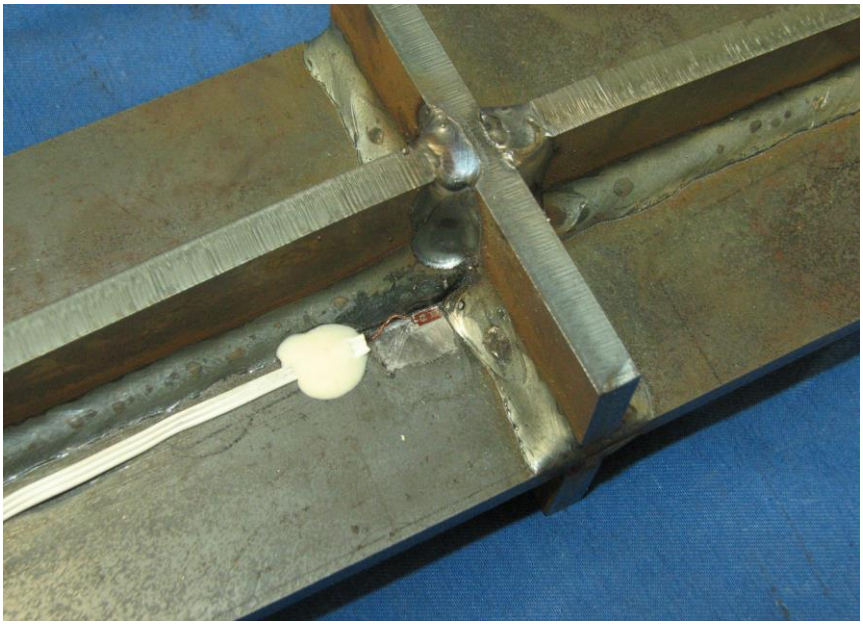

Figure 59. Strain gauge attached to BNS specimen.

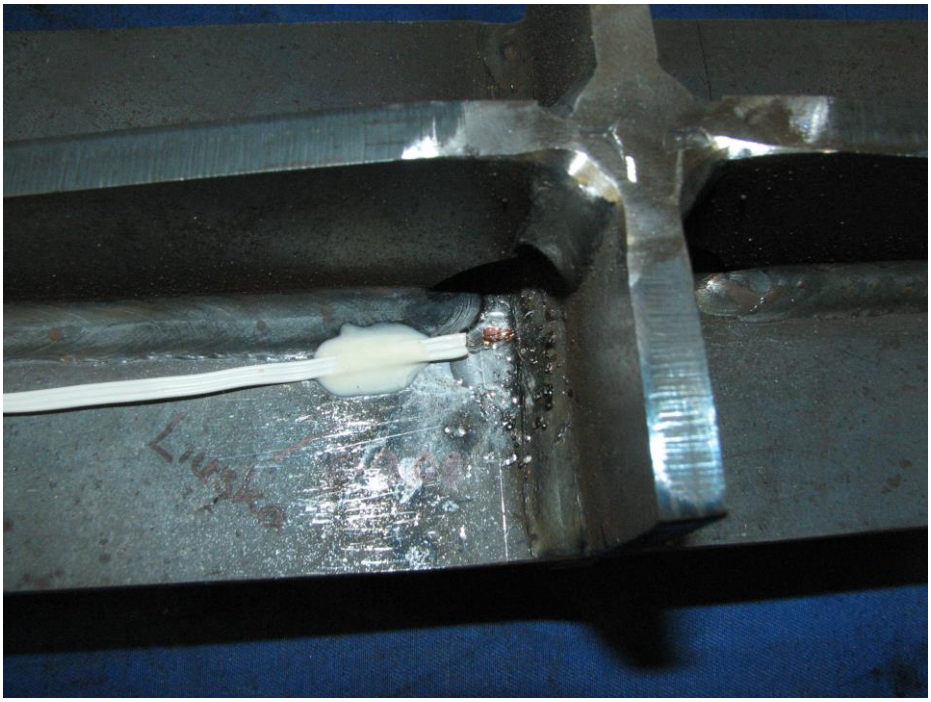

Figure 60. Strain gauge attached to BWS 1 specimen.

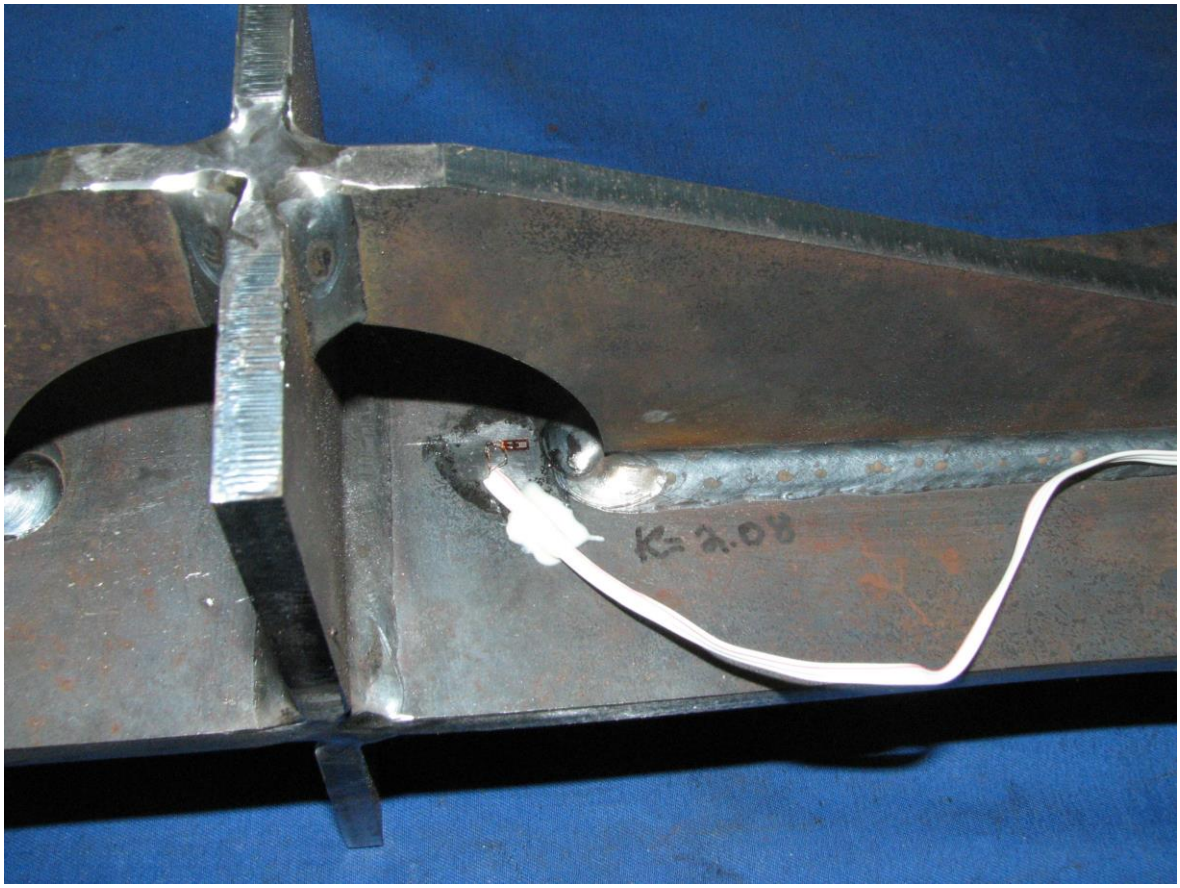

Figure 61. Strain gauge attached to BWS 3 specimen.

Specimens are attached to the fatigue-testing machine shown in figure 62a to start the measurements. Tests were performed until the failure of specimens when fatigue life N (cycles) is gained. This is shown in figure 62b.

Figure 62. Fatigue-testing machine with specimens.

4.1 Results from laboratory measurements and tests

The measured results were categorized and analysed to calculate nominal FAT class, making the comparison of results easy. Table 13 shows that BNS with full penetration weld has the best fatigue strength FAT 109. In that case, the attachment was the weakest point where fretting fatigue applied thus the fatigue strength of the welded corner didn't come out. BWS with a small radius (20 mm) has the second best fatigue strength FAT 96. All BWS specimens failed at bracket scallop's longitudinal side weld toe. Figure 63 shows the failure of BWS specimen 1 and figure 64 shows the failure of BNS specimen 7.

Table 13. Results from laboratory measurements.

Specimen [ID]	Max. Force	Min. force	Nominal stress $\Delta\sigma$ [MPa]	Structural stress $\Delta\sigma$ [MPa]	*N* [cycles]	FAT (nominal)	Crack location	N.B
1 BWS *R*20	192.5	16.6	137.4	179.6	691615	96	Weld toe at scallop	
2 BWS *R*35	191.7	16.5	136.9	211.3	564903	90	Weld toe at scallop	
3 BWS *R*50	191.8	16.2	137.2	210.1	472366	85	Weld toe at scallop	
4 BNS *g/t*=1	282.9	23.6	193	209.5	209582	91	Weld root	
5 BNS *g/t*=0.75	304.5	25.7	207.5	210.1	152249	88	Weld root	
6 BNS *g/t* = 0.5	284.5	24.5	193.4	187.3	158013	83	Weld root	
7 BNS *g/t*=0.25	286	25.5	193.8	189.5	213340	92	Weld root	
8 BNS *g/t*=0	269	14.4	185.5	205.8	378076	109	Attachment	Fretting fatigue

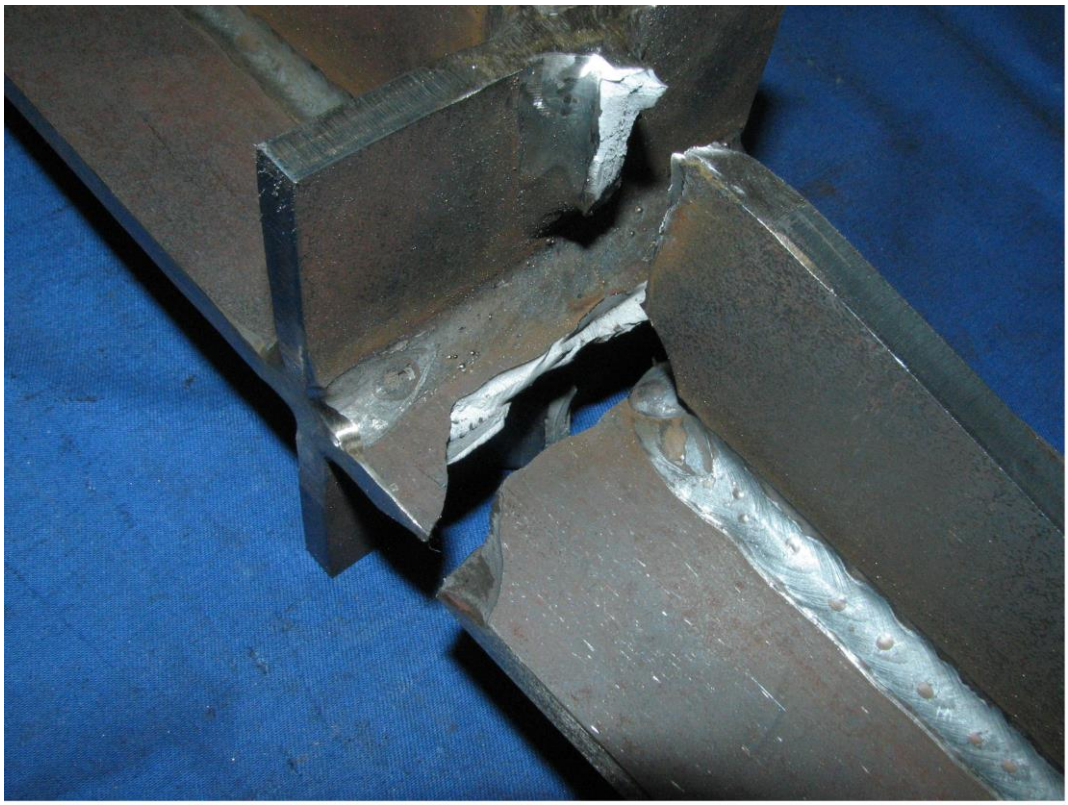

Figure 63. Failure of specimen 1.

Figure 64. Failure of specimen 7.

4.2 Discussion of results from laboratory measurements and tests

Results based on nominal stress show that increasing the size of scallop degreases the fatigue strength of the specimen. Other cases like studies from Fricke and Paetzold (1994) and Miki and Tateishi (1997) show similar results. In BNS specimens degreasing the lack of weld penetration increased the fatigue strength. The problem is that real weld penetration in specimens with a lack of weld penetration was smaller than supposed to be due to welding conditions. The weld penetration in fillet weld specimen was higher than in specimens 5 and 6 that shows in higher FAT number and fatigue strength of fillet weld specimen. According to these tests, scallops should be used only when full penetrated weld is not possible. Scallops with small radius are preferred to be used. Only one test was done to each specimen. More tests should have been done to neglect the possibility that structural flaws and bad weld qualities affected to the results. Degreasing the scallop radius guides higher percentage of the total stress to go through the bracket. This can be seen from structural stress values. That is why nominal stress method should be used to calculate fatigue strengths of these specimens.

5 FEM TO DEFINE STRESS CONCENTRATION FACTORS FOR I-BEAMS WITH SCALLOPS EXPOSED TO TENSILE LOADING

Two different publications from Det Norske Veritas, DNV (2011) and DNV (2014), show stress concentration factors for scallops of four different shapes which are affected by tensile stresses. Specimens are shown in figures 65 and 66 and results are shown in table 14. SCFs are based on the structural hot spot stresses and nominal stresses. SCFs are calculated from as follows:

$$\mathrm{SCF} = \frac{\sigma_{hs}}{\sigma_n}, \tag{13}$$

, where SCF is Stress concentration factor, σ_{hs} is structural hot spot stress and σ_n is nominal stress. (DNV, 2011, p. 13.)

DNV (2011) shows higher SCF values for specimen 1b at point A, shown in figure 65, than DNV (2014) for specimen 1a at point A. Specimen 1a has a half-rounded scallop with 50 mm radius and specimen 1b also has a half-rounded scallop but the radius is unknown (DNV, 2011, pp. 31; DNV, 2014, p. 94). Also research from Cai, Chen and Zhao (2014) gives different results which are seen in figure 67 alongside with the examined specimens 8a and 8b. All of these studies show that SCFs are smaller at the weld toe than in the top of scallop hole. Cai, Chen and Zhao (2014) performed experimental and analytical tests to determine the SCFs at the top of scallop hole and at the weld toe. Because of the incoherence of the results, further research was needed to clarify the SCFs for this detail. Finite element method (FEM) was used to determine the structural hot spot stresses at points A and B for specimens 5, 6 and 7 with half-round scallops.

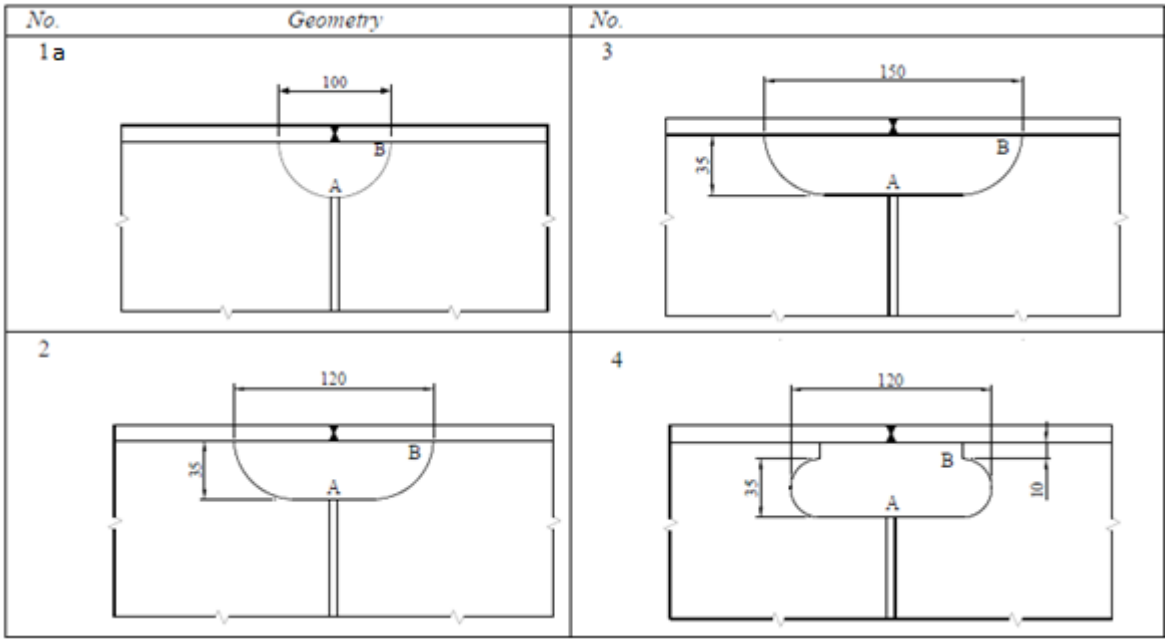

Figure 65. Different scallops shapes from DNV rules (modified from DNV, 2014, p. 94).

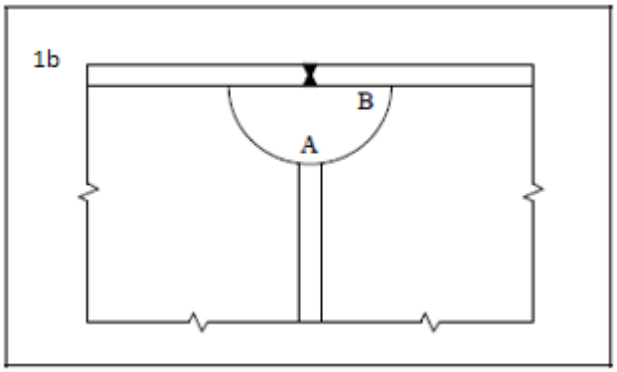

Figure 66. Half-round scallop with unknown radius from DNV rules (modified from DNV, 2011, p. 31).

Table 14. Stress concentration values from DNV rules.

SCF point / Specimen No.	1a	1b	2	3	4
SCF at point A	2.0	2.4	1.27	1.17	1.17
SCF at point B	1.27	1.27	1.27	1.27	1.27

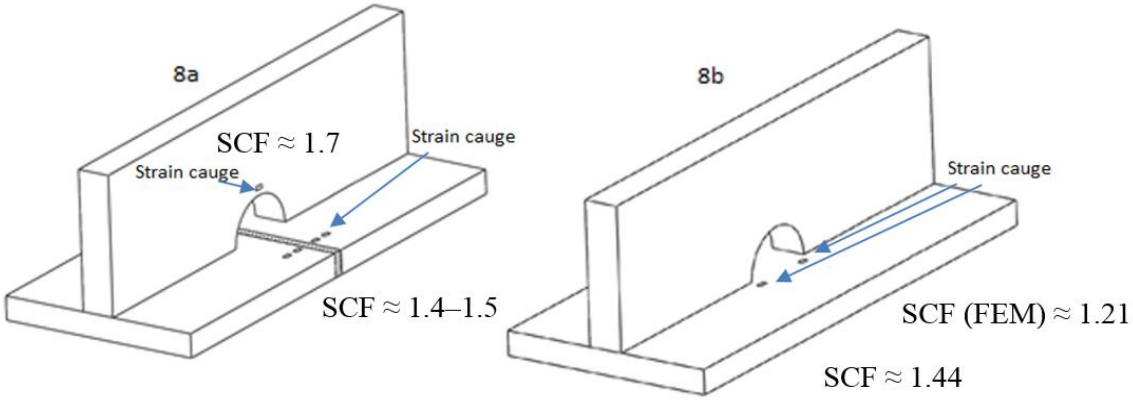

Figure 67. Strain gauges at specimens 8a and 8b and SCFs (modified from Cai, Chen & Zhao, 2014, p. 1011).

5.1 Describing the model

The examined structure is an I-beam with scallops and stiffeners. Material's Young's modulus *E* is 210 GPa and Poisson's ratio is 0.3. The beam is loaded with 100 MPa tensile load shown in figure 68 which describes the geometry of the model. Flange butt welds were deleted for analyses because those were not critical details. Beam was analysed with three different scallop radii. Dimensions of the specimens are shown in table 15.

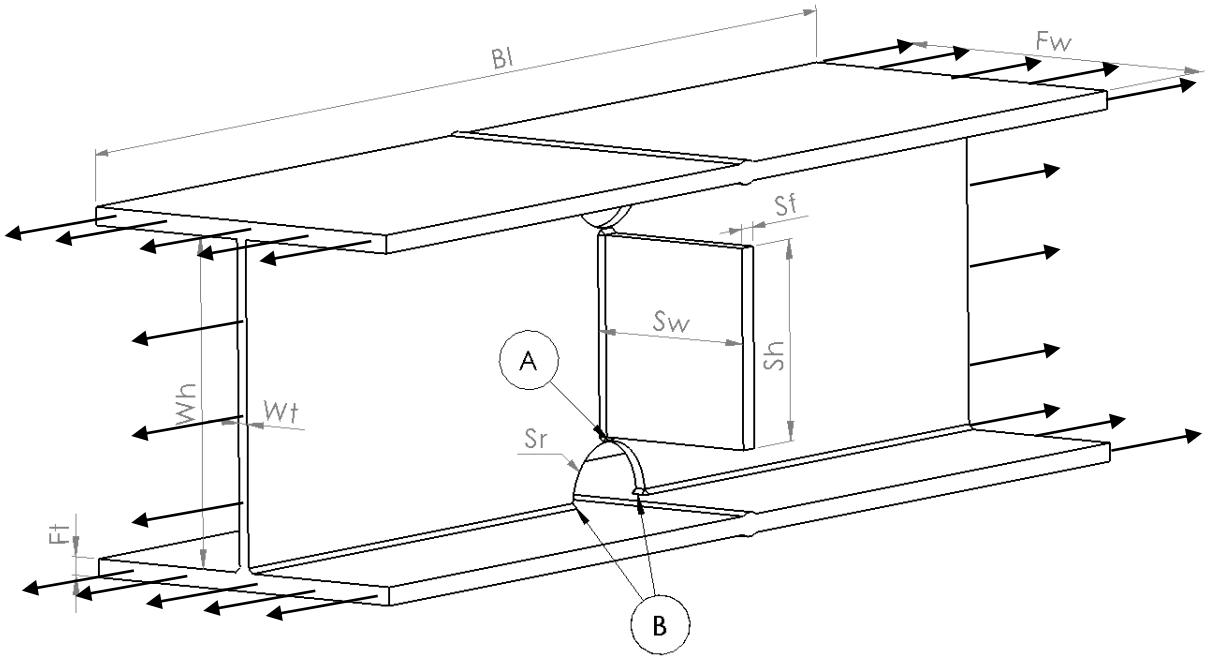

Figure 68. Geometry of analysed model and loading conditions.

Table 15. Dimensions of the specimens.

<table>
<tr><th>Specimen No.</th><th>Scallop radius (Sr)</th><th>Flange thickness (Ft)</th><th>Stiffener thickness (St)</th><th>Web thickness (Wt)</th><th>Beam length (Bl)</th><th>Stiffener width (Sw)</th><th>Web height (Wh)</th><th>Stiffener height (Sh)</th><th>Flange width (Fw)</th><th>Weld throat length</th></tr>
<tr><td></td><td colspan="10">[mm]</td></tr>
<tr><td>5</td><td>50</td><td rowspan="2">15.5</td><td rowspan="2">15.5</td><td rowspan="2">9</td><td rowspan="3">1000</td><td rowspan="3">145</td><td rowspan="3">279</td><td rowspan="3">169</td><td rowspan="3">300</td><td rowspan="3">3</td></tr>
<tr><td>6</td><td>25</td></tr>
<tr><td>7</td><td>20</td><td>24</td><td>24</td><td>24</td></tr>
</table>

For specimens 5 and 6, standard I-beam was chosen from a catalogue. Flange thickness of specimen 3 is the same as the flange thickness of specimens 8a and 8b. Web thickness of specimens 8a and 8b is not represented, but approximation from the drawing shows that it is almost the same as flange thickness. Same web thickness is used on specimen 7 which has a same sized stiffener as specimens 5 and 6.

Symmetry was used to ease the Finite element analysis (FEA). The beam was cut to one eighth model which is shown in figure 69. Using the symmetry degreased the number of used elements and partition work to properly mesh the part.

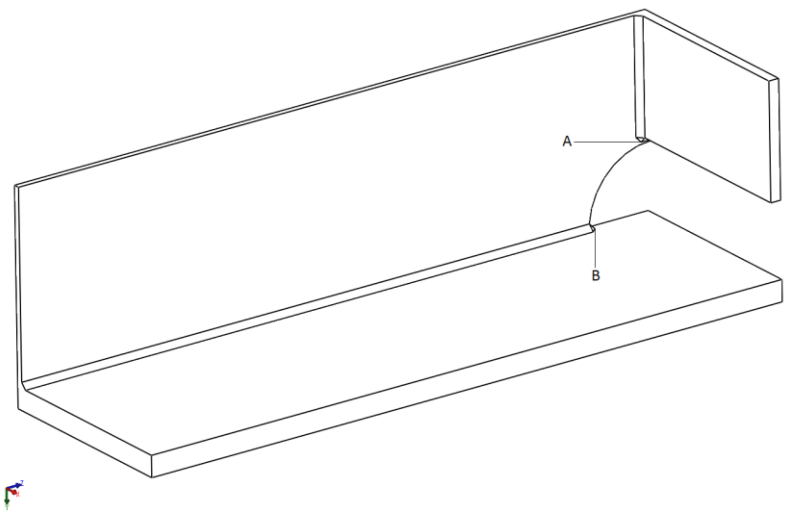

Figure 69. One eighth model of the I-beam.

5.2 Boundary conditions

Boundary conditions prevent the displacements of the analysed model by adjusted conditions. Boundary conditions are shown in figure 70. Point F is made fixed preventing the point to move at all. One eight model was made to correlate the full model using symmetry boundary conditions. Symmetry condition to z-axis direction was adjusted for faces Z. Symmetry condition to x-axis direction was adjusted for face X. Symmetry condition to y-axis direction was adjusted for face Y.

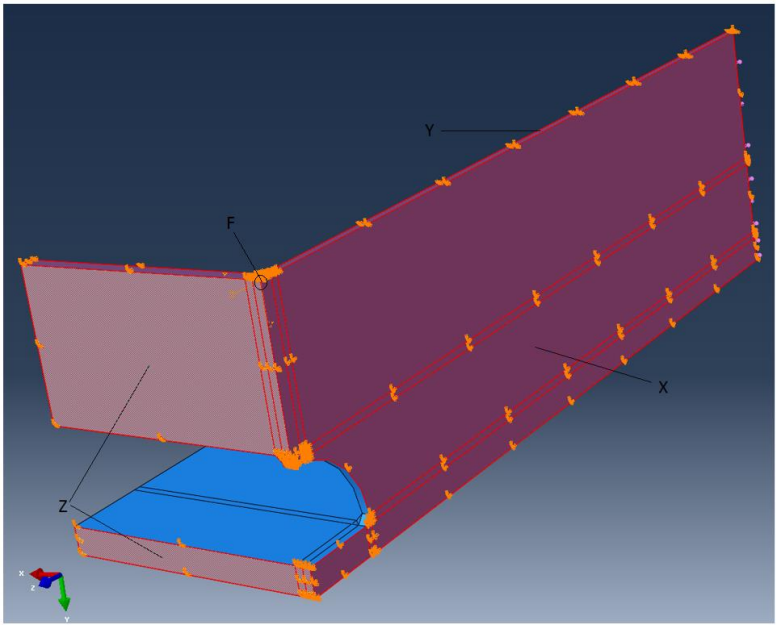

Figure 70. Boundary conditions.

5.3 Loading conditions

Tensile pressure was set to the A side of the I-beam as shown in figure 71. Because the model is symmetrical, the loading is automatically set also to opposite direction. To ease the calculation for SCFs, a round number, 100 MPa, was chosen as the value of pressure.

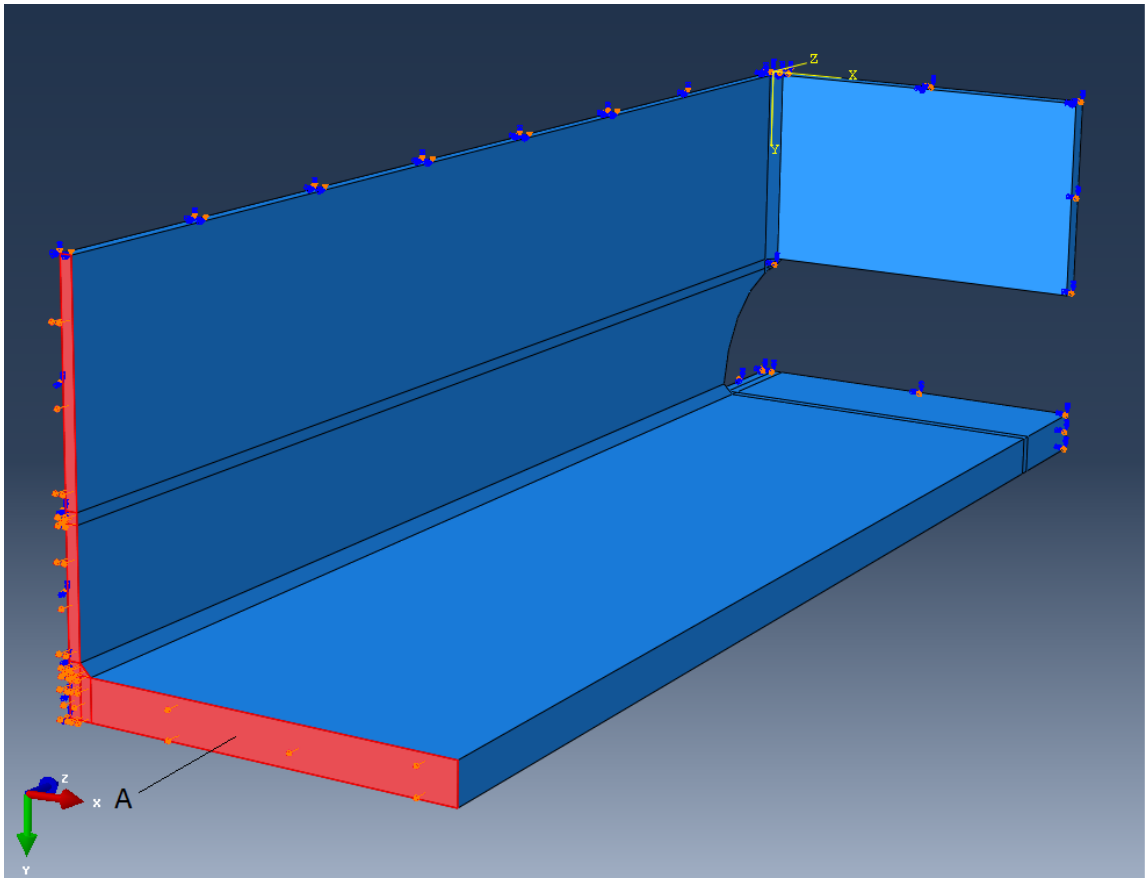

Figure 71. Tension loading affecting to surface A.

5.4 Element types

Solid elements were used to describe the model. Parabolic hexahedral elements were used to get accurate results. Tetrahedral elements are less accurate than hexahedral elements thus those are not used. (Spyrakos, 1996, p. 46.)

5.5 Meshing

Submodels were used to ease meshing of the model and avoid long computation time. One eighth model was first roughly meshed and analysed. After that, submodels were made around details A and B from figure 69. Submodels were connected to the one eighth model by adding submodel boundary conditions to faces that are in connect with the one eighth model. Symmetric boundary conditions were also added to submodels as in the one eighth model. Element sizes of 1 mm or less were used in submodels to increase the number of integration points in critical areas. Element size of 0.5 mm was used to measure SCFs at points B through thickness at the weld toe.

5.6 Results from FEAs

Stress concentration factors at the top of scallops and at scallop corners are gained as results of the FEAs. Gained maximum principal stresses are gathered to tables and compared to results from DNV (2011), DNV (2014) and Cai, Chen and Zhao (2014).

Analysed stresses of specimen 5, beam with 50 mm radius scallop, and hot spot extrapolation points are shown in figures 72 to 75. Hot spot stresses are determined using two extrapolation points at 0.4 * *t* and 1.0 * *t* distances from investigated points. In figures extrapolation points are marked with red spots.

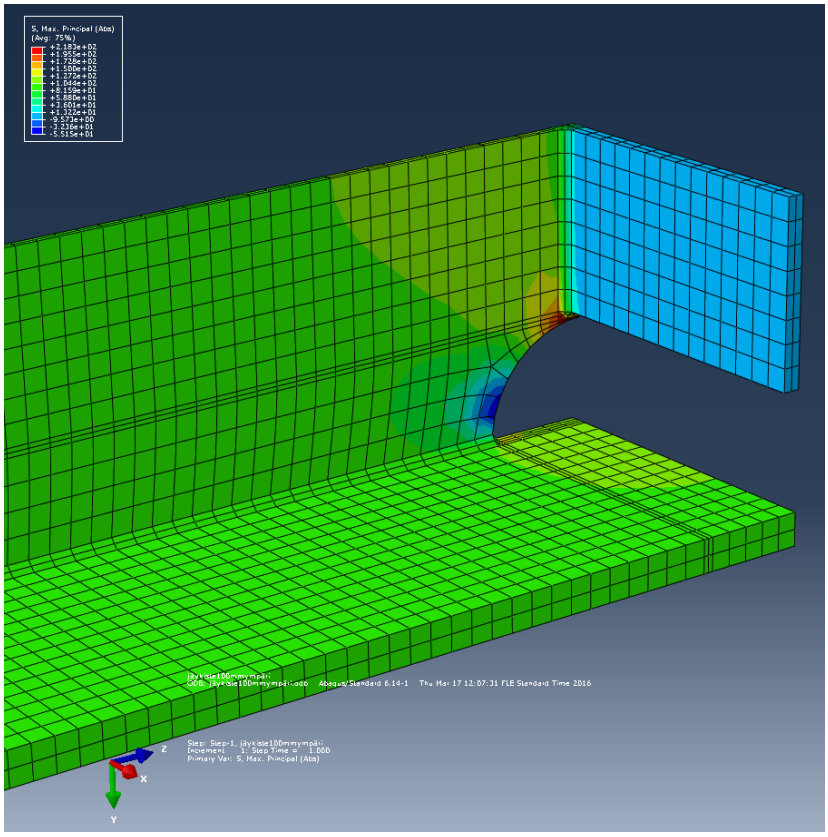

Figure 72. Stresses of one eighth model of specimen 5.

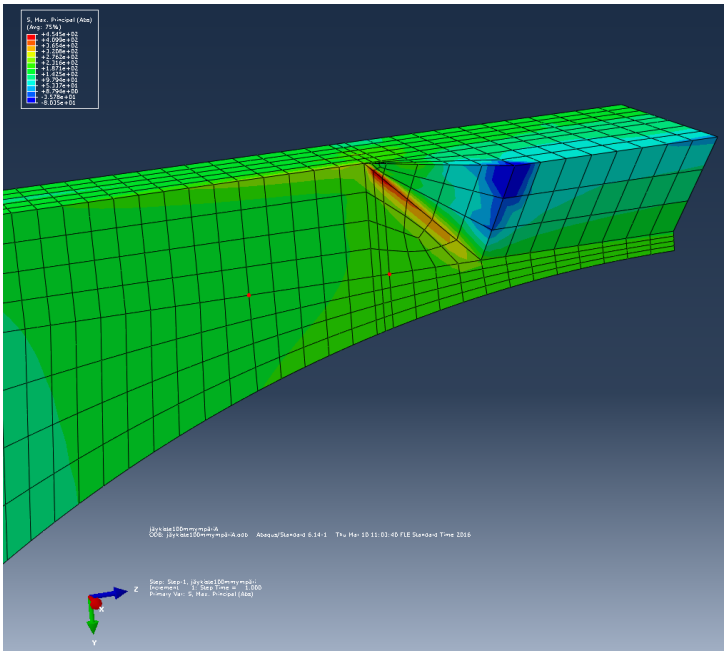

Figure 73. Stresses of submodel and linear surface extrapolation (LSE) points at point A for specimen 5.

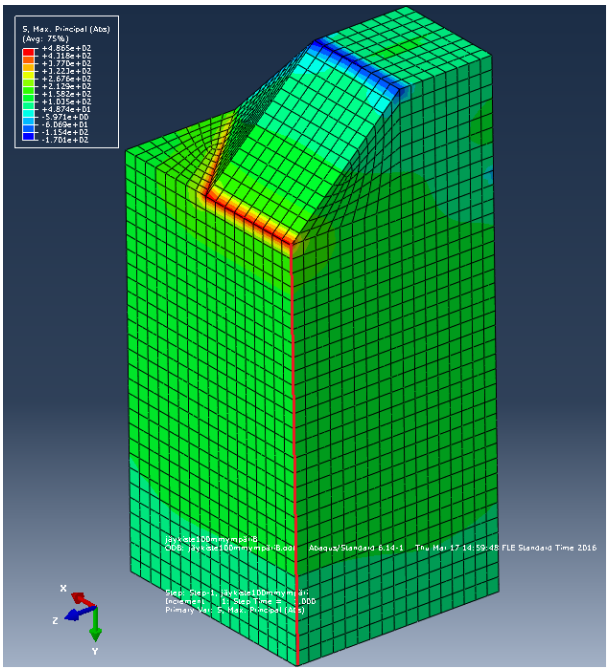

Figure 74. Stresses of submodel and linearization points through thickness at the weld toe (TTWT) at point B for specimen 5.

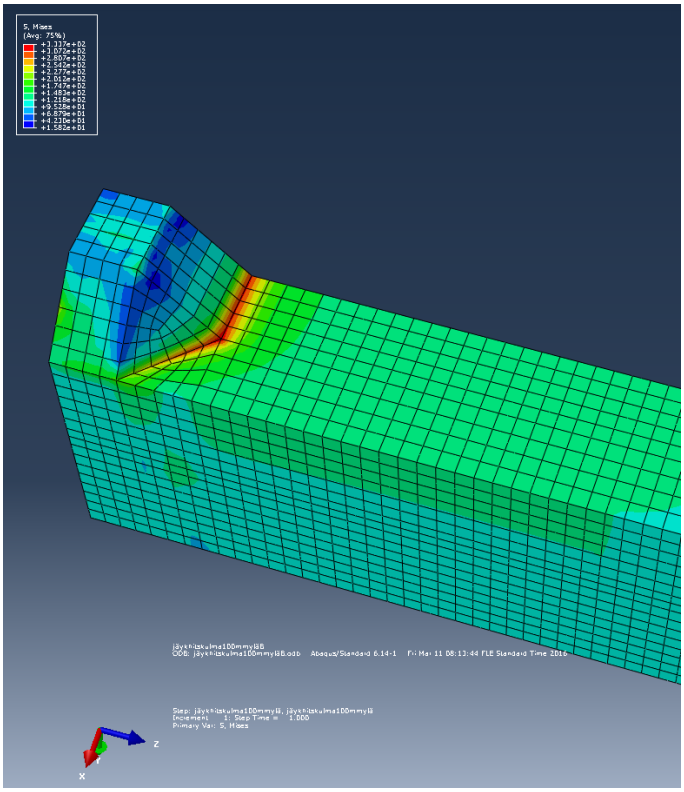

Figure 75. Stresses of submodel and linear surface extrapolation (LSE) points at point B for specimen 5.

Corner of the specimen in figure 74 has been suppressed to measure stresses from every node through material thickness. Same has been done to models in figures 78 and 82. Analysed stresses of specimen 6, beam with 25 mm radius scallop, and hot spot extrapolation points are shown in figures 76 to 79.

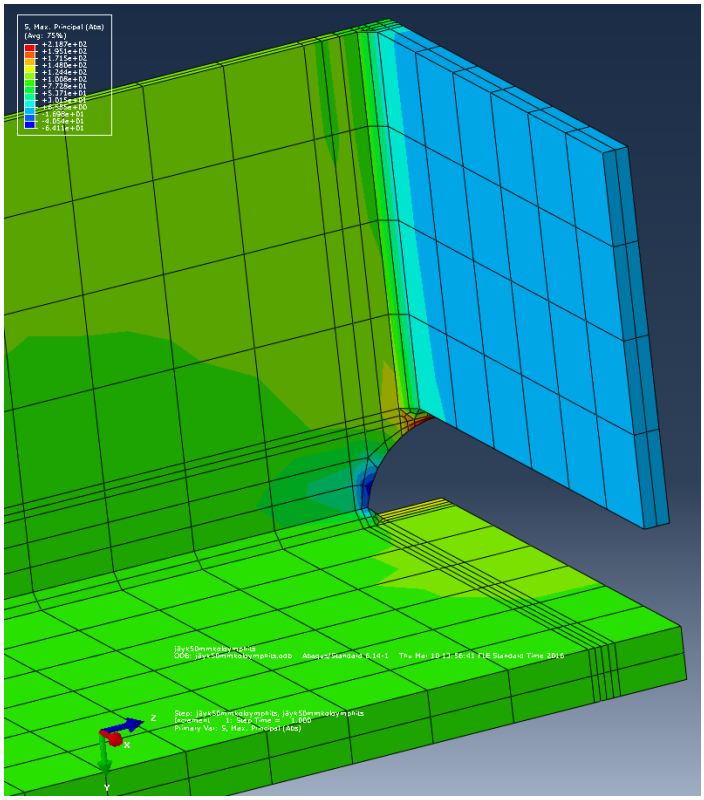

Figure 76. Stresses of one eighth model of specimen 6.

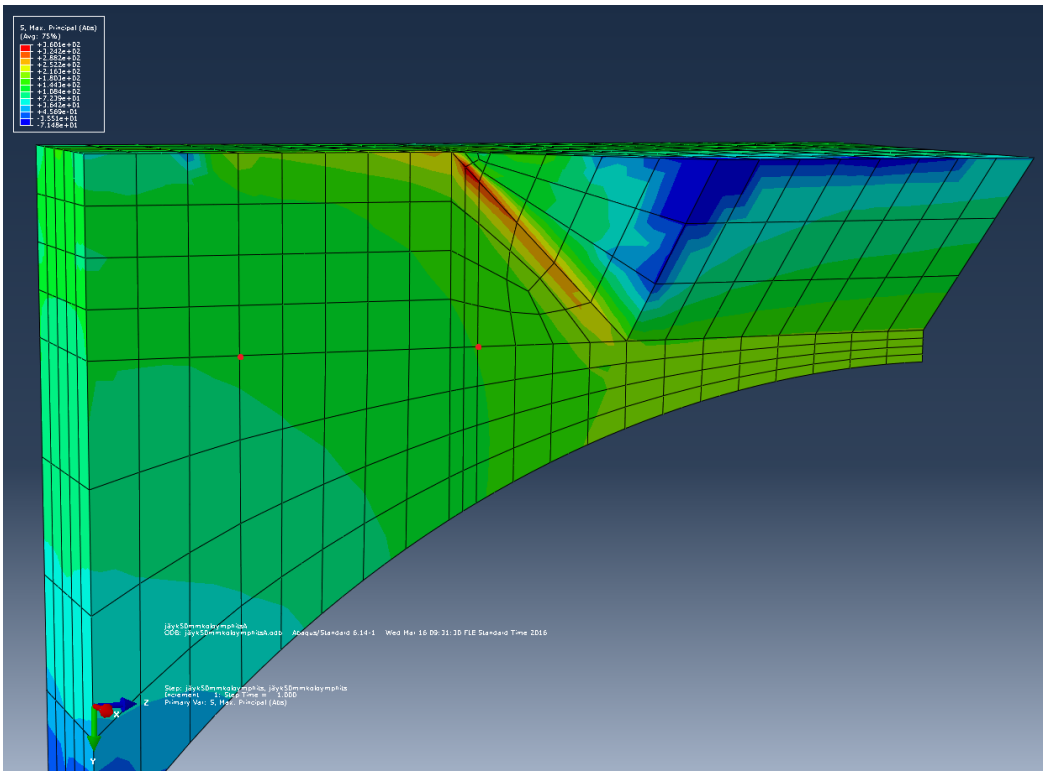

Figure 77. Stresses of submodel and linear surface extrapolation (LSE) points at point A for specimen 6.

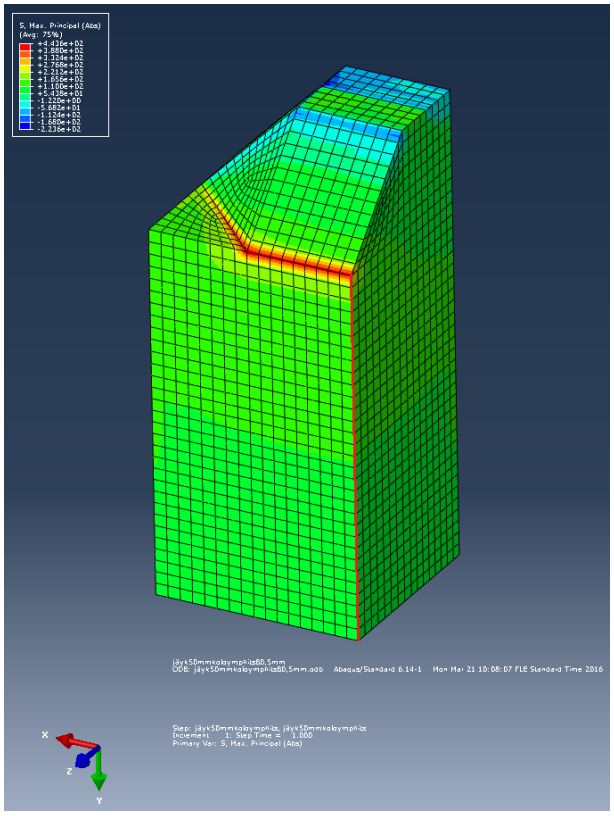

Figure 78. Stresses of submodel and linearization points through thickness at the weld toe (TTWT) at point B for specimen 6.

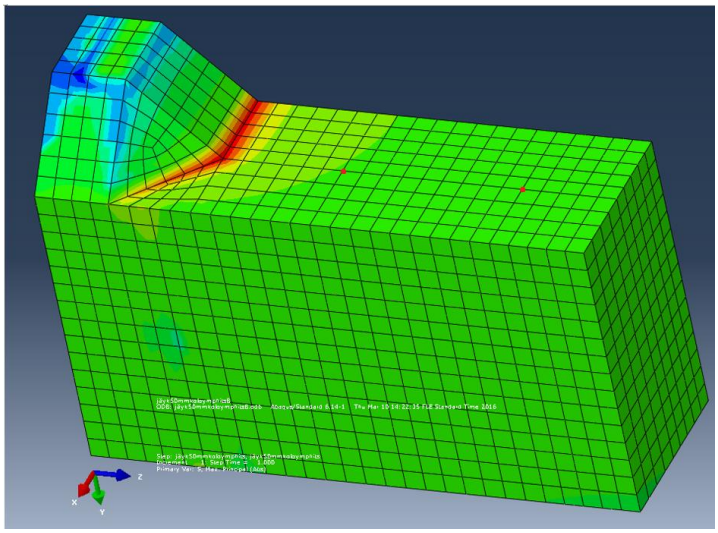

Figure 79. Stresses of submodel and linear surface extrapolation (LSE) points at point B for specimen 6.

Figure 80 shows one eighth model of specimen 7 with maximum principal stresses. Submodels of specimen 7 with hot spot extrapolation points are shown in figures 81 and 82.

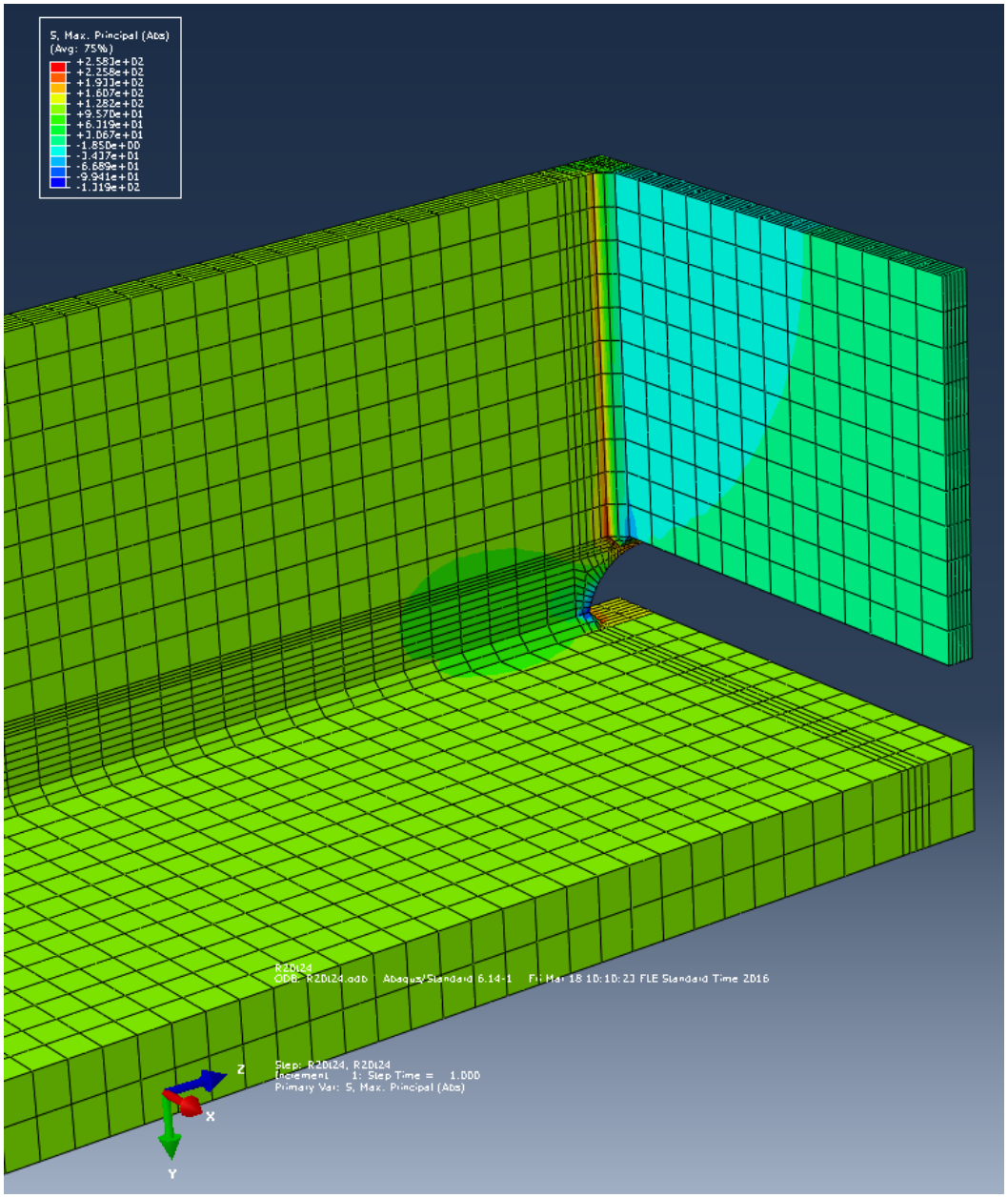

Figure 80. Stresses of one eighth model of specimen 7.

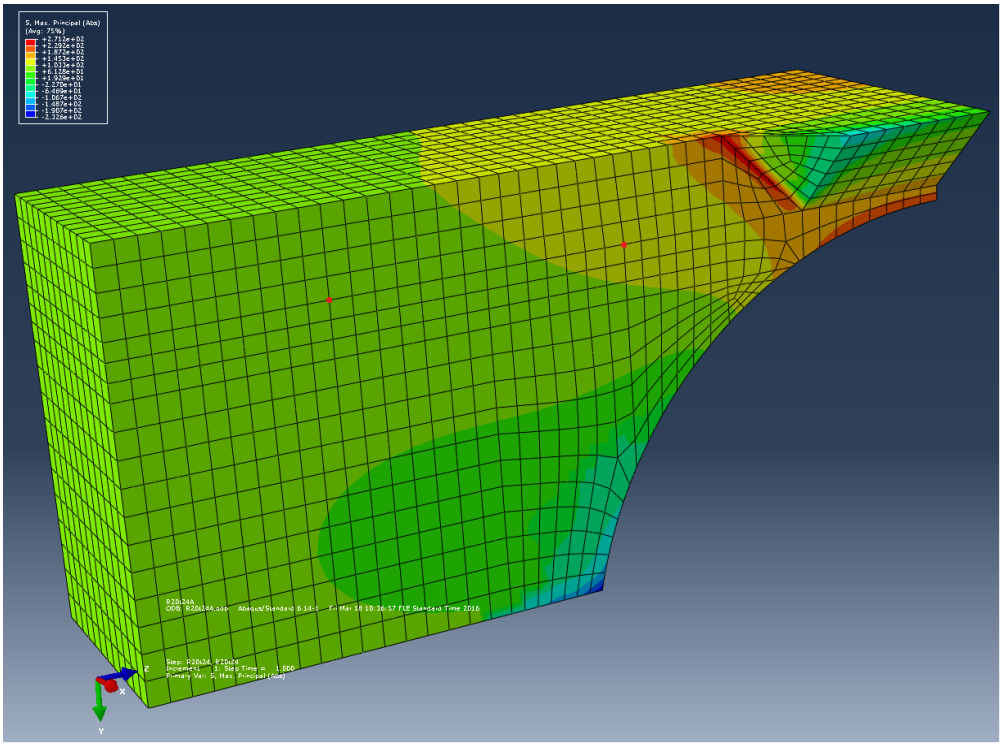

Figure 81. Stresses of submodel and linear surface extrapolation (LSE) points at point A for specimen 7.

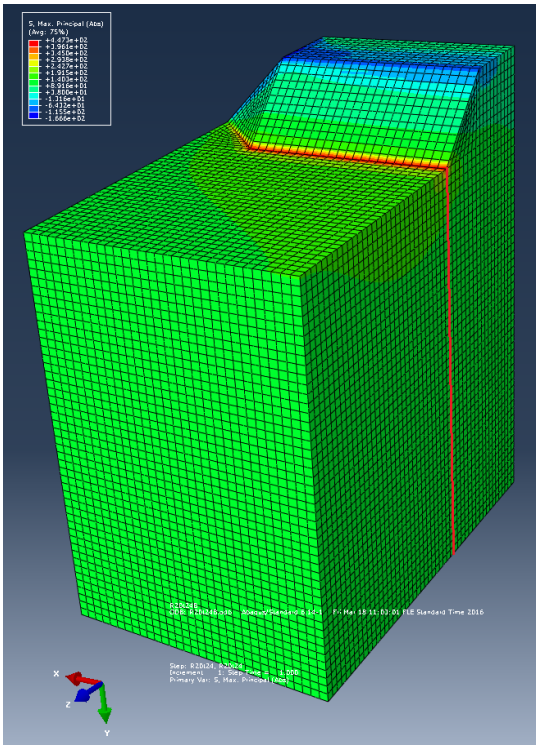

Figure 82. Stresses of submodel and linearization points through thickness at the weld toe (TTWT) at point B for specimen 7.

Maximum principal stresses at linearization points through thickness at the weld toe are plotted for specimens 5, 6 and 7 to figures 83, 84 and 85 to calculate hot spot stress using TTWT method. Membrane and bending stresses are separated from total stress using equations 8 and 9.

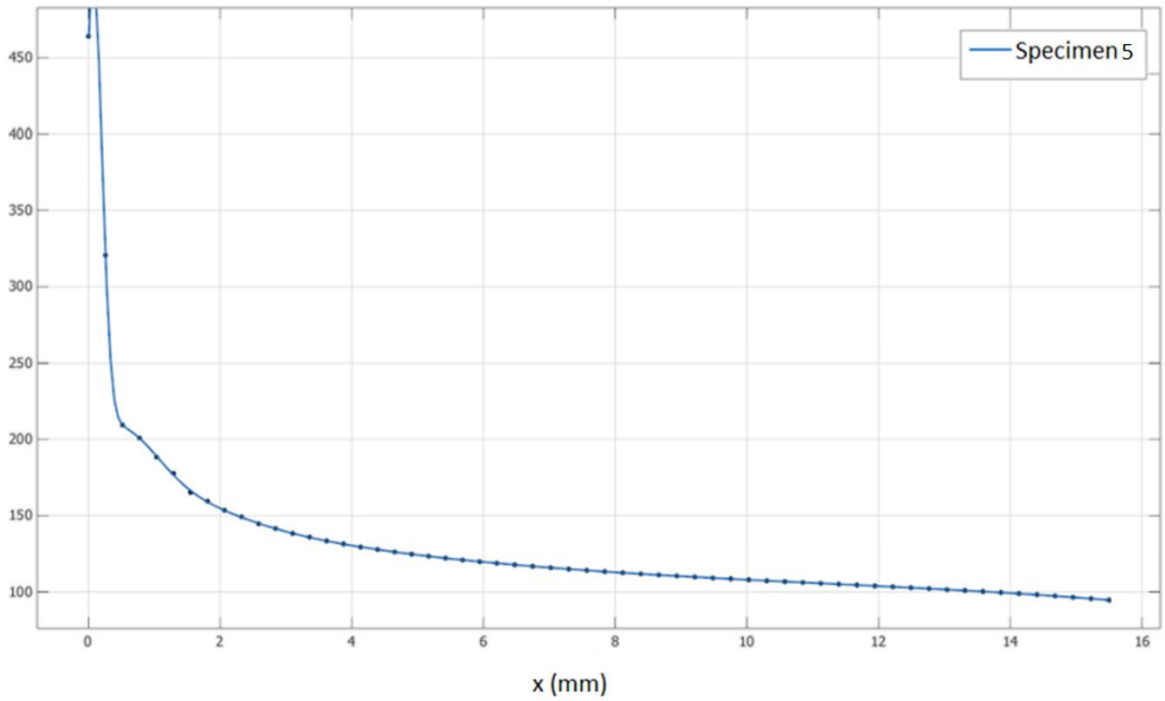

Figure 83. Linearization points TTWT at point B for specimen 5.

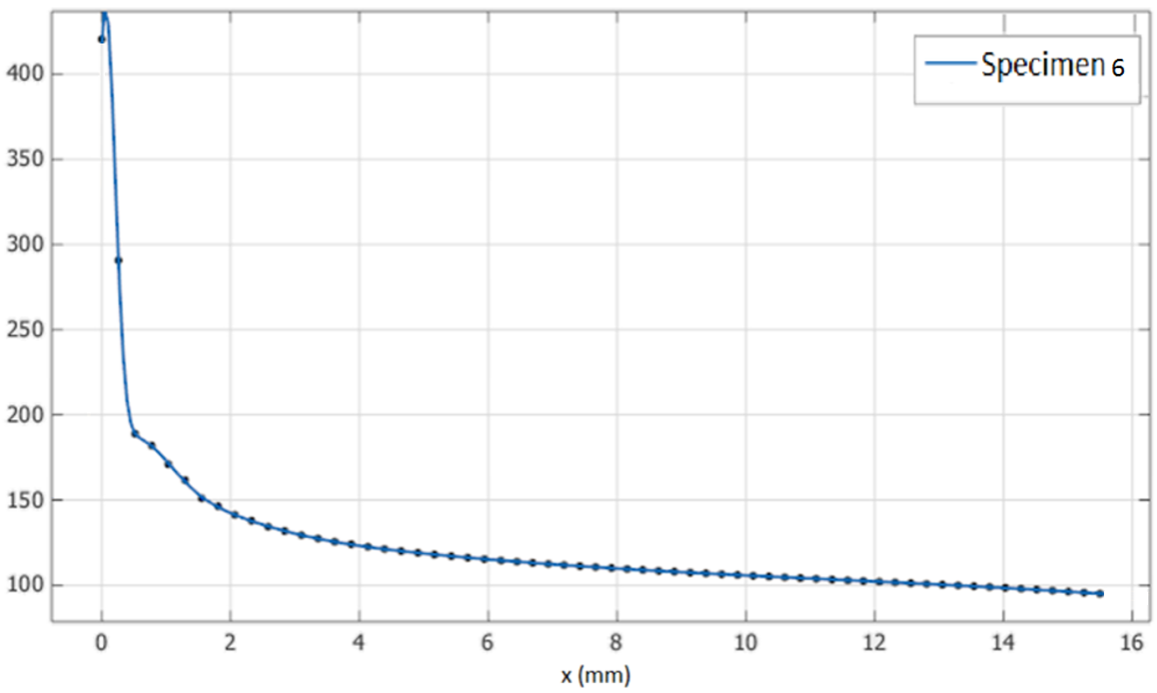

Figure 84. Linearization points TTWT at point B for specimen 6.

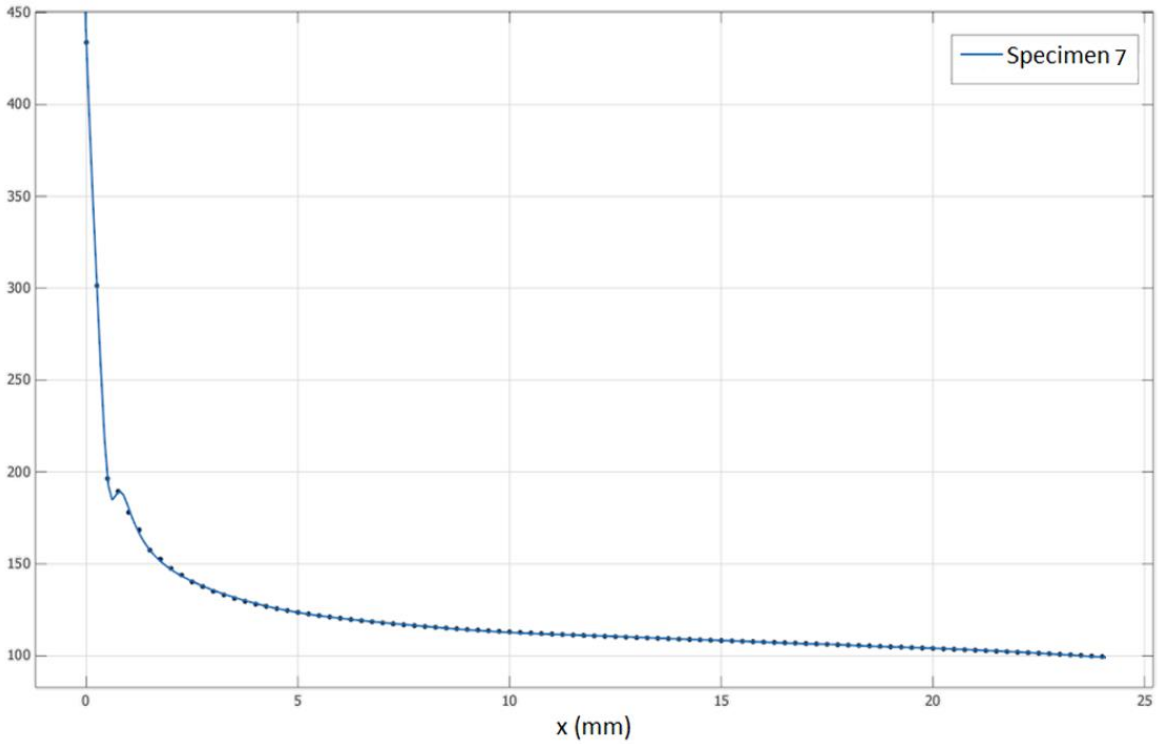

Figure 85. Linearization points TTWT at point B for specimen 7.

Maximum principal stresses measured at extrapolation points 0.4 * *t* and 1.0 * *t* are tabulated to table 16 with membrane and bending stresses over the plate thickness at point B.

Table 16. Maximum principal stresses.

Specimen	Scallop radius [mm]		Max. principal stresses [MPa]			Stresses [MPa]
		extrapolation points	A	B (Z-direction)	Stress	B (Y-direction)
5	50	0.4t	200.8	138.3	Membrane	128.3
		t	168.4	128.6	Bending	56.1
6	25	0.4t	145.4	135.1	Membrane	122.3
		t	111.8	129.3	Bending	46.0
7	20	0.4t	114.1	-	Membrane	120.0
		t	87.6	-	Bending	34.9

Equation 2 was used to calculate LSE SCFs from measured stresses and equation 10 to calculate SCFs from membrane and bending stresses. Results are shown in table 17.

Table 17. Stress concentration factors for A and B points.

Specimen	Scallop radius (mm)	Stress concentration factor at point		
		A	B (Z-direction)	B (Y-direction)
5	50	2.2	1.5	1.8
6	25	1.7	1.4	1.7
7	20	1.3	-	1.6
Specimen (reference)	Scallop radius [mm]	A	B	
1a	50	2.0	1.3	
1b	Unknown	2.4		
8a	Unknown	1.7	-	-
8b		-	1.2 (FEM)	1.4 (Measured)

5.7 Discussion of results from FEA

Analysed SCFs show that degreasing the radius of scallop degreases SCFs. The result is the same as in research by Fricke and Paetzold (1994) which is presented in chapter 3.2. It seems that SCFs for point A are highly dependent on the size of the scallop. SCFs for point B are also dependent on the size of the scallop but the influence is slighter than for point A. SCFs at point B for specimens 5, 6 and 7 are greater than values for specimens 1a and 1b. SCF for detail 8b determined using FEM is close to the values of specimens 1a and 1b. Experimentally measured SCF for specimen 8b gives the same kind of values as specimens 1 and 2 have with linear surface extrapolation (LSE) method. Membrane stresses for specimens 5, 6 and 7 at point B are close to these stresses. It is unknown if only membrane stress is used to calculate the SCFs for specimens 1a, 1b and 8b (FEM) but it seems that bending stress is not included in those. It is not sure how structural hot spot stresses are calculated to make DNV's design rules. Also, the radii of scallops are unknown for details 1b, 8a and 8b. The results gained from FEM are hard to be compared because the lack of information about how previous studies were done. To get more accurate results the effect of effective cross section should be considered. When calculating SCFs using equation 13, σ_n should be replaced with $\sigma_{n,\ effective}$, which is calculated nominal stress using cross section where the area due to scallop cut out has been removed.

6 GUIDANCE FOR USING SCALLOPS

This guidance is based on the results of this Thesis. Fatigue strength is the main criteria in these design rules. It assists engineers to choose whether to use a scallop or not. Instructions for scallop shapes and other remarks are also given. Guidance is divided into three different tables. Table 18 shows design rules for T- and H-shape specimens. Table 19 shows design rules for flange and web with stiffeners and table 20 shows design rules for flange and web without stiffeners. Each table gives design rules for different loading conditions. In this guidance "-" means that the marked option is not specified for that case. "Yes" means that the marked option is recommended to be used. "No" means that the marked option is not recommended to be used.

Table 18. Design rules for T- and H-shape specimens.

T-shape specimens							
Loading	Model	Length of longitudinal attachment	Scallop radius			No Scallop	Remarks
			20 mm	35 mm	> 35 mm		
Tensile (Fillet weld)	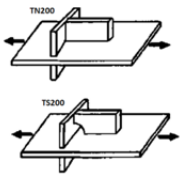	100 mm	-	Yes	-	Yes	Fatigue crack initiates in the bracket end weld toe. Scallop only degreases the length weld in the bracket.
		200 mm	-	No	-	Yes	
Primarily loaded (BNS and BWS fillet weld)	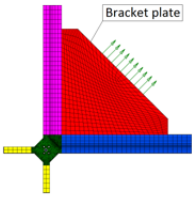	150 mm	Yes	No	No	No	BNS should be used when high quality welding is achieved
Primarily loaded (BNS groove weld)			No	No	No	Yes	

Table 18 continues. Design rules for T- and H-shape specimens.

T-shape specimens							
Loading	Model	Length of longitudinal attachment	Scallop radius			No Scallop	Remarks
			20 mm	35 mm	> 35 mm		
Non-primarily loaded (BNS and BWS fillet weld)	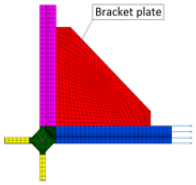		No	No	No	Yes	BNS should be used when high quality welding is achieved
Non-primarily loaded (BNS groove welded)			No	No	No	Yes	
		287.7 mm	No	No	No	Yes	
Non-primarily loaded (fillet welded)			Yes	No	No	No	
H-shape specimens							
Tensile	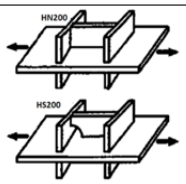	200 mm	-	Yes	-	Yes	Same fatigue strength

Table 19. Design rules for flange and web with stiffeners.

Flange and web with vertical stiffeners (I-beam)								
Loading	Model	Scallop	No Scallop	If scallop is used to ease welding				Remarks
Tensile	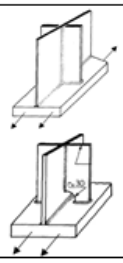	No	Yes	Scallop radius 25 mm	Scallop radius 40 mm			Increasing the scallop radius degreases the fatigue strength
				Yes	-			
Bending		Yes	No	-	-			Scallop radius of 30 mm was used
	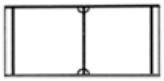	No	Yes	Yes	No			Increasing the scallop radius degreases the fatigue strength
	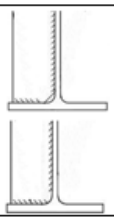	-	-	-	-	Web gap	No Gap	Web gaps smaller than 6,35 mm should be avoided
						Yes	Yes	
Flange and web with vertical and horizontal stiffeners (I-beam)								
Bending	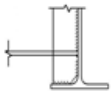	-	-	-	-	-	-	Web gaps smaller than 6,35 mm should be avoided

Table 20. Design rules for flange and web without stiffeners.

	Flange and web (I-beam)							
Loading	Model	Scallop	No scallop	If scallop is used to ease welding				Remarks
				Scallop radius 25 mm	Scallop radius 40 mm			
Tensile	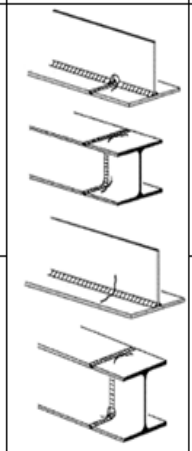	No	Yes	Yes	No	Scallop shape	Boxing weld	Increasing the scallop radius degreases the fatigue strength
Bending		No	Yes	Yes	No	Half-round or triangular[1]	No[2]	

[1] See figure 35.

[2] Boxing weld should not be used if good quality welding endings are provided.

7 CONCLUSIONS AND SUMMARY

Fatigue is a notable phenomenon in bridge failures and also in decks and offshore structures. Scallops are used in these structures for different reasons. In this thesis the convenience of scallops was investigated using results from previous studies, finite element analyses and experimental laboratory measurements.

Laboratory fatigue tests and FEAs did to T- and H-shaped specimens in LUT and earlier studies showed that convenience of scallops depends on the loading condition, weld penetration depth, scallop radius and length of longitudinal attachment.

Fatigue strength is almost the same for T-shaped specimens with or without scallops (radius 35 mm), shown in figure 15, when 100 mm long longitudinal attachment is used. When 200 mm long attachment is used, it is recommended to avoid scallops. Fatigue cracks developed at weld toes of bracket ends. Scallops degrease the effective length of brackets which is seen in slightly better fatigue strength than in specimens without scallops. When bracket length is increased the effect of the scallop degreases. Fatigue strength is almost the same for H-shaped specimens with 200 mm long longitudinal attachment with or without scallops (radius 30 mm).

FEAs show that for primarily loaded specimens, shown in figure 17, 20 mm scallops are recommended to be used when fillet weld is used. Avoiding scallops is recommended if full penetration weld is used in BNS specimen. Bracket end weld toe is the critical location for fatigue failure in non-primarily loaded cases for BNS and BWS specimens. Specimens with and without scallops (20 mm radius) have almost the same fatigue strength at bracket end weld toe. When full penetration weld is used in corner weld area BNS specimen have better fatigue strength at weld crossing than BWS specimen thus, BNS specimen with high-quality welding should be used. Laboratory tests show that when non-primarily loaded specimens represented in figure 17 were full penetration welded, scallops should be avoided. When fillet weld is used specimen with 20 mm radius scallop has the best fatigue strength. In all T- and H-shape specimens, raising the scallop radius degreases fatigue strength at the scallop corner weld toe.

Based on laboratory tests and FEAs, design rules for flange and web connections with stiffeners were made. In cases where tensile loading is affecting to specimens with transverse stiffeners, using of scallops in stiffeners should be avoided. If scallops are used to ease welding, scallops with small radii like 25 mm should be chosen. When bending is affecting to the structure, scallops should be used in stiffeners but scallops in web should be avoided. Instead of scallops also, web gaps are used as seen in figure 22. In cases where bending is affecting to structure, using a web gap or not doesn't make a much difference in fatigue strength. In cases with vertical and horizontal stiffener affected to bending, web gaps smaller than 6.35 mm should not be used to avoid brittle fracture.

Based on Eurocode, IIW rules and other laboratory tests and FEAs, design rules for flange and web connections without stiffeners were made. In tensile loading cases for specimen shown in table 20, scallops are not recommended to be used. Scallops with small radii like 25 mm should be chosen if scallops are used to ease the welding. Same results fit to cases where tensile loading is replaced with bending. In most cases half-round scallops are used. In bending cases scallop shape should be half-round or triangular. One test result shows that boxing welds increase peak stress in scallop details decreasing fatigue strength. Boxing weld might be better not to be used when good welding quality can be provided to weld endings. Weld endings are common areas for welding defects and cause stress raisers.

In manufacturing point of view, scallops should be used to ease the welding and surface treatment process. Scallop radius should be 50 mm when plate thickness is over 25 mm and 35 mm when plate thickness is 25 mm or less. When scallops are over weld seams, the distance between the toe of a fillet weld and the toe of a butt weld should not be less than 5 mm.

The fatigue strength of scallops can be increased by adding filler plates or reinforced plastic strips and by improving scallop shapes like increasing curvature ratios of scallops. Also, full penetration welding and surface treatments like TIG dressing, hammer peening and grinding increase fatigue strength but also increase manufacturing costs.

As a rule of thumb, scallops should be avoided because those are stress raisers for the structure and take a lot of time to manufacture. There are some exceptions when scallops

should be used, then good quality welding should be provided and full weld penetration is recommended to be used in load-carrying corner weld areas. Additional holes should be made to the structure if scallops were worked as air or drain holes.

7.1 Proposed future work

Fatigue strength of specimen with different scallop types and shapes should be researched to determine if triangular shaped scallops are better than commonly used half-round scallops. Laboratory tests and finite element method should be used to give reliable results.

REFERENCES

American Bureau of Shipping. 1995. Guide on improvement for structural connections and sample structural details - service experience and modifications - for tankers. [E-document]. [Referred 4.4.2016]. 23 p. Available on PDF file: https://www.eagle.org/eagleExternalPortalWEB/ShowProperty/BEA%20Repository/Rules&Guides/Current/75_StructConn&SampleStructDetails_Tankers/Pub75_TankerModifications

American Bureau of Shipping. 2007. Guide for shipbuilding and repair quality standard for hull structures during construction. [E-document]. [Referred 6.4.2016]. 37 p. Available on PDF file: http://www.eagle.org/eagleExternalPortalWEB/ShowProperty/BEA%20Repository/Rules%26Guides/Archives/87_Shipbuilding%26RepairQualStand_HullStruct_Const/Pub87_SRQS_Guide

American Institute of Steel Construction. 2010. ANSI/AISC 360-10, specification for structural steel buildings. [E-document]. [Referred 4.4.2016]. 552 p. Available on PDF file: https://www.aisc.org/WorkArea/showcontent.aspx?id=41132.

Bowman, M.D., Fu, G., Zhou, Y.E., Conner, R.J. and Godbole, A.A. 2012. Fatigue evaluation of steel bridges. NCHRO Report 721. WASHINGTON, D.C.: Transportation research board. 115 p.

Bramat, M., Gerbeaux, and Vix, J.-M. 1973. Comportement en fatigue sous flexion plane de poutres composées par soudage. Soudage et Techniques connexes 27. pp. 129–140.

British Columbia Ministry of Transportation. 2007. Bridge Standards and Procedures Manual: Supplement to CHBDC S6-06. Volume. Canada. 173 p.

Cai, S., Chen, W. and Zhao, Y. 2014. Experimental and Analytical Study on the KT-joints of the All-welded Steel Truss Bridge. [E-document]. [Referred 4.4.2016]. Atlantic press. pp. 1008–1014. Available on PDF file: http://www.atlantis-

press.com/php/pub.php?publication=icmce-14&frame=http%3A//www.atlantis-press.com/php/paper-details.php%3Fid%3D14940

DeLong, D.T. and Bowman, M.D. 2010. Fatigue Strength of Steel Bridge Members with Intersecting Welds. [E-document]. [Referred 4.4.2016]. Publication FHWA/IN/JTRP-2009/19. Joint Transportation Research Program, Indiana Department of Transportation and Purdue University, West Lafayette, Indiana, 2010. 204 p. Available on PDF file: http://dx.doi.org/10.5703/1288284314287

DNV. 2011. DNV-RP-C203, fatigue design of offshore steel structures. [E-document]. [Referred 4.4.2016]. 176 p. Available on PDF file: https://rules.dnvgl.com/docs/pdf/DNV/codes/docs/2011-10/RP-C203.pdf

DNV. 2014. Classification Notes, N. 30.7. Fatigue assessment of ship structures [E-document]. [Referred 4.4.2016]. 151 p. Available on PDF file: https://rules.dnvgl.com/docs/pdf/DNV/cn/2014-04/CN30-7.pdf

DNV. 2016. Hull structural design - Ships with length 100 metres and above. [E-document]. [Referred 4.4.2016]. 187 p. Available on PDF file: http://rules.dnvgl.com/docs/pdf/dnv/rulesship/2016-01/ts301.pdf

Dong, P. 2001. A structural stress definition and numerical implementation for fatigue analysis of welded joints. International Journal of Fatigue, vol. 23, no. 10. pp. 865–876.

Dowling, N.E. 2007. Mechanical behavior of materials: engineering methods for deformation, fracture, and fatigue. 3rd ed. Upper Saddle River (NJ): Pearson Prentice Hall, 912 p.

EN 1993-1-9. 2005. Eurocode 3: Design of steel structures. Part 1-9: Fatigue. 34 p.

Fisher, J.W. 1977. Bridge fatigue guide: design and details. American Institute of Steel Construction, Chicago. 58 p.

Fisher, W. E. & Stallmeyer, J. E. 1958. Behavior of welded build-up beams under repeated loads. University of Illinois, Urbana, Illinois. 104 p.

Fricke, W. 2010. Guideline for the Fatigue Assessment by Notch Stress Analysis for Welded Structures. IIW-Doc XIII-2240r2-08/XV-1289r2-08, International Institute of Welding.

Fricke, W. 2014. Session 1: Fatigue assessment by notch stress analysis for welded structures. Fatigue Seminar in Lappeenranta, August 21, 2014. 30 p.

Fricke, W. and Kahl, A. 2005. Comparison of different structural stress approaches for fatigue assessment of welded ship structures. Marine structures, vol. 18. pp. 473–488.

Fricke, W. and Paetzold, H. 1995. Fatigue strength assessment of scallops - an example for the application of nominal and local stress approaches. Marine Structures, vol. 8. pp. 423–447.

Glenn, I.F., Dinovitzer, A., Paterson, R.B., Luznik, L. and Bayley, C. 1999. Fatigue resistant detail design guide for ship structures. Ship Structure Committee. Report SSC-405. 205 p.

Glinka, G. and Krzyżecki, A. 1981. Fatigue life calculation and testing of full-scale welded I-beams. Fatigue & Fracture of Engineering Materials & Structures, vol. 4, No. 1. pp. 35–48.

Gurney, T.R. 1979. Fatigue of welded structures. 2nd ed. London, United Kingdom: Cambridge University press. 456 p.

Gurney, T.R. and Maddox, S. 1972. A re-analysis of fatigue data for welded joints in steel. The Welding Institute, Abington, Rep. E/44/72.

Heshmati, M. and Al-Emrani, M. 2012. Fatigue strength of cope-hole details in steel bridges. Gothenburg, Sweden: Chalmers University of Technology, Department of Structural Engineering. 16 p.

Hobbacher, A. 2014. Recommendations for fatigue design of welded joints and components. IIW-document XIII-2460-13/XV-1440-13, International Institute of Welding. 164 p.

Imam, B. and Chryssanthopoulos, M.K. 2010. A review of metallic bridge failure statistics. IABMAS 2010, vol. 7. 15 p.

InfraRYL 2006. 2008. Infrarakentamisen yleiset laatuvaatimukset, Osa 3 Sillat ja rakennustekniset osat. Helsinki: Rakennustieto. 278 p.

Jordan, C.R. and Krumpen, R.P. 1990. Design guide for ship structural details. Ship Structure Committee. Report SSC-331. 142 p.

Krantz, B. and Sonsino, C.M. 2010. Verification of FAT values for the application of the notch stress concept with the reference radii $r_{(ref)}$=1.00 and 0.005 mm. Welding in the World 54. pp. 218–224.

Kühn, B., Lukić, M., Nussbaumer, A., Günther, H.-., Helmerich, R., Herion, S., Kolstein, M.H., Walbridge, S., Androic, B., Dijkstra, O. and Bucak, Ö. 2008. Assessment of Existing Steel Structures: Recommendations for Estimation of Remaining Fatigue Life. [E-document]. [Referred 4.4.2016]. 90 p. Available on PDF file: http://eurocodes.jrc.ec.europa.eu/doc/background/EUR23252EN.pdf

Mahmoud, H.N., Connor, R.J. and Fisher, J.W. 2005. Finite Element Investigation of the Fracture Potential of Highly Constrained Details in Steel Plate Members. Computer-Aided Civil and Infrastructure Engineering, vol. 20, issue 5. pp. 383-392.

Matoba, M., Kawasaki, T., Fuji, T. and Yamauchi, T. 1983. Evaluation of fatigue strength of welded steel structures, hull's members, hollow section joints, piping and vessel joints. IIW-Doc XIII-1081-83, International Institute of Welding.

Miki, C. and Tateishi, K. 1997. Fatigue strength of cope hole details in steel bridges. International Journal of Fatigue, vol. 19, no. 6. pp. 445–455.

Munse, W.H. and Grover, L.M. 1964. Fatigue of welded steel structures. New York: Welding research council. 210 p.

National Board of Housing, Building and Planning. 2003. Swedish Regulations for Steel Structures, BSK 99. [E-document]. [Referred 4.4.2016]. 192 p. Available on PDF file: http://www.boverket.se/globalassets/publikationer/dokument/2003/swedish_regulations_for_steel_bsk99.pdf

Niemi, E. 1999. Designer's guide for hot spot fatigue analysis. IIW-Doc XIII-WG3-01-99, International Institute of Welding. pp. 1–22.

Niemi, E. 2003. Levyrakenteiden suunnittelu. Helsinki: Teknologiainfo Teknova. 136 p.

Niemi, E. Kilkki, J., Poutiainen, I. and Lihavainen, V., 2004. Väsymättömän hitsausliitoksen suunnittelu. Lappeenrannan teknillinen yliopisto: LTY Digipaino. 121 p.

Okumoto, Y., Takeda, Y., Mano, M. and Okada, T. 2009. Design of Ship Hull Structures - A Practical Guide for Engineers. Berlin Heidelberg: Springer-Verlag. 578 p.

Radaj, D. 1990. Design and Analysis of Fatigue Resistant Welded Structures. Woodhead Publishing. 378 p.

Rautaruukki Corporation. 2014. Optim QC structural steels. [Online]. [Referred 4.4.2016]. Available: http://www.oxycoupage.com/FichiersPDF/Ruukki_Pdf/English/Optim-QC-structural-steels.pdf

Sakano, M., Mikami, I. and Yonemoto, E. 1993. Fatigue life prediction for plate girder specimens with 4 types of vertical stiffener connections. Technology Reports of Kansai University, No. 35. pp. 277–284.

Sakano, M., Mikami, I., Yonemoto, E., Kano, K. and Yasuike, H. 1992. Fatigue tests for plate girder specimens with 4 types of vertical stiffer connections: Technology Reports of Kansai University, No. 34. pp. 149–160.

Solomon, B., Björk, T. and Nykänen, T. 2010. Fatigue analysis of brackets with and without scallop for bridge and other deck structures using effective notch stress. Lappeenranta University of Technology. 20 p.

Spyrakos, C.C. 1996. Finite element modeling in engineering practice: includes examples with ALGOR. Pittsburg, PA: Algor Inc. 322 p.

Xiao, Z. and Yamada, K. 2005. Fatigue Strength of Intersecting Attachments. Journal of Structural Engineering, vol. 131 no. 6. pp. 924–932.